Co-funded by the Erasmus+ Programme of the European Union

Renewable Energies
(part C, Solar and Geothermal)

Master Degree in Innovative Technologies in Energy Efficient Buildings for Russian & Armenian Universities and Stakeholders

Marco Fossa
University of Genova, Italy

Rev. 18/11/2016

Renewable Energies
Energy from the sun, Fundamentals

Solar Resource and utilization

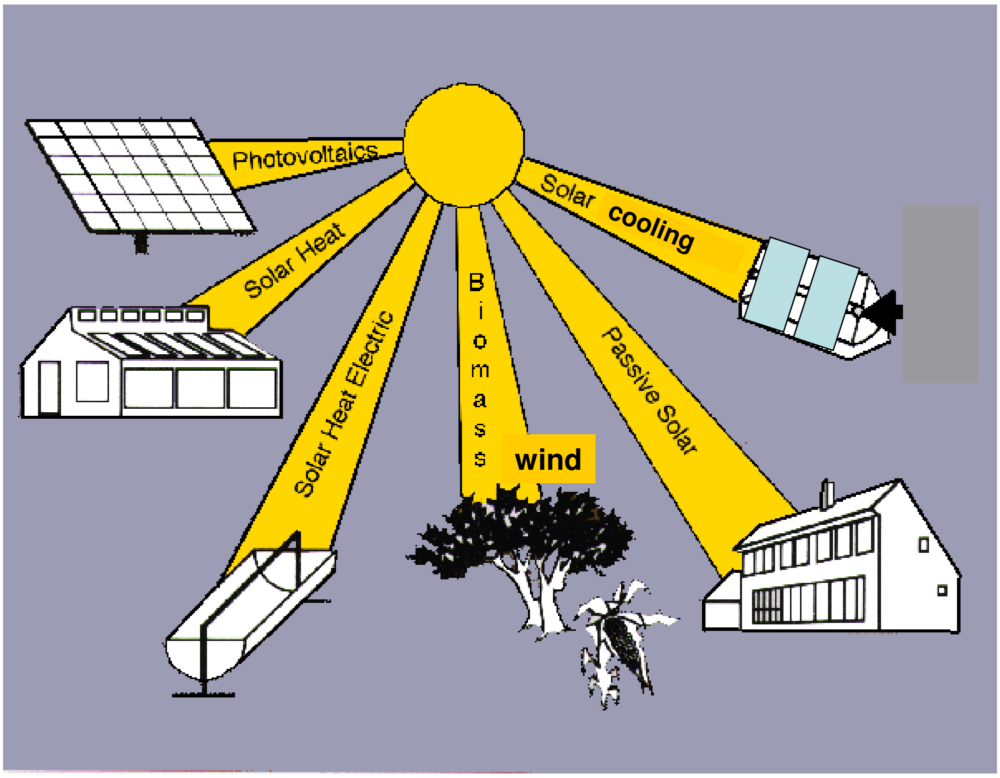

Solar Resource and utilization

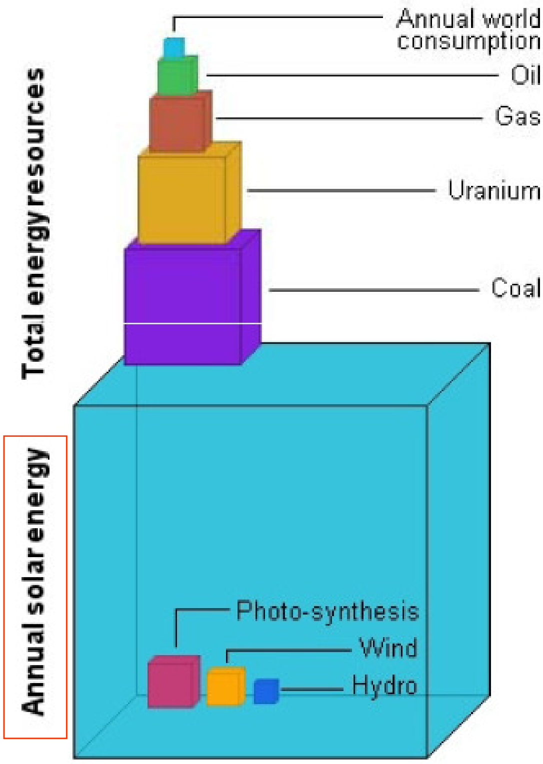

Source: World Energy Council

The Sun (I)

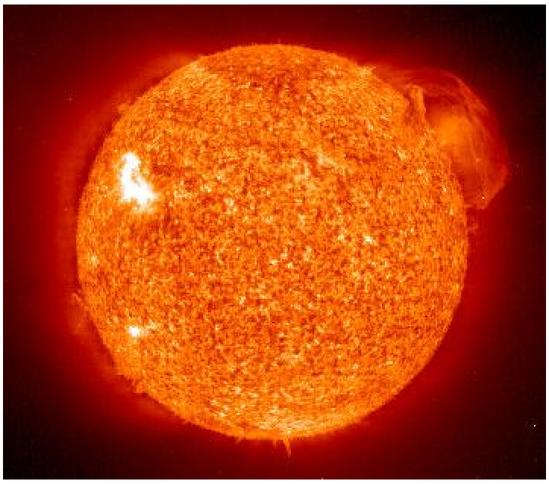

Mean diameter	1.392×10^{9} m 109 Earths
Surface area	6.0877×10^{18} m^2 11 990 × Earth
Volume	1.4122×10^{27} m^3 1 300 000 Earths
Mass	1.9891×10^{30} kg 332 946 Earths
Temperature of surface (effective)	5 778 K
Temperature of core	~15.7×10^{6} K
Sidereal Rotation period	25.05 days (at Equator)
	34.3 days (at Poles)
Composition by mass	
Hydrogen	73.46 %
Helium	24.85 %

The Sun (II)

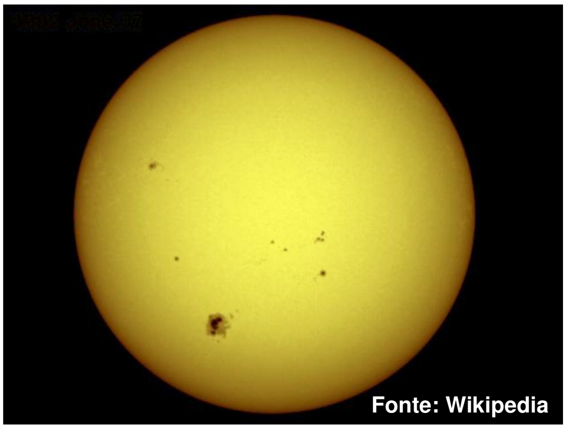

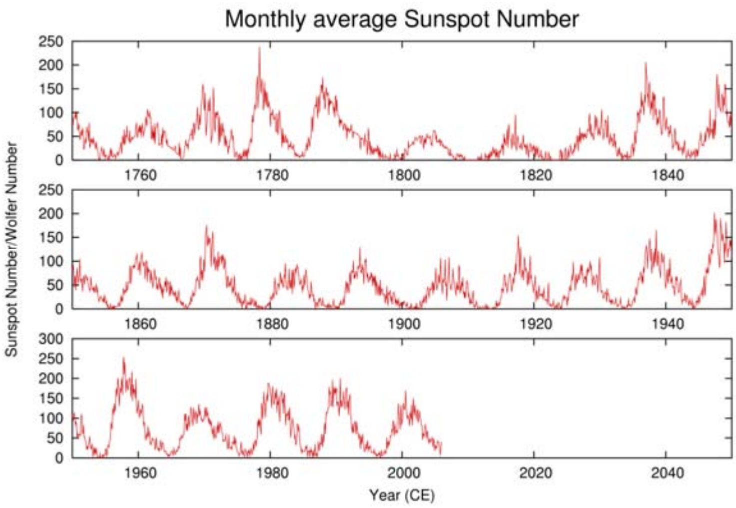

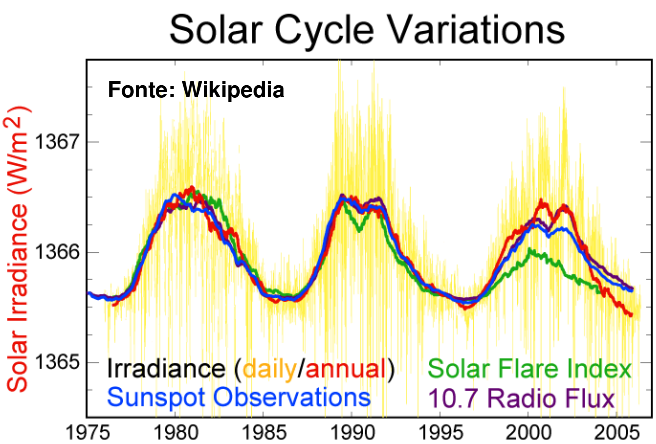

The Sun and the earth

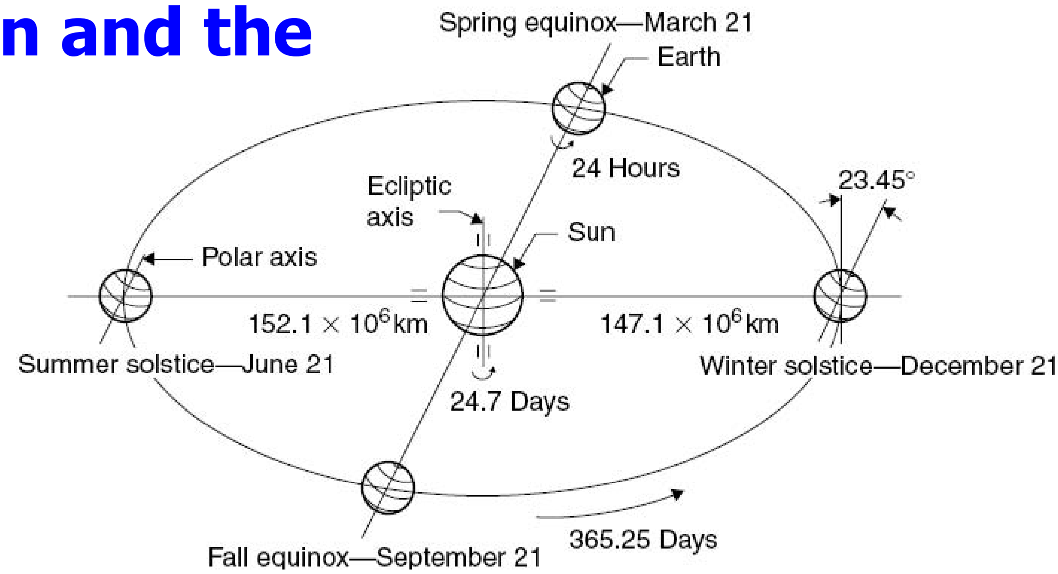

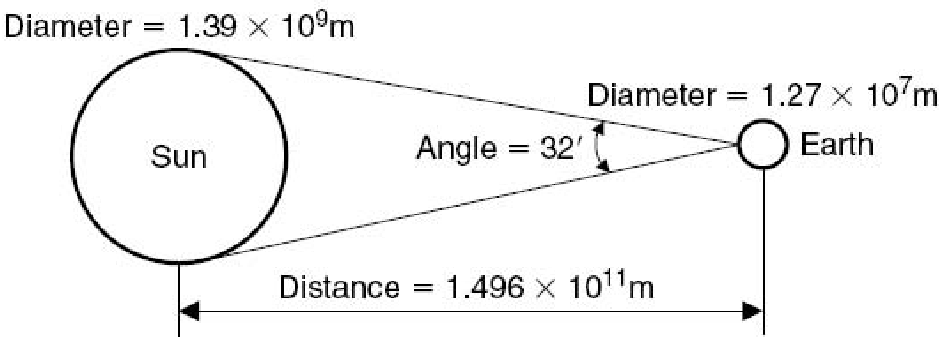

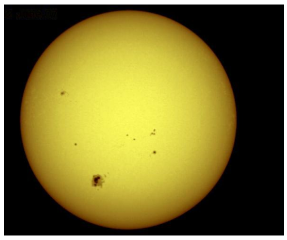

The Sun and the earth (II)

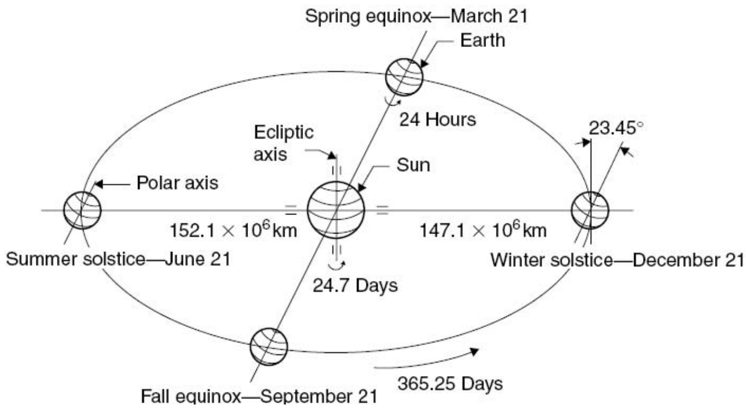

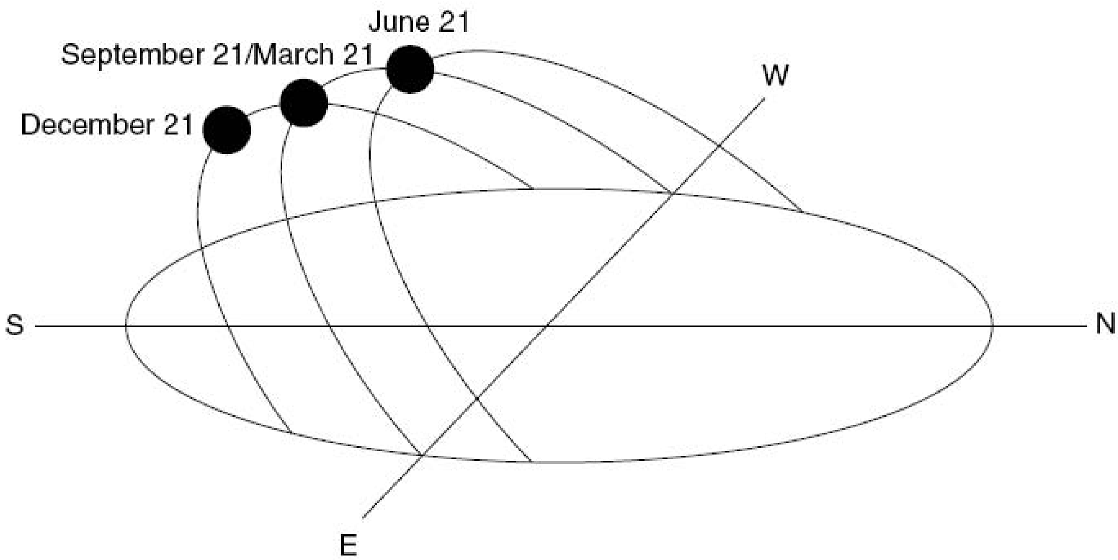

The Sun and the earth, Declination angle

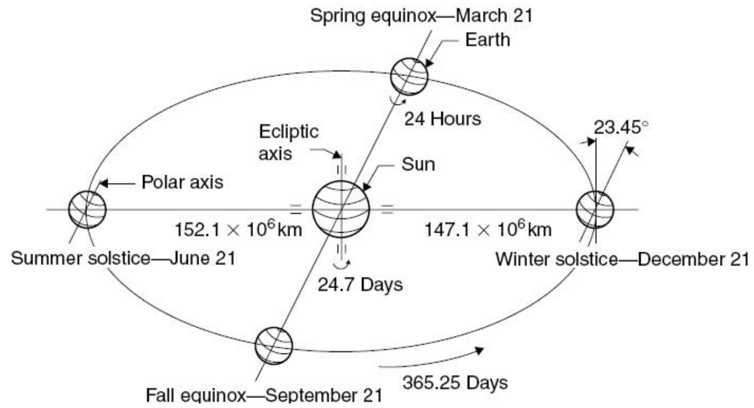

Sun Declination angle

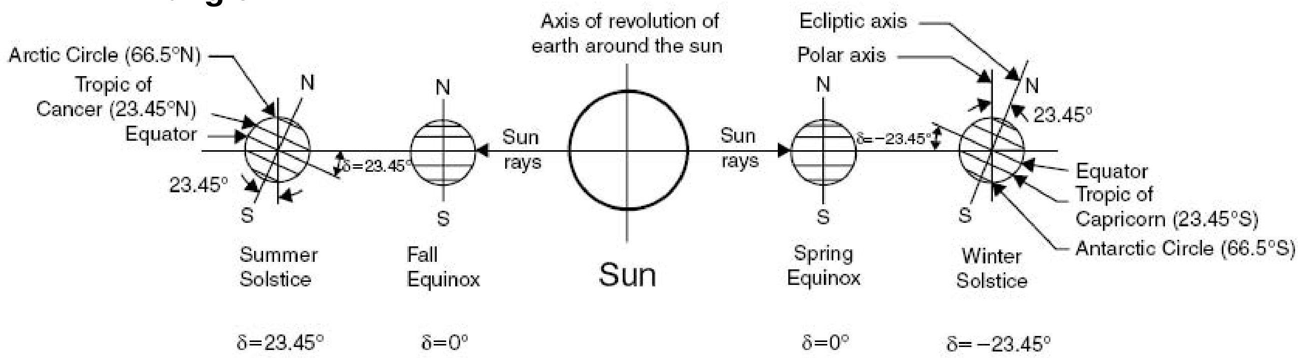

Declination and hour angle

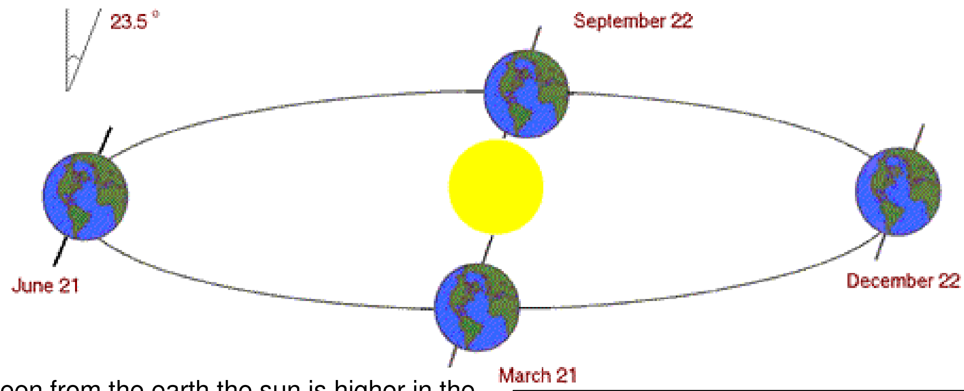

Seen from the earth the sun is higher in the sky in summer. This is due to the **sun declination** , which is the angle between a plane perpendicular to the ecliptic plane (and to sun-earth joining line) and the earth rotational axis.

This angle is also equal to the sun angle at noon as measured from the earth equatorial plane.

The Cooper formula is an approximate but reliable expression for the declination, in terms of the day number n:

$$\delta = 23.45\pi / 180 * \sin(2\pi * (284 + n) / 365)$$

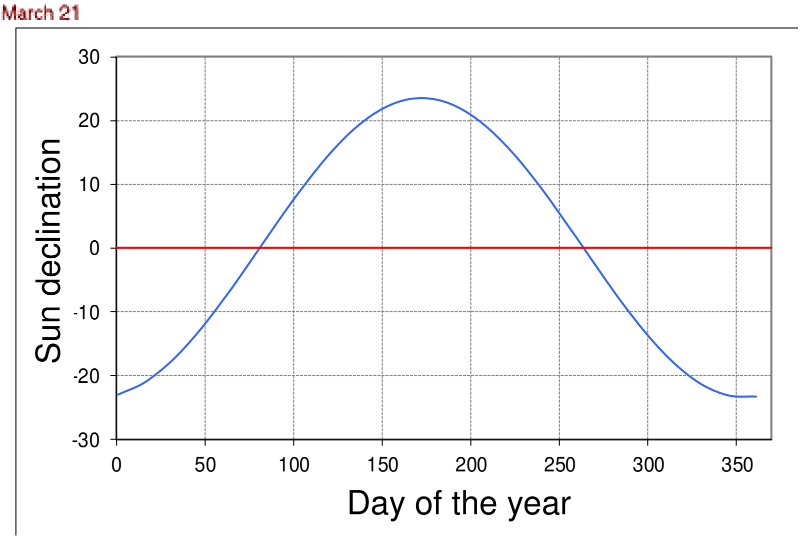

Zenith angle and solar altitude

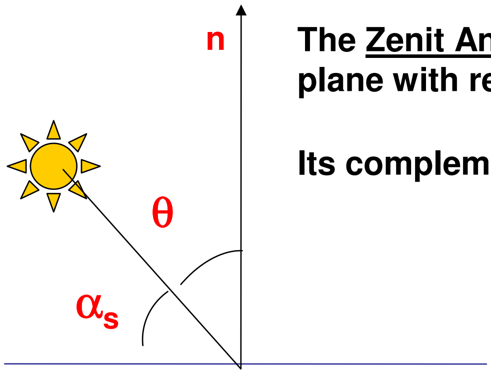

The Zenit Angle θ is measured in the local horizontal plane with respect to plane normal.

Its complementary angle is the solar altitude α

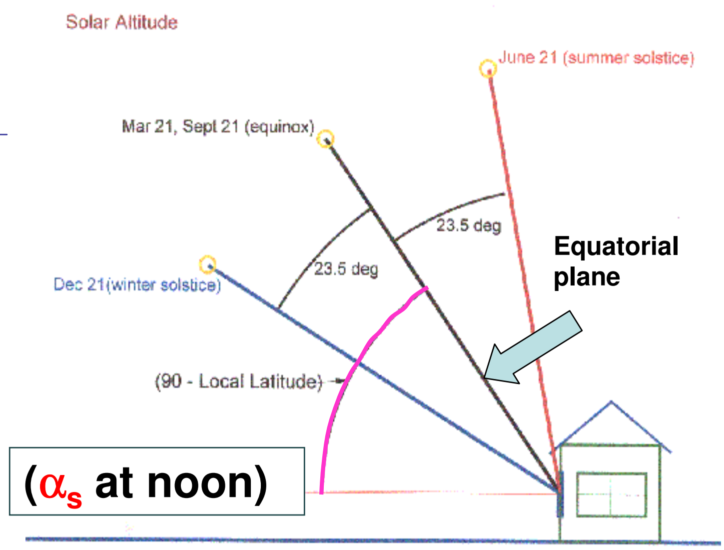

Hour and Zenith angles

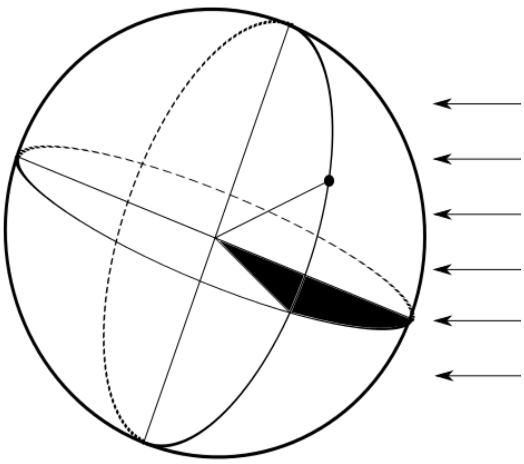

The hour angle ω is measured in the equatorial plane, as the sun ray projection with respect to the north-south direction

The Azimuth angle γ_s is measured in the local horizontal plane, with respect to N-S direction as the projection of the sun ray on local horizontal plane

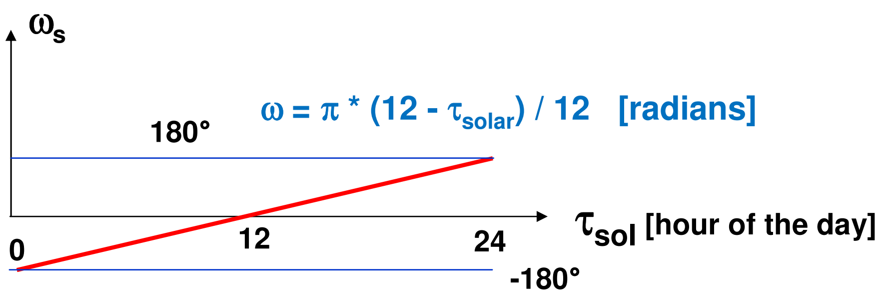

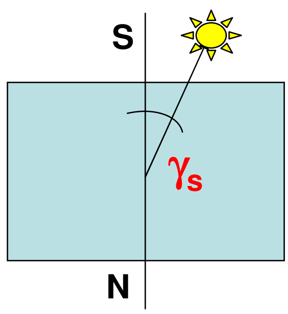

Hour angle at sunrise and sunset

The Zenit Angle θ depends on hour, declination and latitude angle φ.

It can be demonstrated that

$$\cos(\theta) = \sin(\varphi)\sin(\delta) + \cos(\varphi)\cos(\delta)\cos(\omega)$$

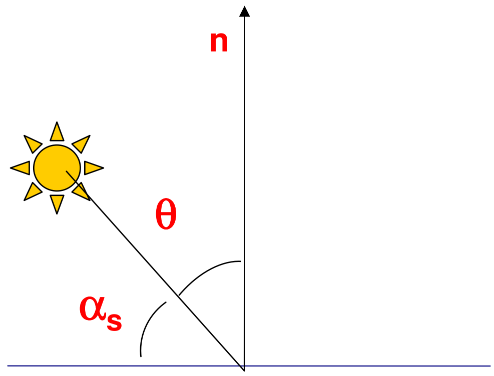

At sunrise and sunset theta is 90° and hence ω_{ss} (sunset and sunrise, positive sign at sunset) is

$$\omega_{ss} = \mathrm{acos}[-\mathrm{atan}(\varphi)\mathrm{atan}(\delta)]$$

Solar and local Time

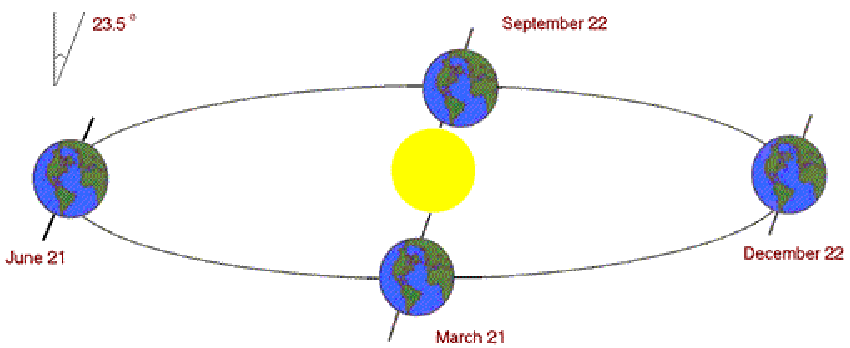

Solar time, local time and hour angle

In order to describe the sun position in time, we need to know the relationships existing between the local time, the time zone and the solar time τ_{sol}. The local time is the same in any time zone, while the sun position depends on the local longitude, which is typically different from the reference longitude of the time zone.

The solar time has its 12pm when the sun is at its apex, say at Noon.
In order to correct the local time for the local longitude it is needed to subtract (Longlocal – Longsm)/15 (in hours). Longlocal is in degrees and Longsm è is the longitude of the reference meridian of the time zone.

Furthermore one needs to correct the local time with respect to the Equation of Time in order to have the Solar time.

The hour angle ω represents the sun position with respect to the north-south direction, as measured in the equatorial plane.

The length of the day

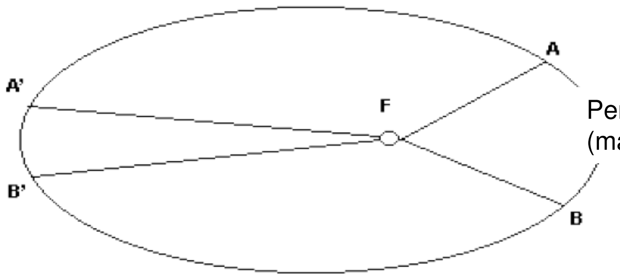

Solar day is measured with respect to su (apparent position) in the sky. By definiti is the time elapsed from 2 solar noons (highest position in the sky. Its duration is about 24h.

Sideral day is referred to a far star and is measured with respect to star position in the sky. Its duration is about 23h56'

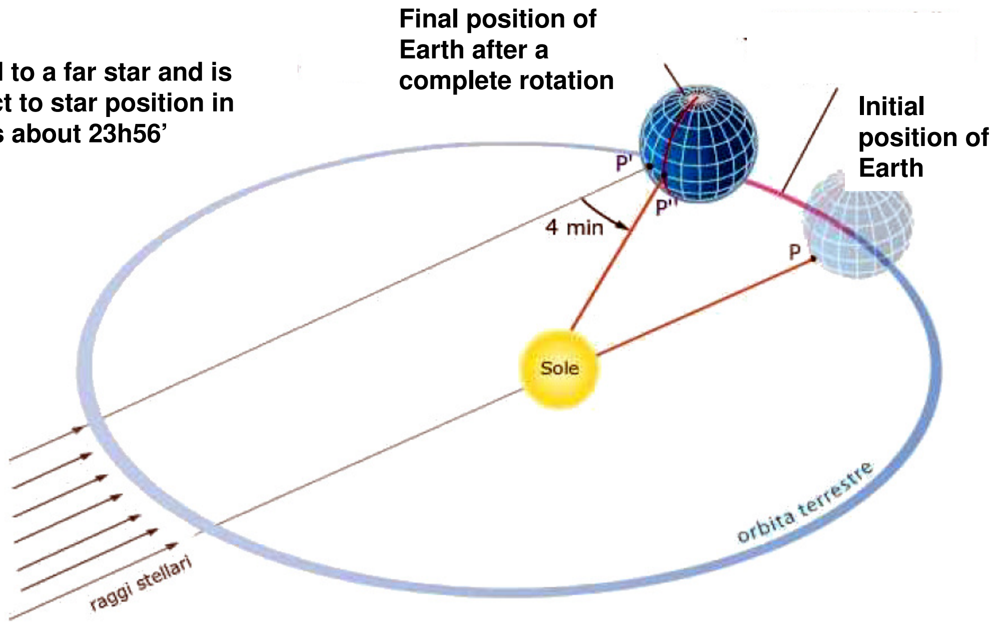

Equation of time

Revolution of earth around the sun is not constant in terms of angular speed. In addition the inclination of the earth axis varies with respect to the revolution plane. The combined effect is a variable length of the solar day, as defined as the time interval between 2 subsequent noon instants.
The solar day is not constant..! Formulas allow to take into considerations these phenomena.

Equation of Time (Eqt), in minutes:

$Eqt = -14.2 \sin(\pi(n + 7) / 111)$, for year day n between 1 and 106
$Eqt = 4.0 \sin(\pi(n - 106) / 59)$ for year day n between 107 and 166
$Eqt = -6.5 \sin(\pi(n - 166) / 80)$ for year day n between 167 and 246
$Eqt = 16.4 \sin(\pi(n - 247) / 113)$ for year day n between 247 and 365

$$T_{solar} = T_{local} + Eqt / 60 - (Long_{SM} - Long_{Local}) / 15 - DLS \quad [Hours]$$

Notice: DayLight Saving correction often apply from 1st april to 30 october (+ 1 hour, DLS=0, +1)
Long is positive East of Greenwich

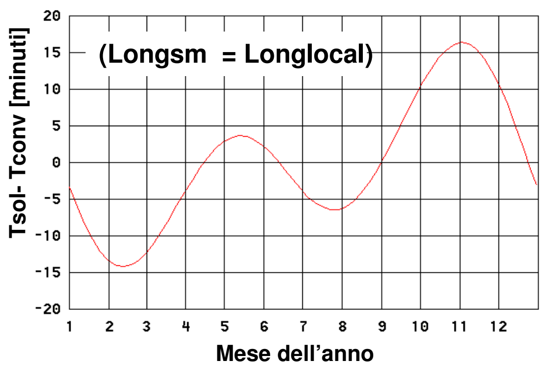

Equation of time

La rotazione della terra intorno al sole avviene a velocità angolare non costante, per effetto della conservazione del momento angolare. Un altro effetto è legato alla inclinazione dell'asse terrestre rispetto al piano di rotazione. Si genera pertanto una differenza rispetto al tempo convenzionale (locale) che trascorre in maniera uniforme

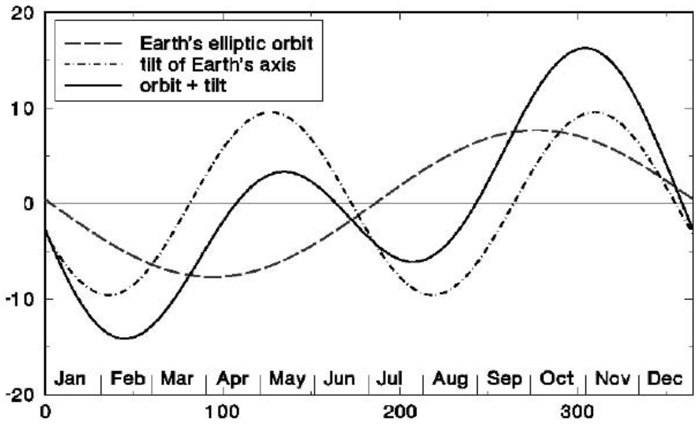

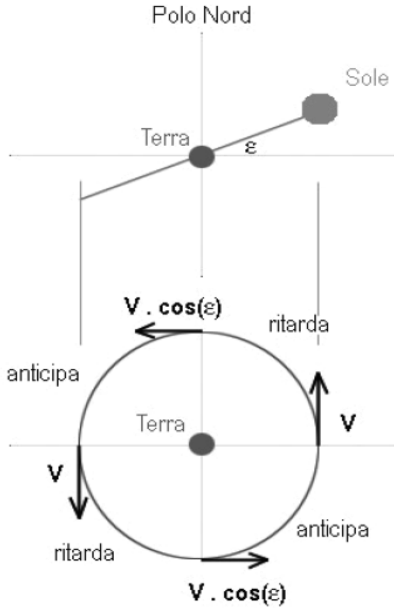

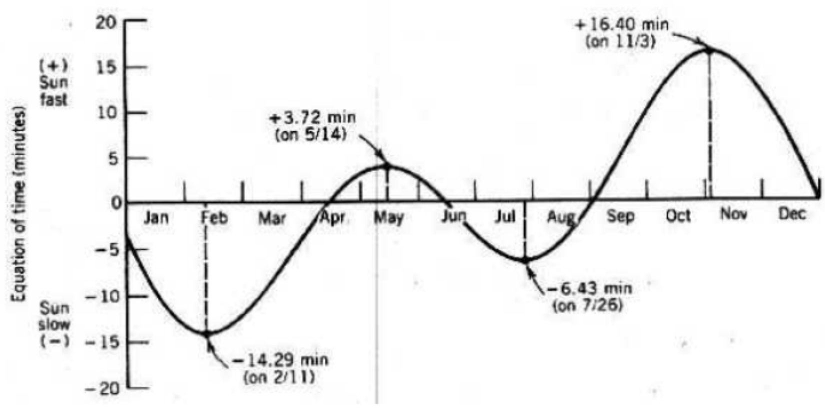

Equation of time (...Analemma)

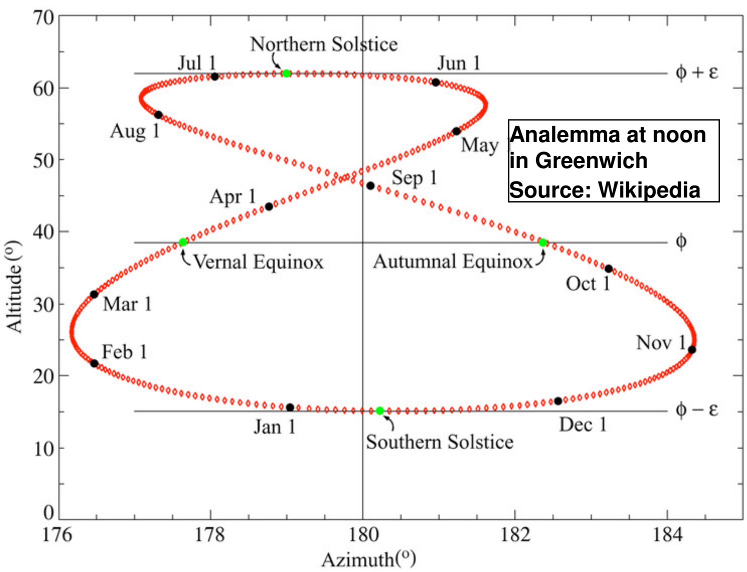

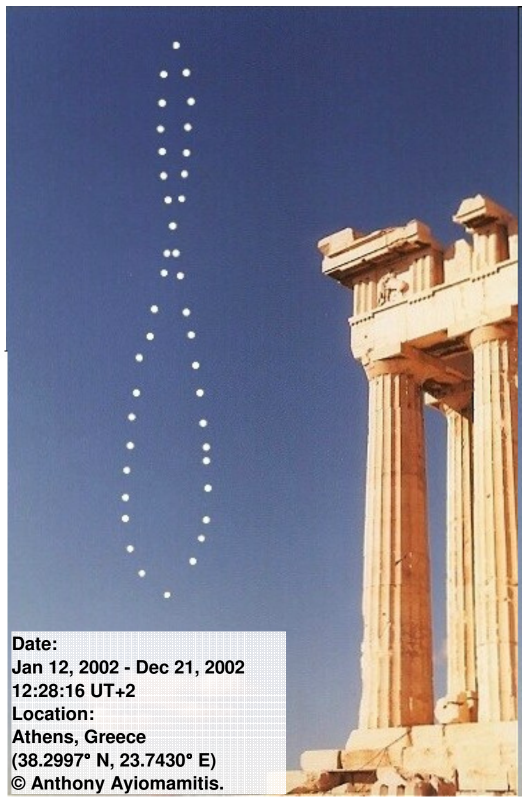

Equation of time
(Fao Penman model for crop evo-transpiration)

The solar time angle at midpoint of the period is:

$$\omega = \frac{\pi}{12}\left[(t + 0.06667(L_z - L_m) + S_c) - 12\right]$$

- t — standard clock time at the midpoint of the period [hour]. For example for a period between 14.00 and 15.00 hours, t = 14.5,
- L_z — longitude of the centre of the local time zone [degrees west of Greenwich]. For example, L_z = 75, 90, 105 and 120° for the Eastern, Central, Rocky Mountain and Pacific time zones (United States) and L_z = 0° for Greenwich, 330° for Cairo (Egypt), and 255° for Bangkok (Thailand),
- L_m — longitude of the measurement site [degrees west of Greenwich],
- S_c — seasonal correction for solar time [hour].

The seasonal correction for solar time is:

$$S_c = 0.1645 \sin(2\,b) - 0.1255 \cos(b) - 0.025 \sin(b)$$

$$b = \frac{2\pi\,(J - 81)}{364}$$

J is the number of the day in the year.

Azimuth Angle

La posizione del sole rispetto all'asse nord-sud è invece detto angolo azimutale (γ_s).
L'angolo orario è più facile da utilizzare dell'angolo azimutale in quanto esso è misurato nel piano dell'orbita apparente del sole.

Solar Azimuth
The azimuth angle is the angle within the horizontal plane measured from true South or North. The azimuth, when in reference to the South is usually called the bearing. If the sun is East of South, the Bearing is positive, else the bearing is negative.

Alt = Altitude Azm = Azimuth Decl = Declination
HAngle = Hour angle alt_R = Altitude in radians azm_R = Azimuth in radians
lat_R = Latitude in radians hour_R = Hour angle in radians x_azm = x component of azimuth
y_azm = y component of azimuth
TODEGREE = Constant equal to 180/pi

sin(Azm_R) = cos(Decl_R)sin(Hang_R)/cos(Alt_R)

$$\gamma_s = arcsen\,\frac{\cos\delta\; sen\,\omega}{\cos\alpha_s}$$

<u>This equation, however, fails at certain points, e.g. when the altitude is 90°.</u>

Therefore another equation is used which breaks the azimuth in its x and y components.
x_azm = sin(hour_R) * cos(decl_R)
y_azm = (-(cos(hour_R))*cos(decl_R)*sin(lat_R))+(cos(lat_R)* sin(decl_R))
azimuth = atan(x_azm/y_azm)*TODEGREE

Solar chart

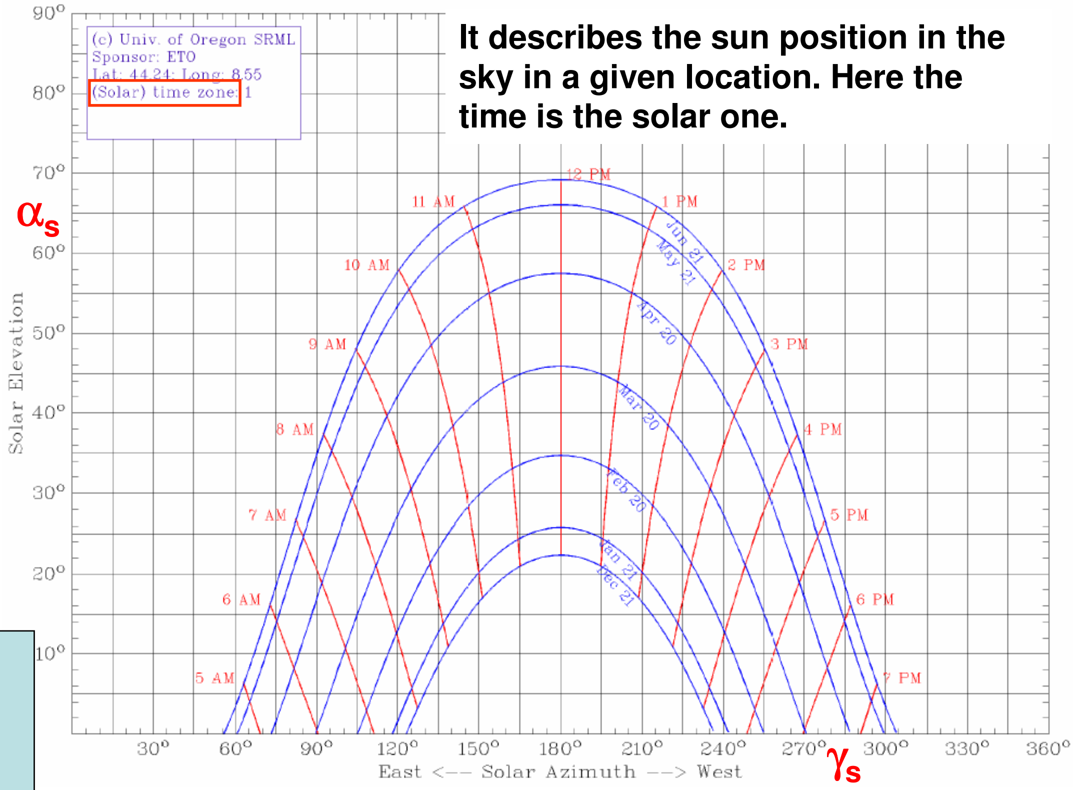

It describes the sun position in the sky in a given location. Here the time is the solar one.

Fonte: University of Oregon

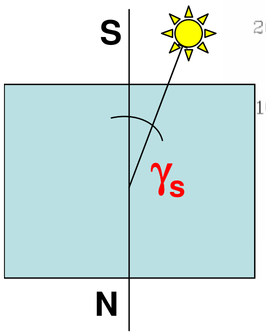

γ_s= sign(ω)*acos[cosθsinφ–sinδ)/(sinθcosφ)]

Solar chart

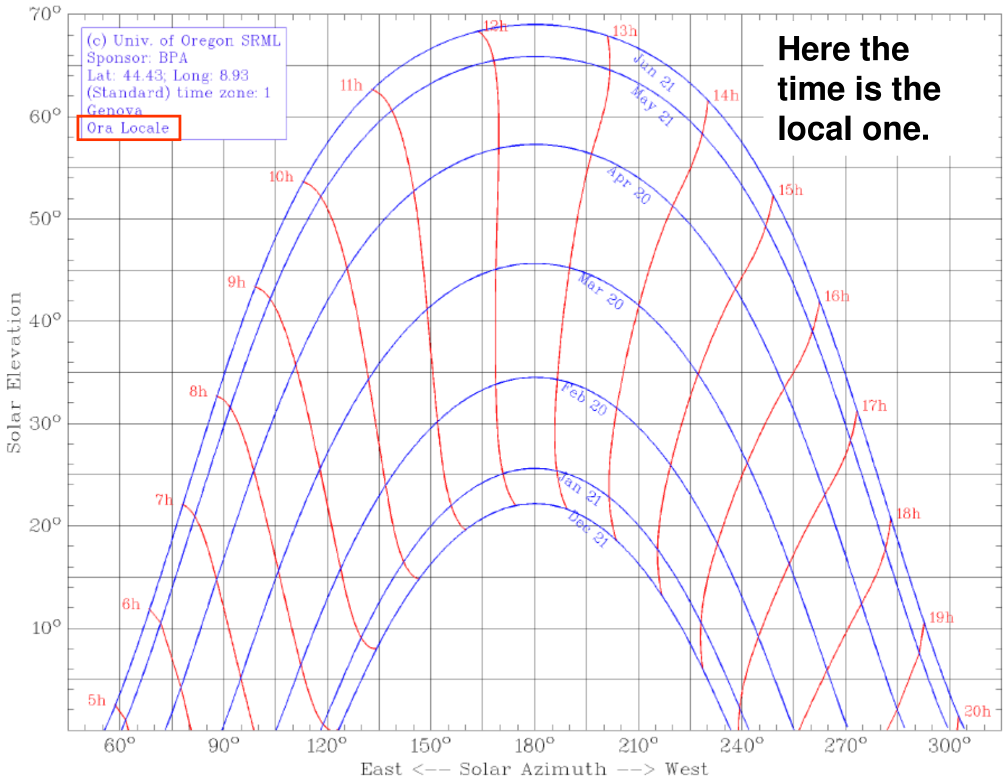

Here the time is the local one.

Fonte: University of Oregon

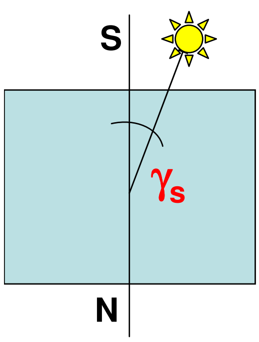

Solar angles

$\gamma_s = \text{sign}(\omega) * \text{acos}[\cos\theta \sin\varphi - \sin\delta)/(\sin\theta \cos\varphi)]$

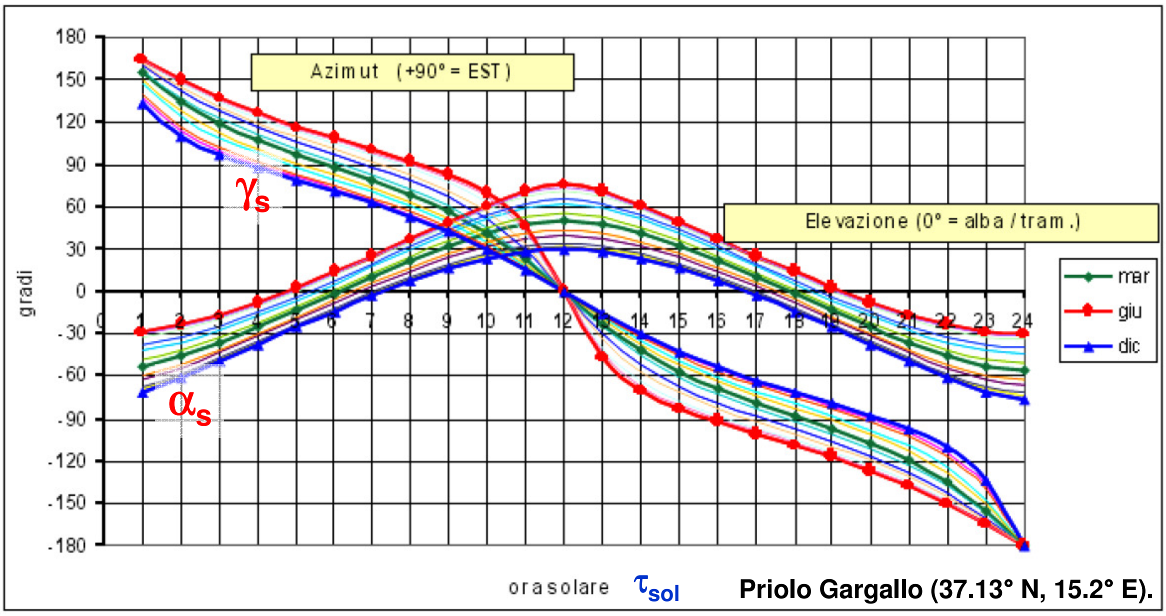

Angles related to tilted surfaces

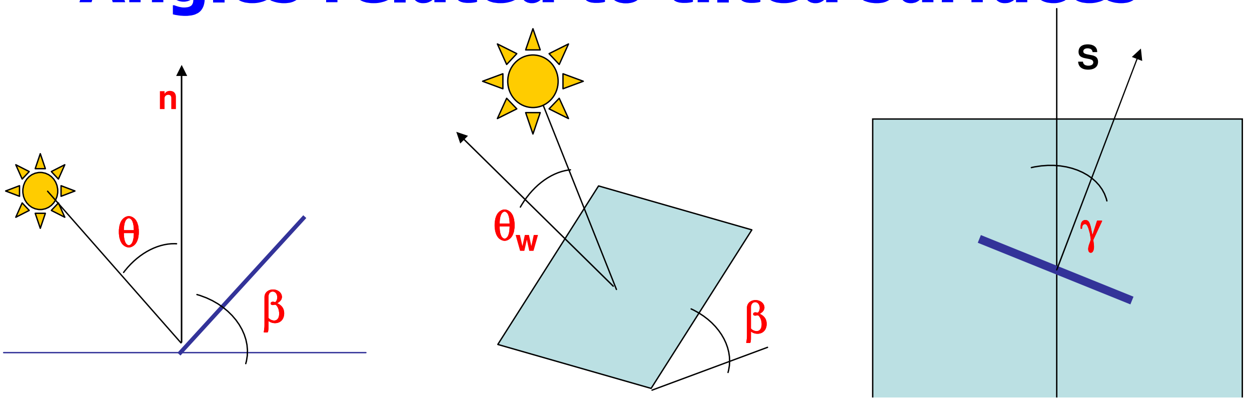

β = Tilt of the surface $\cos(\theta) = \sin(L-\beta)\sin(\delta) + \cos(L-\beta)\cos(\delta)\cos(h)$

θ_w = zenith angle of the surface

γ = azimuth angle of the surface

$\cos\theta_w = \cos\theta\cos\beta + \sin\theta\sin\beta\cos(\gamma_s - \gamma)$

$\cos\theta_w = \sin\delta\sin\varphi\sin\beta - \sin\delta\cos\varphi\sin\beta\cos(\gamma) + \cos\delta\cos\varphi\cos\beta\cos\omega + \cos\delta\sin\varphi\sin\beta\cos(\gamma)\cos\omega + \cos\delta\sin\beta\sin(\gamma)\sin\omega$

$\cos\theta_w = \cos\theta\cos\beta + \sin\theta\sin\beta\cos(\gamma - \gamma_{sun})$

$\cos\theta_w = \sin\delta\sin(\varphi-\beta) - \cos\delta\cos(\varphi-\beta)\cos\omega$ South Facing

Black body emission

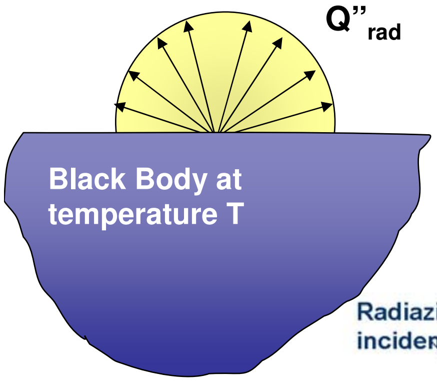

The Black Body is:

-The perfect absorber

-The best emitter

-The isotropic emitter

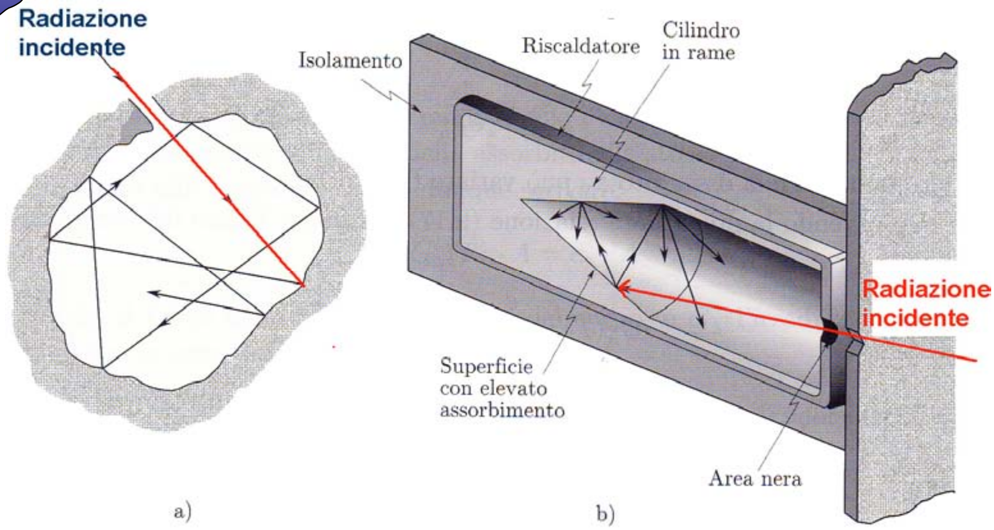

Black body emission (II)

$$e_{\lambda,n} = \frac{C_1}{\lambda^5\left[exp\left(\frac{C_2}{\lambda\,T}\right)-1\right]}$$

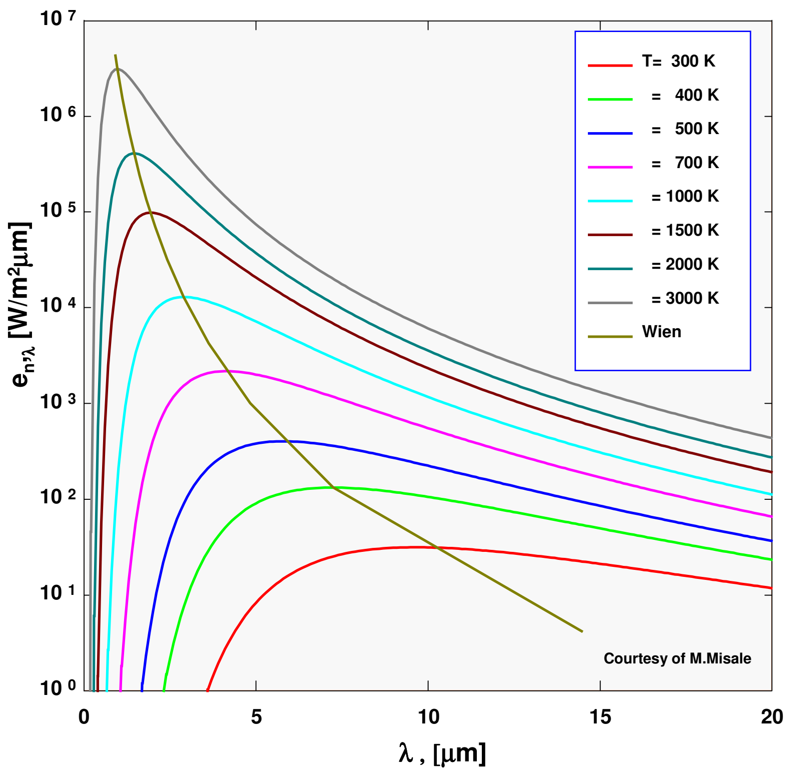

Black body emission (III)

Wien law:

$$\lambda_{max} T = 2897.6 \quad (\mu m\ K)$$

Total emissive Power

$$E_n = \int_o^{\infty} e_{\lambda,n}\, d\lambda = \sigma T^4$$

$$\sigma = 5.67 \cdot 10^{-8} \qquad [W/m^2 K^4]$$

Fraction of Blackbody radiation

$$F_{0-\lambda} = \frac{\int_o^{\lambda} e_{\lambda,n}\, d\lambda}{\sigma T^4} = F(\lambda T)$$

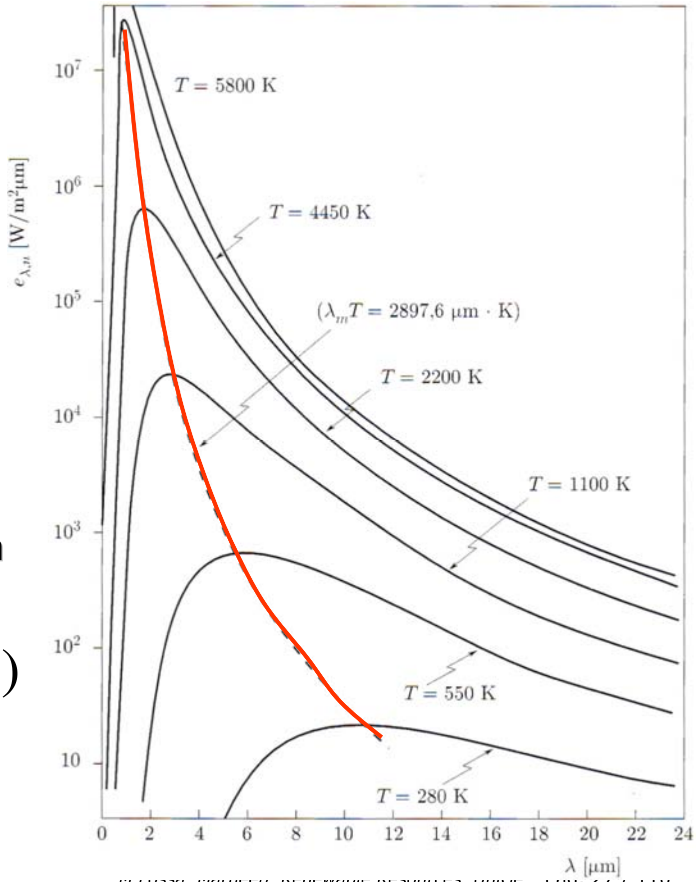

Sun irradiance

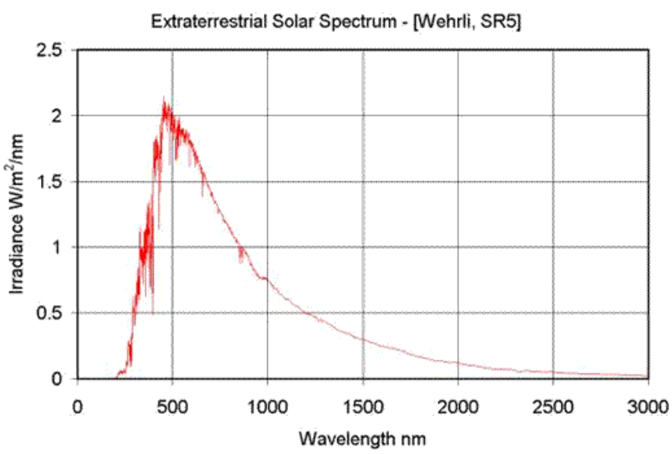

Sun Irradiance outside the atmosphere on a perpendicular surface in on average 1367 (W/m²). This value varies of about ±3% due to the earth position with respect to sun (elliptic orbit). The closest position is 4 jan while the farmost one is 5 july.

Extraterrestrial irradiance at normal incidence is:

G_o= 1367 * (Rav / R)² W/m²

where Rav is the average sun to earth distance and R is the current distance. An approximate expression for that ratio is :

(Rav / R)² = 1.00011
+ 0.034221 * cos(b)
+ 0.001280 * sin(b)
+ 0.000719 * cos(2b)
+ 0.000077 * sin(2b)

dove b = 2πn / 365 [radianti] e *n* è il giorno dell'anno (Per esempio il 15 febbraio è il giorno numero 46)

Another expression is :

G_o= 1367 * [1+0.033 cos(360n/365)] W/m²

On horizontal surface:

$G_{o,H}$ = G_o cos θ = G_o [sin(φ)sin(δ) + cos(φ)cos(δ)cos(ω)]

Daily Insolation (extraterrestrial, average) is evaluated trough the integration in time of $G_{0,H}$ between sunrise and sunset:

$(E_{o,H})_{day}$= 1367 *3600*24/π [1+0.033 cos(360n/365)] [sin(φ)sin(δ)ω_s + cos(φ)cos(δ)sen(ω_s)] [J/m²day]

ω_s at sunset in radians

Sun irradiance

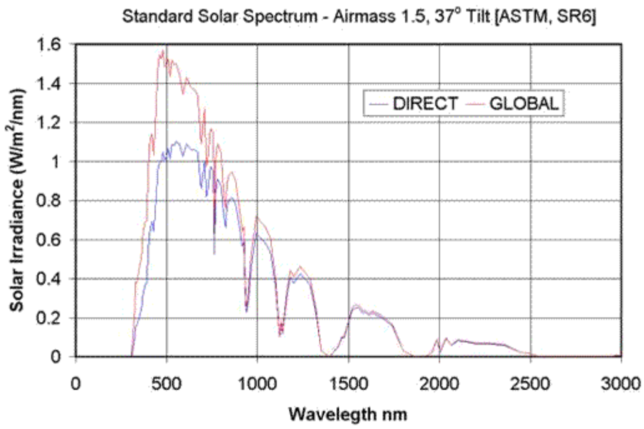

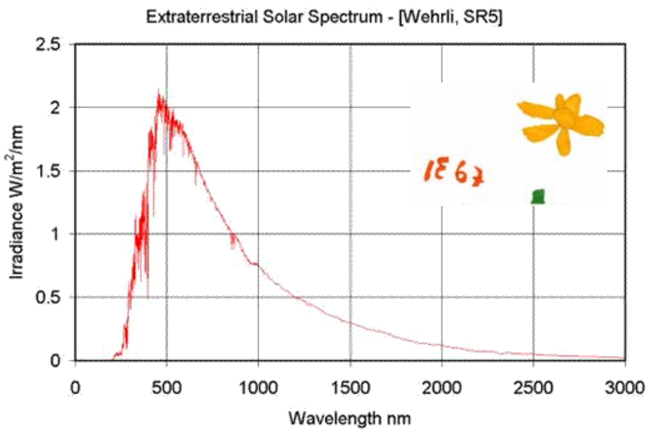

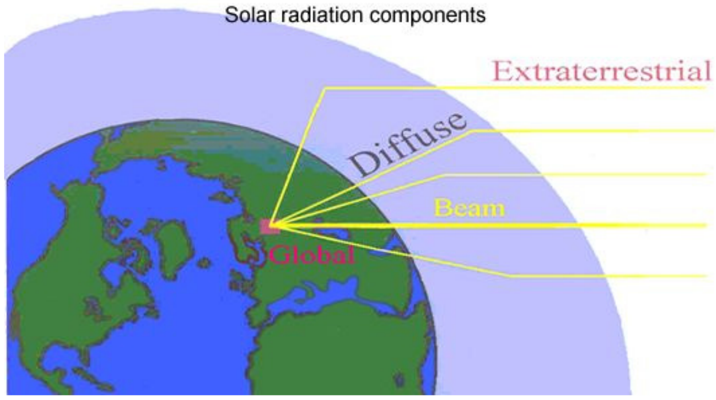

Sun irradiance (III)

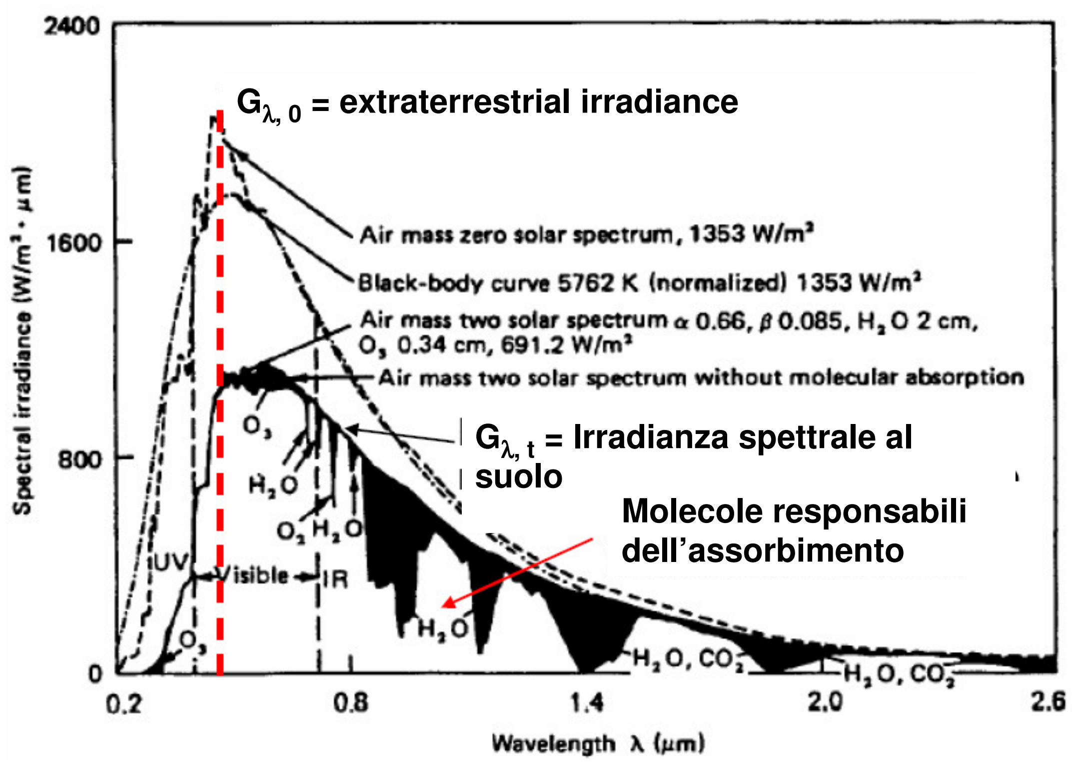

Definitions

Solar: terms and meaning

Irradiance **("Irradianza")is the rate of radiant energy falling on a surface per unit area of the surface (units, watts per square meter [W/m^2] symbol, G),**

Irradiation **is incident energy per unit area on a surface (units, joules per square meter [J/m^2]), obtained by integrating irradiance over a specified time interval. Specifically, for solar irradiance the terms used is *insolation*.**

The symbols used in many books are *H* for insolation for a day and *I* for insolation for an hour.

The appropriate subscripts used for *G*, *H*, and *I* are beam or direct (*B*), diffuse (*D*), and ground-reflected (*G or R*) radiation.

Radiance, the amount of radiation such as light or radiant heat that passes through or is emitted from a particular area, and falls within a given solid angle in a specified direction [W/m^{2}St]

Earth Energy Balance(I)

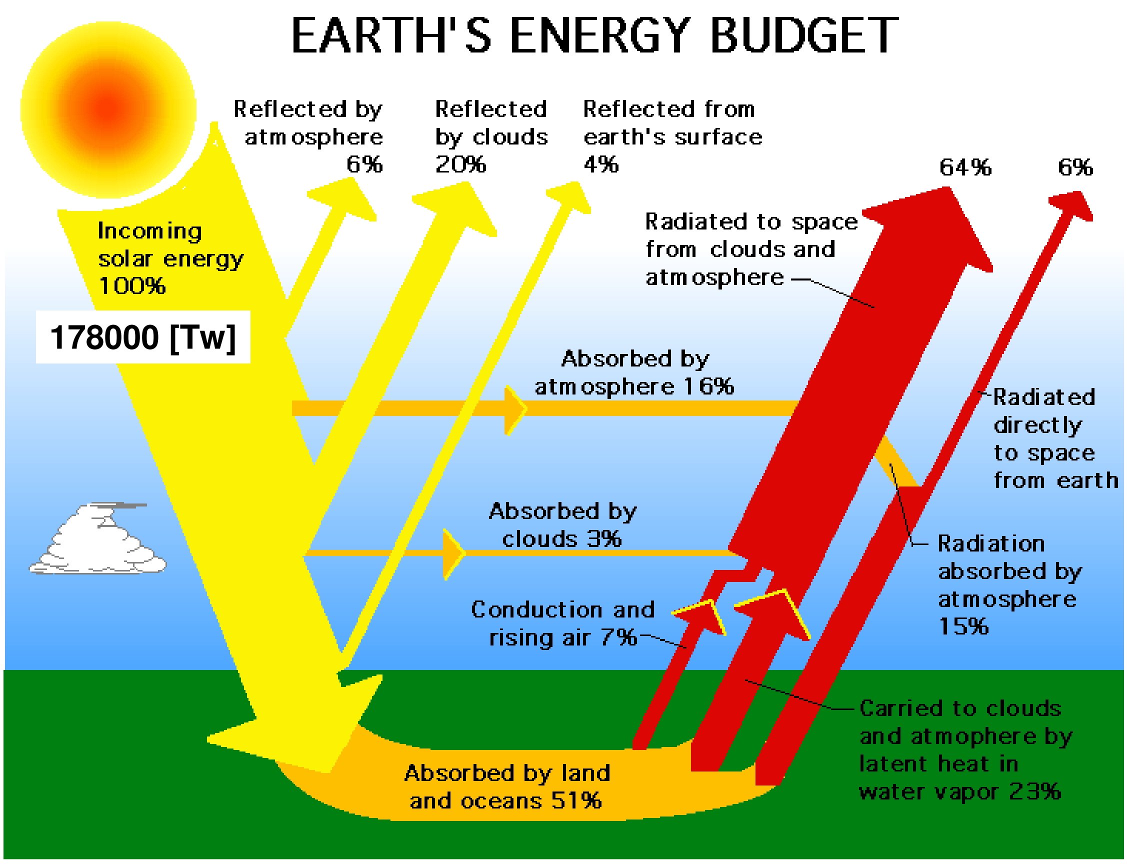

Irradiance at earth surface (I)

Sun energy at ground depends on ray path inside atmosphere. That path, made dimensionless, is the Air Mass m (or AM) given (for a Flat Earth..) as
m = 1/ cos(θ)

$$AM = \frac{1}{\cos\theta_z + 0.50572(96.07995 - \theta_z)^{-1.6364}}$$

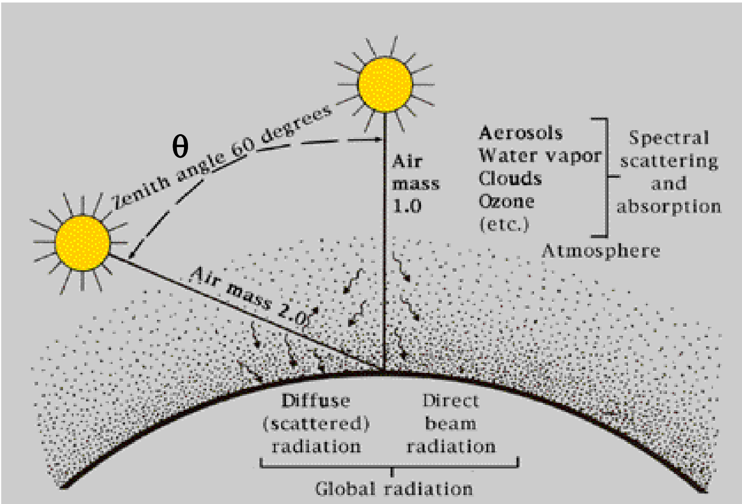

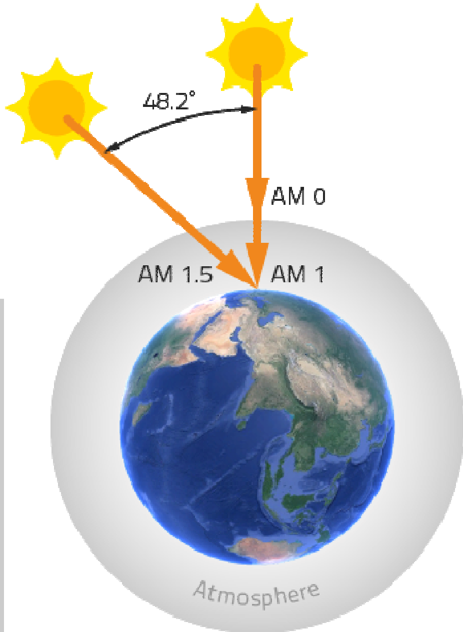

Irradiance at earth surface (II)

Sun energy at ground depends on ray path inside atmosphere. That path, made dimensionless, is the Air Mass m (or AM) given (for a Flat Earth..) as
m = 1/ cos(θ)

$$AM = \frac{1}{\cos\theta_z + 0.50572(96.07995 - \theta_z)^{-1.6364}}$$

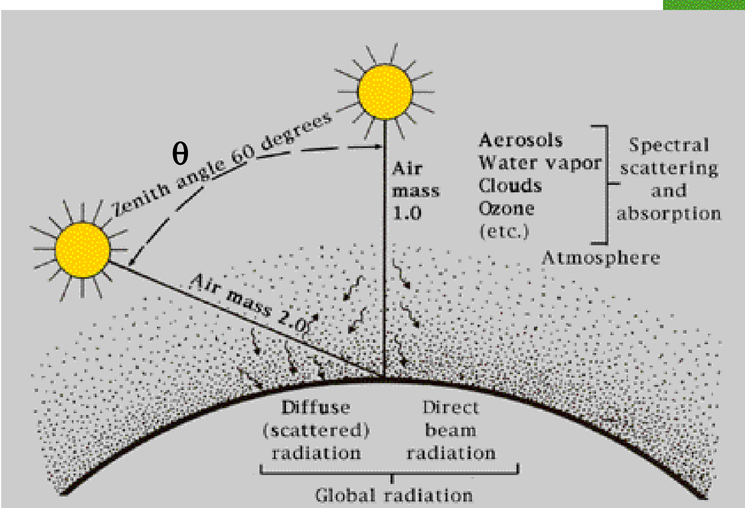

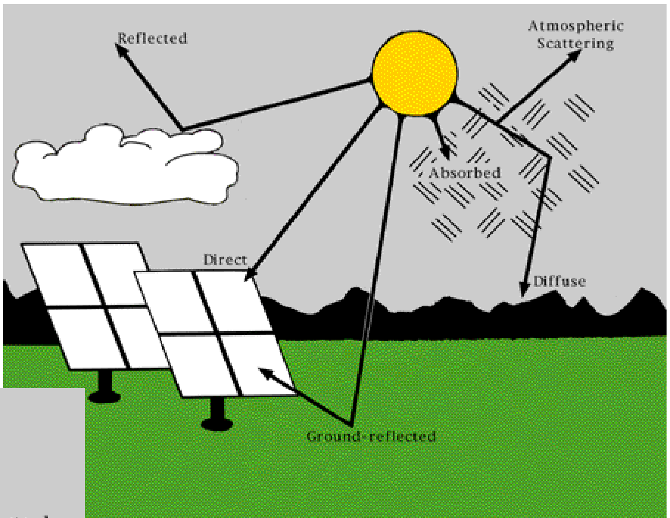

$G_{earth} = G_0\, \tau^{m}$

$G_{earth} = G_{diff} + G_{beam}$

With clear sky G_{earth} depends on air mass and atm. ave. trasmissivity τ, which in turns depends on opaque gas concentration (H_20, O_3 CO_2)

Irradiance at earth surface (II)

K_t = (<u>Clearness index</u>)

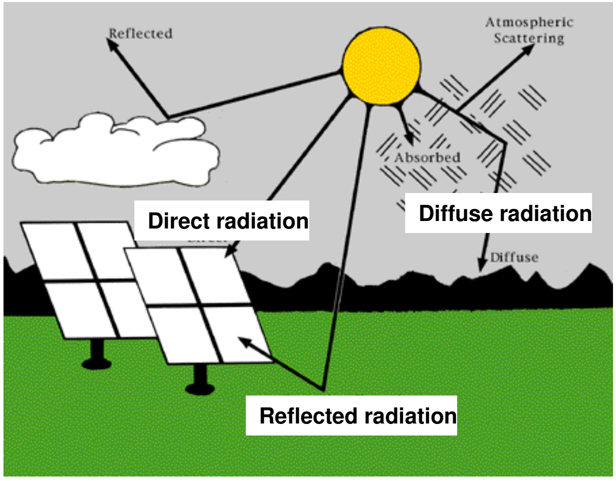

$K_t = E_H / E_{0,H}$

It is the ratio between ground Insolation divided by the ET insolation , on horizontal

It can be defined on a hourly basis, on a monthly average hourly basis or, more often as <u>monthly average daily value</u>

$\bar{K}_t = f(n / N)$ n= hours of clear sky,

N = max hours of clear sky (sr to ss)

$(\bar{K}_t)_{day} = a + b\,(n/N)$ <u>Page Formula</u>
(daily average)

$E_H = E_{H,dir} + E_{H,diff}$

$(\bar{K}_t)_d = (\bar{E}_H)_d / (\bar{E}_H)$

Correlations:
Herbs (diffusa, 1982), Iqbal (1983)
Liu & Jordan (diffusa, 1960)

Irradiance at earth surface (II)

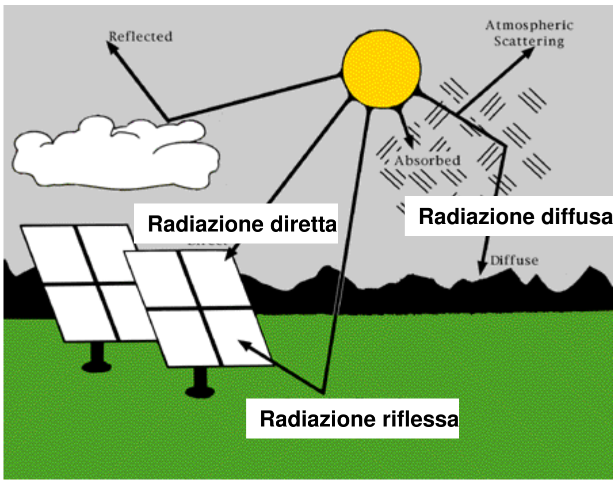

Correlations:
Herbs (diffuse, 1982), Iqbal (1983),
Liu & Jordan (diffusa, 1960)

$(\bar{K}_t)_d = (\bar{E}_H)_d / (\bar{E}_H)$

$$K_{diff} = 1.39 - 4.027\,K_t + 5.331\,K_t^2 - 3.108\,K_t^3$$

Liu e Jordan (anno 1960)

$$K_{diff} = 0.881 - 0.972\,K_t$$

Norma UNI 8477 (anno 1985)

Insolation in Italy, yearly values

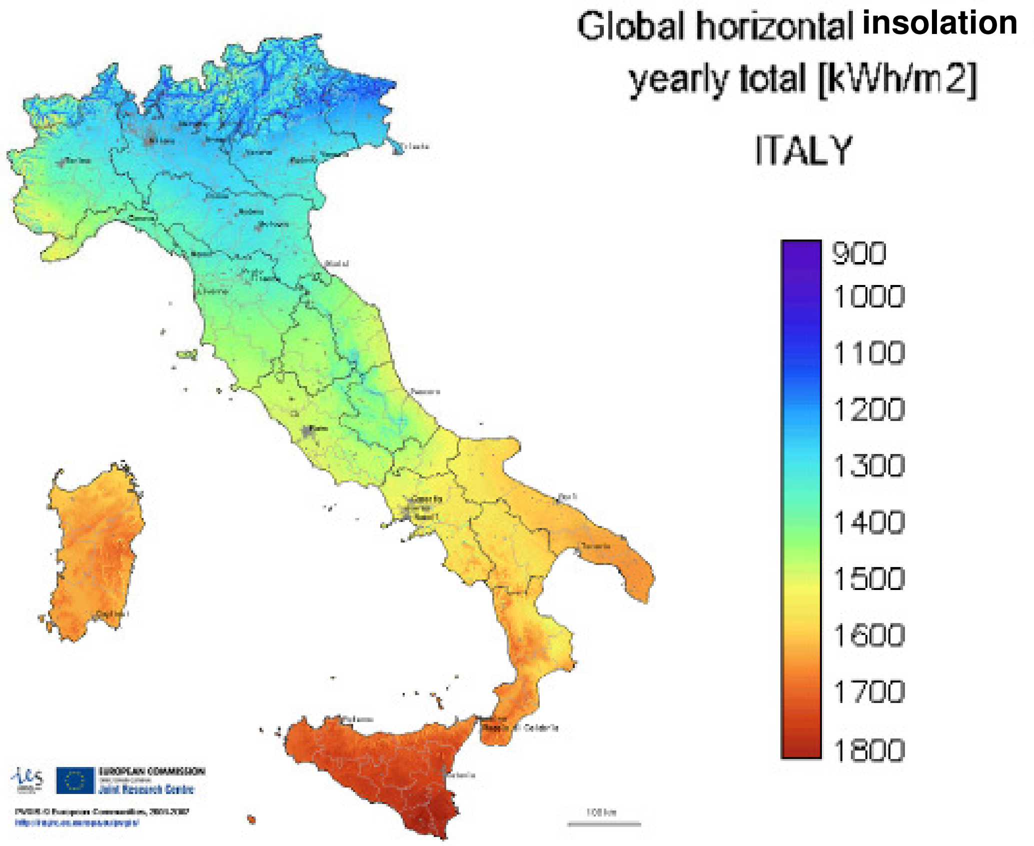

Direct and diffuse Insolation

Clear sky, Genoa, june

Insolation

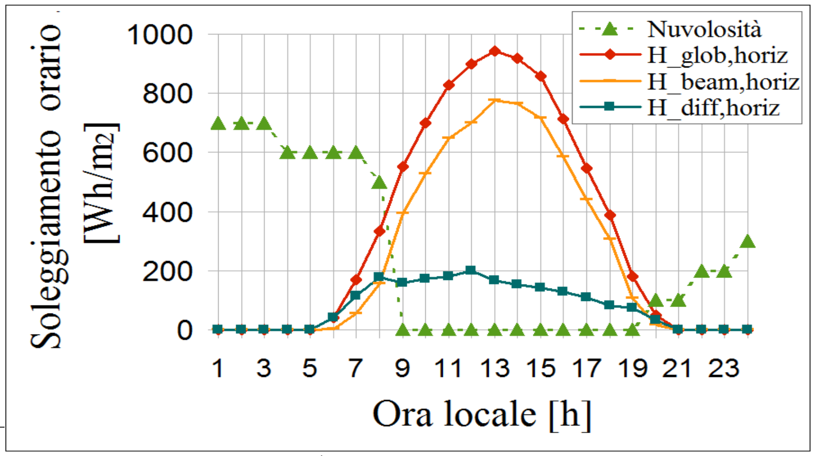

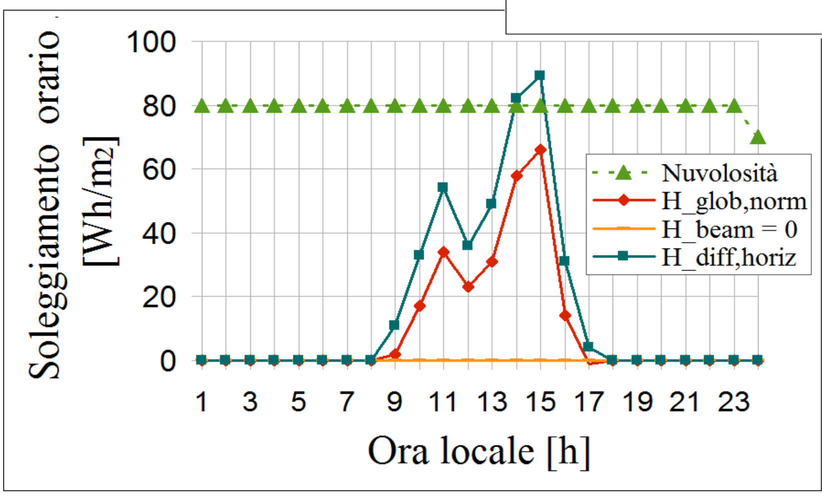

Overcast sky, November, Genoa, Italy

Irradiance at earth surface (III)

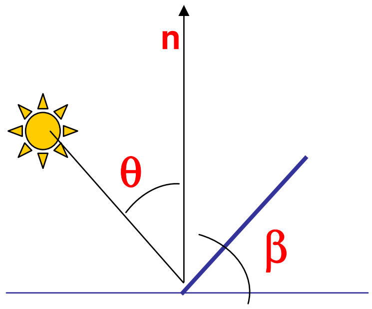

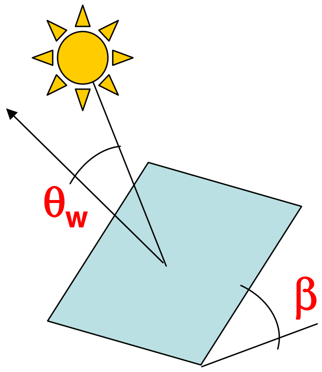

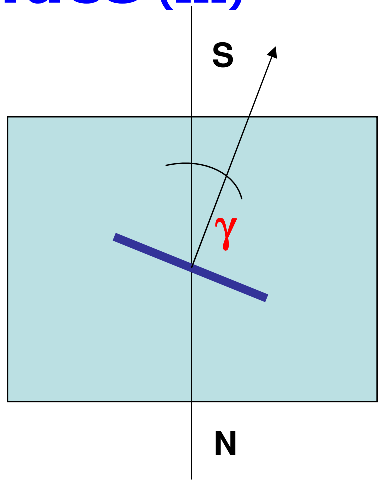

β = Tilt angle

θ_w = Surface zenith angle

γ = surface azimuth angle

R_b <u>beam radiation tilt factor</u>

Isotropic sky ....!

$E_T = E_{T, dir} + E_{T, diff} + E_{T, rifl} = E_H(1 - E_{H,diff} / E_H)R_b + E_{H, diff}(1+\cos\beta)/2 + E_H \rho(1-\cos\beta)/2$

(su <u>base giornaliera</u> media mensile – <u>Monthly average daily</u> insolation)

$E_{H,diff} / E_H = 1.39 - 4.027K_t + 5.331K_t^2 - 3.108K_t^3$ (Liu and Jordan, 1960)

$E_{H,diff} / E_H = 1.391 - 3.56K_t + 4.189K_t^2 - 2.137K_t^3$ (ω_s<81.2°, Herbs, 1982)

$E_{H,diff} / E_H = 0.881 - 0.972K_t$ (UNI 8477, 1985)

$R_b = E_{T, dir} / E_{H, dir} = R_b(\phi, \gamma, \omega_s, \omega_{s, app}, \beta, \gamma) = \cos(\theta_w)/\cos(\theta)$ either on inst. or ave basis

Irradiance at earth surface (IIIb)

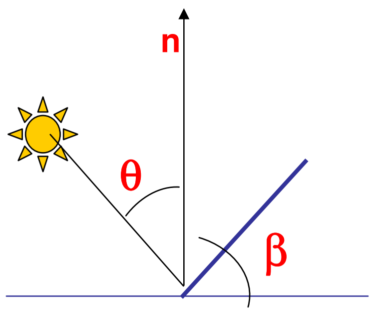

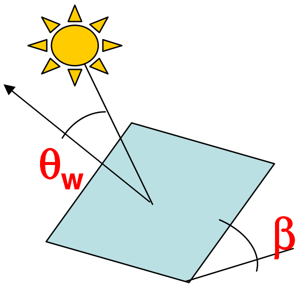

β = Tilt angle

θ_w = Surface zenith angle

γ = surface azimuth angle

R_b <u>beam radiation tilt factor</u>

It represents the <u>beam</u> energy gain (or loss) by the tilted surface with respect to the horizontal surface.

For tilted surfaces $R_{b,ave}$ is typically higher than unity in winter (sun is low at the horizon, and tilted, south facing, surface “sees” it better) but can be lower than the unity in summer, where the sun is more “perpendicular” to the horizontal surface

$R_b = E_{T, dir} / E_{H, dir} = R_b(\phi, \gamma, \omega_s, \omega_{s, app}, \beta, \gamma)$

$= \cos(\theta_w)/\cos(\theta)$ either on instantaneous or daily average basis

Irradiance on vertical surfaces

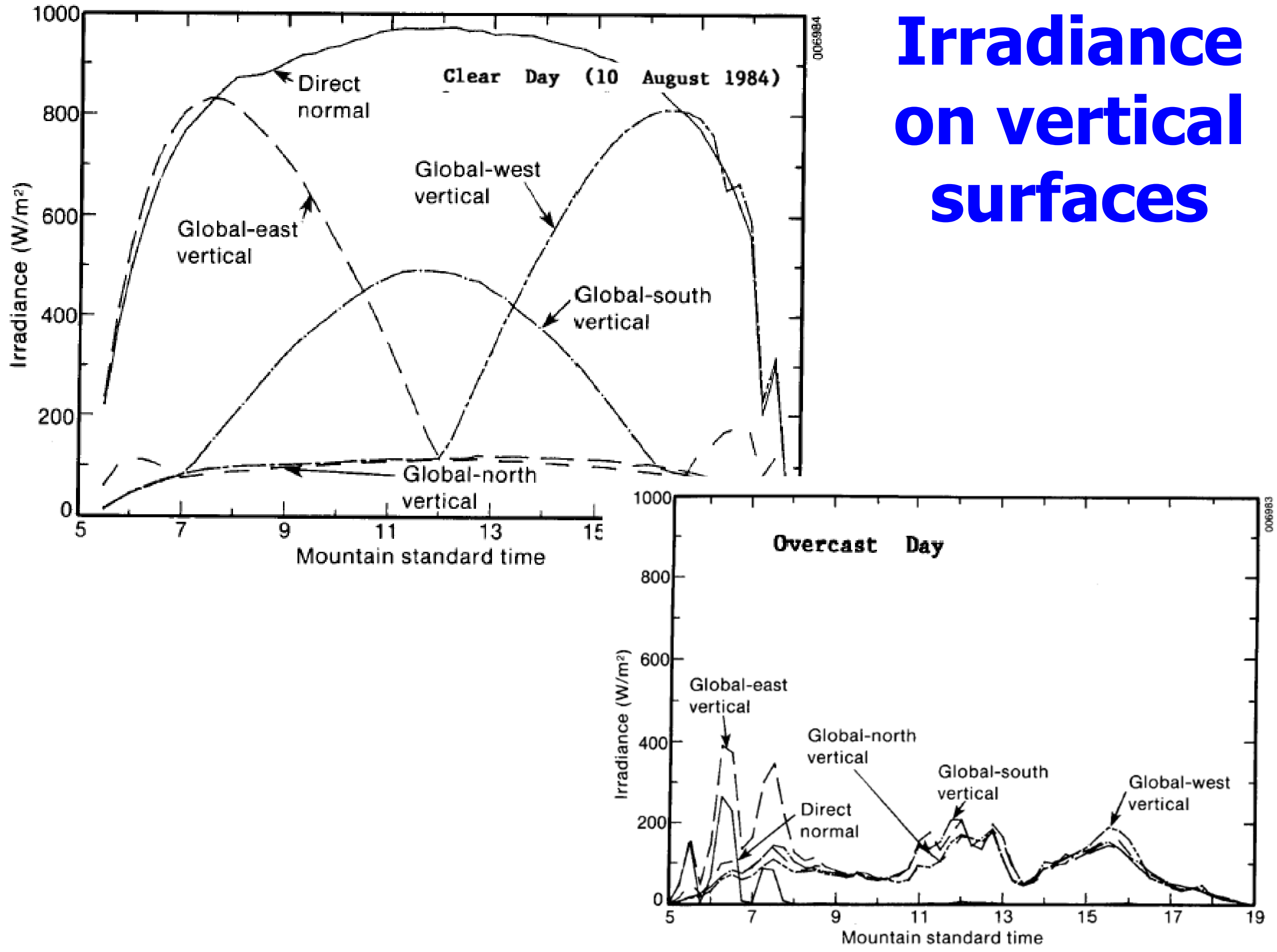

Sky diffuse radiation

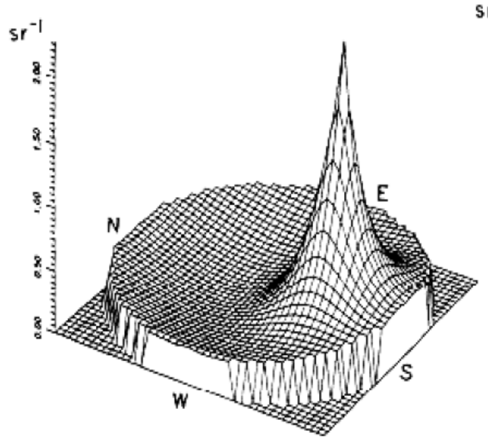

Radianza a cielo sereno (k_t = 0,75 e k_d = 0,05)

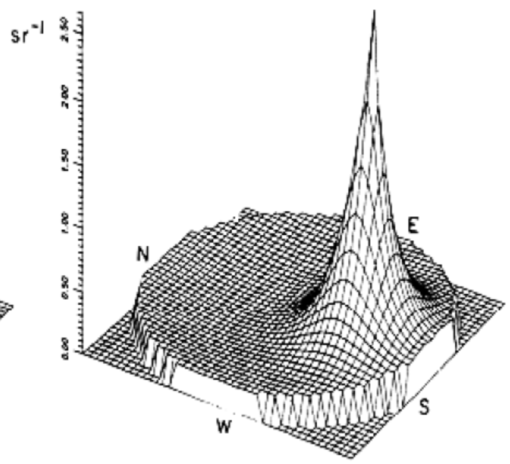

Radianza a cielo parzialmente coperto (k_t = 0,55 e k_d = 0,55)

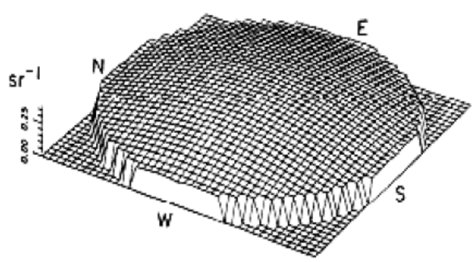

Radianza a cielo coperto (k_t = 0,05 e k_d = 0,95)

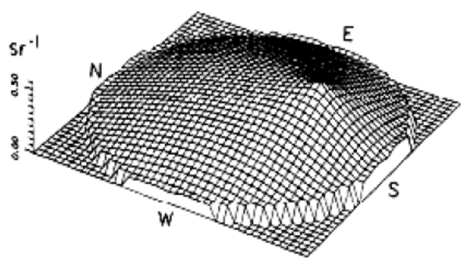

Radianza a cielo quasi coperto (k_t = 0,35 e k_d = 0,95)

Diffuse radiation

$$H_{d,t}=H_{d,h}\cdot(1-F_1)F_d+H_{d,h}\cdot F_1\frac{a}{b}+H_{d,h}\cdot F_2\sin(\beta)$$

Isotropic **Circumsolar** **Horizon anisotropy**

$H_{d,h}$ = **Diffuse insolation on horizontal**

F_d = isotropic diffuse view factor

F_1 = **Circumsolar anisotropy coefficient**

F_2 = **Horizon anisotropy coefficient**

a = $\max(0,\cos\theta_w)$

b = $\max(0.087,\cos\theta)$

(*) Perez et al. (1986, 1987, 1988 e 1990a)

Diffuse radiation (II)

Circumsolar
circumsolare

Isotropic
diffusa isotropa

Horizon anisotropy
orizzonte

$$G_t = (G_B + G_D A)R_B + G_D(1-A)\left[\frac{1-\cos(\beta)}{2}\right]\left[1+\sqrt{\frac{G_B}{G_B+G_D}}\sin^3\left(\frac{\beta}{2}\right)\right] + (G_B+G_D)\rho\left[\frac{1-\cos(\beta)}{2}\right]$$

$$A = \frac{G_{Bn}}{G_{on}}$$

Subscripts:

B=beam

D=Diffuse

t= tilted

on=Extraterrestrial, normal

Bn= Beam, on tilted normal to sun

(Reindl et al., 1990a,b)

Irradiance at earth surface (IV)

Rb = Rb (ϕ, γ, ω, β, γ=0) = cos (θ_w)/cos (θ) **Instantaneous value**

$$R_B = \frac{\sin(\varphi - \beta)\sin(\delta) + \cos(\varphi - \beta)\cos(\delta)\cos(\omega)}{\sin(\varphi)\sin(\delta) + \cos(\varphi)\cos(\delta)\cos(\omega)}$$

Example

Calculate beam radiation factor and beam irradiance for surface located at 35° North latitude, tilted 45° when solar time is 2.00pm the 10th of march.

Beam irradiance on horizontal: 900W/m²

Irradiance at earth surface (V)

Diffuse Insolation $E_{H,diff}$ and beam Insolation $E_{H, dir}$ [MJ/m²/day] In Italian locations

Prospetto VIII — Irradiazione solare giornaliera media mensile diretta $\overline{H}_{bh}$ e diffusa $\overline{H}_{dh}$ sul piano orizzontale

N°	GENNAIO		FEBBRAIO		MARZO		APRILE		MAGGIO		GIUGNO		LUGLIO		AGOSTO		SETTEMBRE		OTTOBRE	
	$\overline{H}_{dh}$ MJ/m²	$\overline{H}_{bh}$ MJ/m²	$\overline{H}_{dh}$ MJ/m²	$\overline{H}_{bh}$ MJ/m²	$\overline{H}_{dh}$ MJ/m²	$\overline{H}_{bh}$ MJ/m²	$\overline{H}_{dh}$ MJ/m²	$\overline{H}_{bh}$ MJ/m²	$\overline{H}_{dh}$ MJ/m²	$\overline{H}_{bh}$ MJ/m²	$\overline{H}_{dh}$ MJ/m²	$\overline{H}_{bh}$ MJ/m²	$\overline{H}_{dh}$ MJ/m²	$\overline{H}_{bh}$ MJ/m²	$\overline{H}_{dh}$ MJ/m²	$\overline{H}_{bh}$ MJ/m²	$\overline{H}_{dh}$ MJ/m²	$\overline{H}_{bh}$ MJ/m²	$\overline{H}_{dh}$ MJ/m²	$\overline{H}_{bh}$ MJ/m²
1	3,4	5,4	4,2	8,3	5,3	11,6	6,2	16,0	6,3	20,6	6,0	23,5	5,4	24,2	4,8	22,2	4,9	16,0	4,3	10,3
2	2,4	[illegible]	3,5	4,0	5,1	6,5	6,7	9,1	7,9	10,6	8,4	12,1	7,7	14,9	7,0	11,0	5,6	7,8	4,0	4,5
3	2,5	[illegible]	[illegible]	3,9	5,2	6,9	6,6	11,7	7,4	15,7	7,9	16,2	[illegible]	[illegible]	6,4	15,6	5,4	10,6	4,1	6,4
4	2,4	[illegible]	[illegible]	4,6	4,9	7,2	6,7	9,0	7,9	10,3	8,4	11,5	[illegible]	[illegible]	7,1	10,4	5,6	7,6	3,9	4,8
5	2,8	[illegible]	[illegible]	[illegible]	5,3	7,3	6,8	10,4	7,8	13,0	8,0	15,7	[illegible]	[illegible]	[illegible]	16,0	5,5	10,8	4,2	6,2
6	2,8	3,2	[illegible]	[illegible]	[illegible]	6,7	6,9	7,9	8,0	11,3	8,4	12,7	7,7	[illegible]	[illegible]	[illegible]	5,7	10,0	4,2	6,4
7	2,6	2,5	[illegible]	[illegible]	[illegible]	6,0	6,9	8,2	8,0	11,2	8,2	14,0	7,7	[illegible]	[illegible]	[illegible]	5,6	9,3	4,2	5,2
8	2,5	2,7	3,5	[illegible]	[illegible]	[illegible]	6,7	9,6	7,9	10,7	8,4	12,2	7,8	14,7	[illegible]	[illegible]	[illegible]	7,5	4,0	5,1
9	2,9	2,5	4,0	[illegible]	[illegible]	[illegible]	[illegible]	11,3	7,6	14,7	7,8	16,9	6,6	20,3	[illegible]	[illegible]	[illegible]	[illegible]	4,3	7,7
10	3,0	3,6	3,9	6,2	[illegible]	[illegible]	6,3	14,3	6,8	18,5	6,7	21,3	5,9	22,7	5,4	[illegible]	[illegible]	14,0	4,0	9,2
11	2,3	1,9	3,4	3,5	5,0	[illegible]	6,7	8,9	7,9	11,2	8,4	12,2	7,8	14,6	6,9	11,9	[illegible]	8,5	3,9	5,2
12	2,3	2,0	3,4	4,1	4,9	[illegible]	6,7	8,6	7,9	11,4	8,4	12,1	7,9	14,0	7,0	10,8	[illegible]	8,4	3,8	5,3
13	2,9	2,8	4,0	4,7	5,5	7,4	6,9	10,3	7,8	13,1	7,8	16,8	6,8	19,6	6,3	16,6	5,7	10,7	4,3	6,8
14	2,5	2,0	3,6	4,3	5,1	7,0	6,6	10,7	7,7	13,3	8,0	15,6	7,1	18,5	6,6	14,4	5,4	10,0	4,0	5,9
29	3,3	5,6	4,2	7,7	5,5	10,6	6,5	14,6	6,6	16,9	[illegible]	[illegible]	[illegible]	[illegible]	[illegible]	[illegible]	[illegible]	[illegible]	[illegible]	[illegible]
30	2,5	2,1	3,6	4,1	5,2	5,7	6,7	10,7	7,7	13,4	8,2	14,2	7,5	16,4	7,0	12,2	5,4	10,2	3,9	6,8
31	2,9	3,5	3,9	5,8	5,3	8,6	6,5	13,0	7,3	16,5	7,5	18,2	6,8	19,8	6,2	17,0	5,3	12,5	4,1	8,4
32	2,6	2,7	3,7	4,5	5,2	7,0	6,7	10,7	7,6	14,3	7,9	16,2	7,0	18,6	6,5	15,2	5,3	11,0	4,0	6,9
33	2,5	2,3	3,6	4,3	5,1	7,5	6,6	11,1	7,5	14,7	7,7	17,6	6,7	19,9	6,3	15,9	5,2	11,4	4,0	6,3
34	2,9	3,6	3,9	5,3	5,3	8,5	6,7	10,7	7,7	13,2	7,6	17,0	6,9	19,0	6,4	15,9	5,4	11,8	4,2	7,4
35	2,5	2,8	3,6	4,6	5,1	7,4	6,7	10,2	7,8	12,8	8,2	14,5	7,4	17,4	6,8	13,7	5,5	9,9	4,0	6,6

N= 35 → Genova

Insolation measurements (I)

The Campbell-Stokes Pattern Sunshine Recorder employs a glass sphere to focus the sun's rays to an intense spot, which will char a mark on a curved card mounted concentrically with the sphere. As the earth rotates, the position of the spot moves across the card. When the sun is obscured, the trace is interrupted. At the end of the day the total length of the trace, less gaps, is proportional to the duration of sunshine

Different cards are used for different seasons. Each card is marked with hourly
Intervals

Fonte: wittich & visser

.

Fonte: wittich & visser

Insolation measurements (II)

The Eppley Precision Spectral Pyranometer (PSP) is a World Meteorological Organization First Class Radiometer, designed for the measurement of total solar radiation (the sum of direct and diffuse). It comprises a rectangular multi-junction wire-wound Eppley thermopile glued to the back of the sensor disk. This disk is coated with Parson's black lacquer (for non-wavelength selective absorption). The dome consists of a pair of precision ground and polished hemispheres of Schott optical glass. Both hemispheres are made of clear WG295 glass which is uniformly transparent to energy between 0.285 to 2.8µm

Eppley Normal Incident Pyrheliometer (NIP)

The Eppley Normal Incidence Pyrheliometer (NIP) is a World Meteorological Organization First Class Pyrheliometer designed for the measurement of solar radiation at normal incidence. The NIP incorporates a wire-wound thermopile at the base of a tube. The aperature subtends an angle of 5.725°. The inside of this brass tube is blackened and suitably diaphragmed. The tube is filled with dry air at atmospheric pressure and sealed at the viewing end by an insert carrying a 1 mm thick, Infrasil II window. Two flanges, one at each end of the tube, are provided with a sighting arrangement for aiming the pyrheliometer directly at the sun.The pyrheliometer is mounted on a power-driven equatorial mount for continuous readings. See Solar Trackers.

Fonte: University of Oregon, http://solardat.uoregon.edu/

Insolation measurements (III)

Schenk Star pyranometer

The Schenk Star pyranometer is a black and white star type pyranometer that has six black and six white segments. The temperature difference between the black and white painted sectors is proportional to the incident solar radiation. Because the measurement is a temperature difference, the measurement should not be affected as much by ambient temperature.

Fonte: University of Oregon

Ascension Technology's Rotating Shadow Band Pyranometer (RSP) uses a solar cell pyranometer (manufactured by LI-COR to measure global and diffuse irradiance and calculates direct normal beam irradiance. The RSP has a shadow band that rotates once a minute to block the sun from directly shining on the pyranometer. The pyranometer is measuring global irradiance before and after the shadow band starts its rotation to block the sun. The diffuse value is the minimum value that is obtained when the band sweeps in front of the sun. Direct irradiance on a horizontal surface is then calculated by subtracting the diffuse from the global irradiance. The direct normal beam irradiance is then obtained by projecting the direct horizontal irradiance onto the normal in the direction of the angle of incidence

Renewable Energies
Energy from the sun, Solar collectors

Solar collectors, low temperature

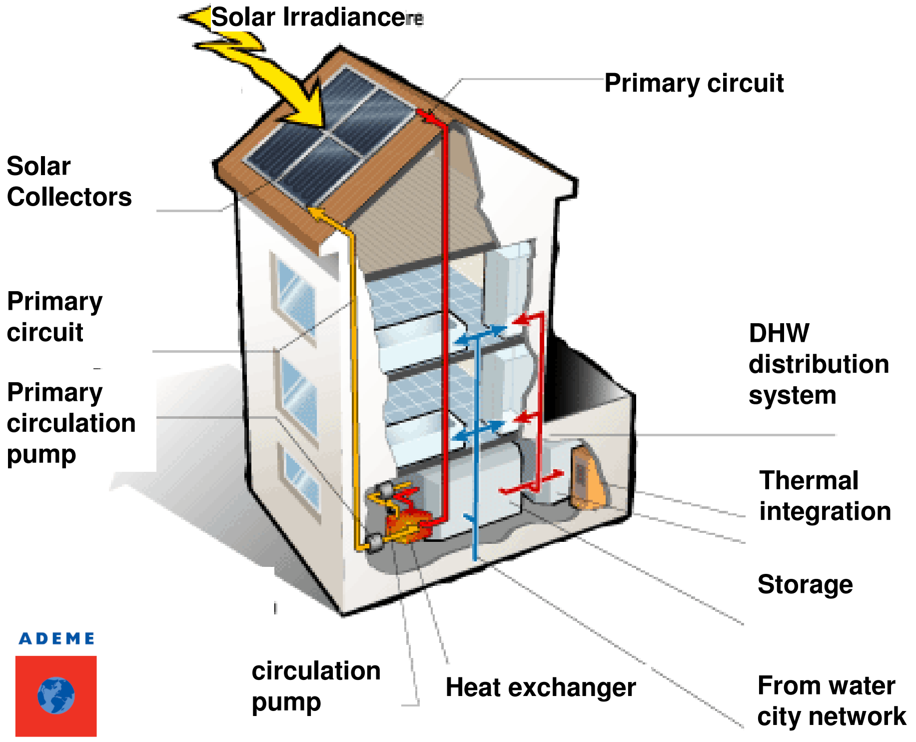

Solar collectors, fundamentals

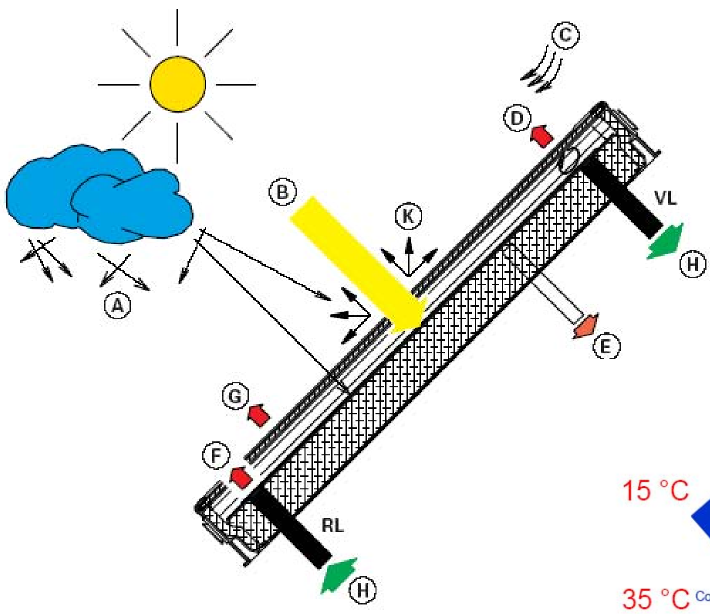

A) Diffuse radiation
B) Beam radiation
C) Convection due to wind
D) Thermal losses to the environment (glass side)
E) Thermal losses to the environment (back side)
F) Radiation from absorber
G) Radiation from glass cover
H) Heat carrier fluid
K) Reflections

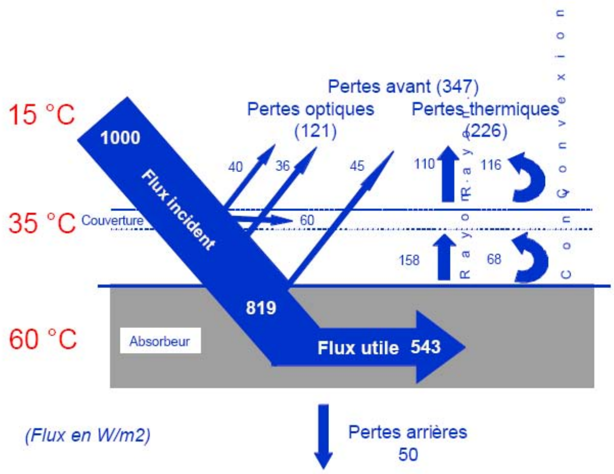

Fundamentals (II)

Requirements for an efficient thermal collector
1) High transmissivity of glass

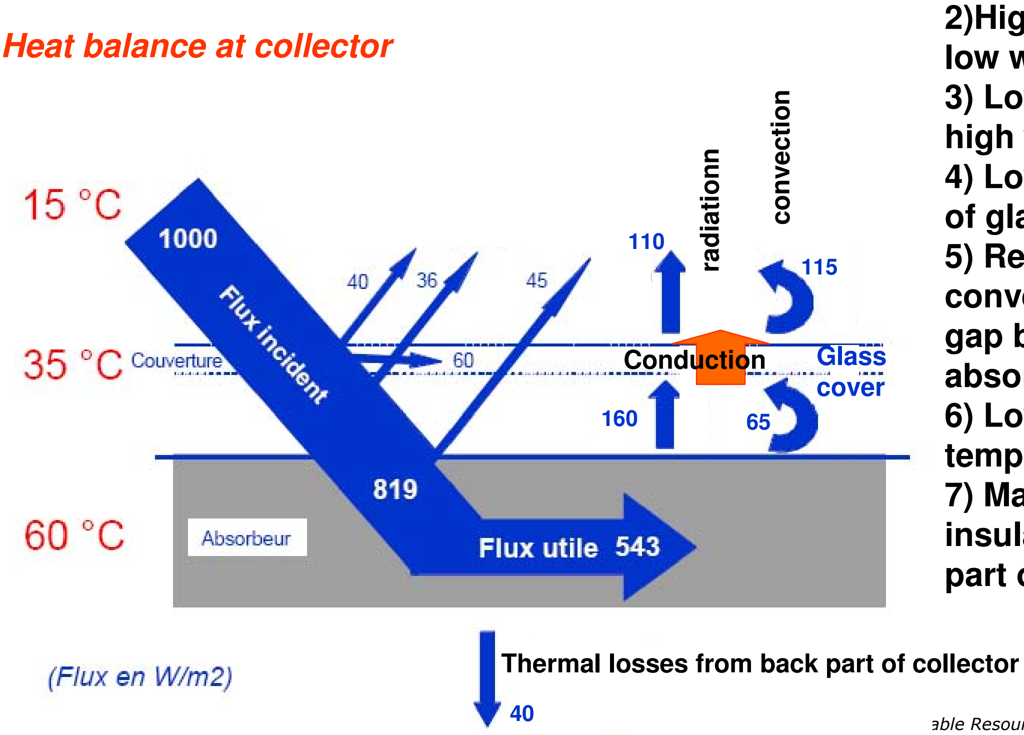

2)High absorptivity at low wavelengths
3) Low emissivity at high wavelength
4) Low conductance of glass cover
5) Reduced convection in the air gap between absorber and glass
6) Low operating temperatures
7) Maximum insulation in the back part of collector

Historical notes (I)

ATTESTATO di privativa industriale (13 ottobre 1886 - Vol. 40, N. 412), per anni tre, a datar MF1 l 30 settembre 1886, rilasciato al signor Battaglia Ales per un trovato che ha pe *multiplo solare.*

TAVOLA CCX

Il *collettore multiplo solare,* c l'invenzione, ha per iscopo di rac che cadono su d'una determinata ficie terrestre a qualunque latitu in un fascio di forma speciale in supeficie limitata, onde ottenere ed un numero di calorie capace di

TRANSLATION:

Year 1886

Certificate of industrial copyright, valid 3 years

released to Mr Battaglia Alessandro, born in Genova, Italy, for his invenction:

"Solar multiple collector"

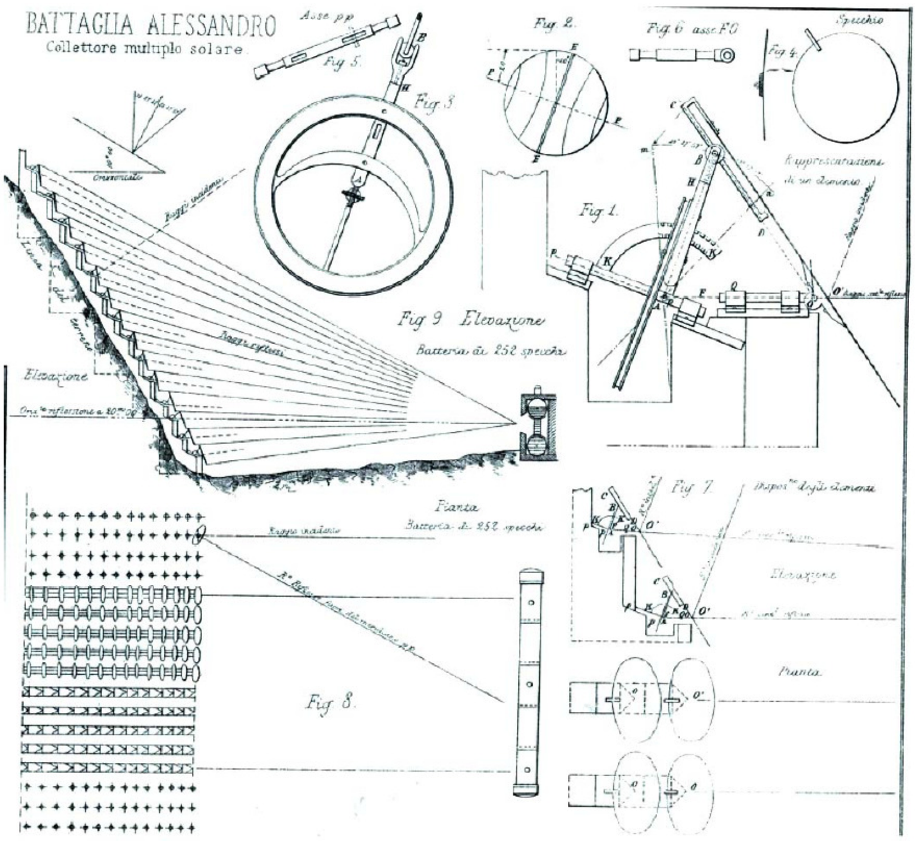

MF1 TRANSLATION:

Year 1886

Certificate of industrial copyright, valid 3 years

released to Mr Battaglia Alessandro, born in Genova, Italy, for his invenction:

"Solar multiple collector"

Marco Fossa, 07/06/2011

Historical notes (II)

Giovanni Francia, 1911-1980, Professor at University of Genova

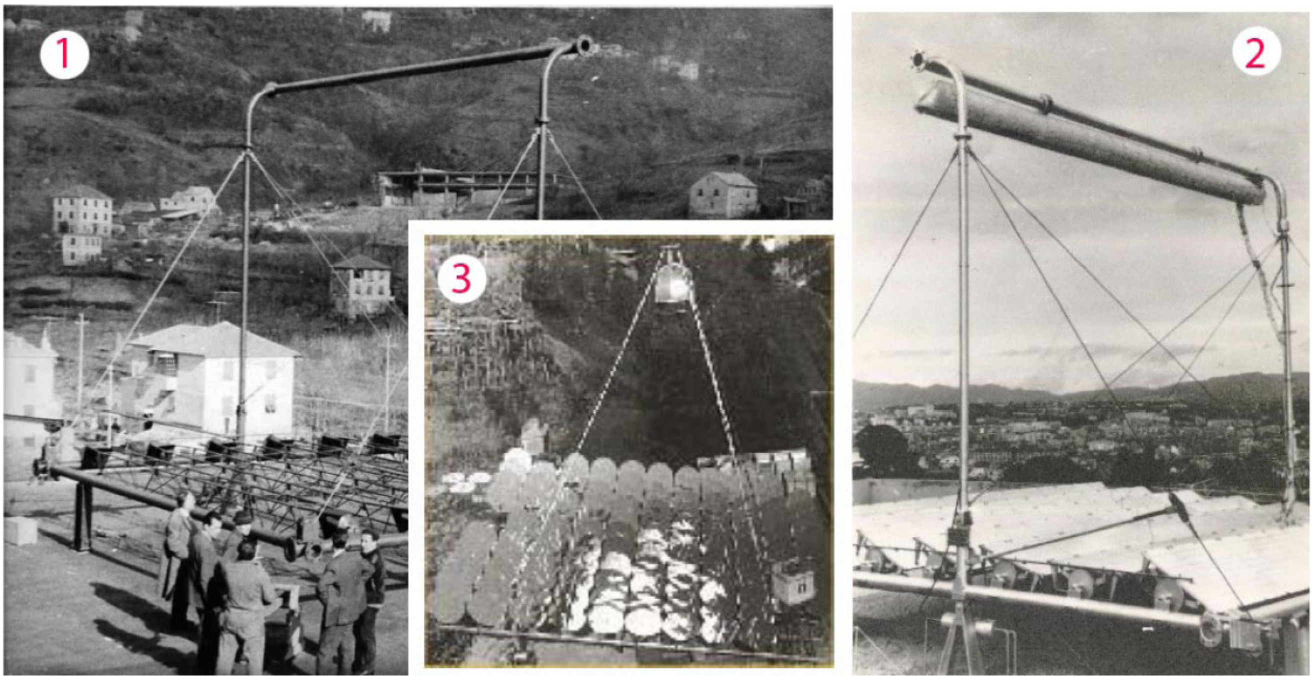

Fonte: Cabibbo-Gses

1, 2 Prototype of linear Fresnel concentrator, 1964

3 Prototype of tower concentrator (Sant'Ilario, Genova, 1965)

Historical notes (III)

Giovanni Francia, 1911-

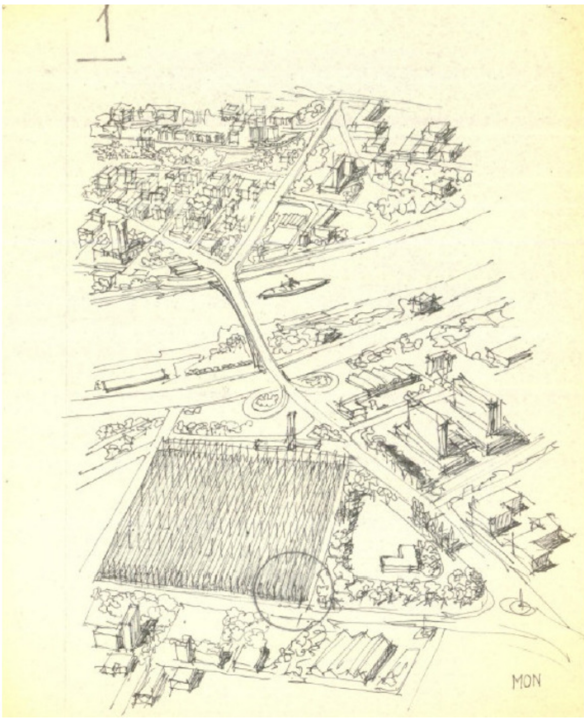

Fresnel concentrators for a Solar City (1964)

Fonte: Cabibbo-Gses

Radiant properties(I)

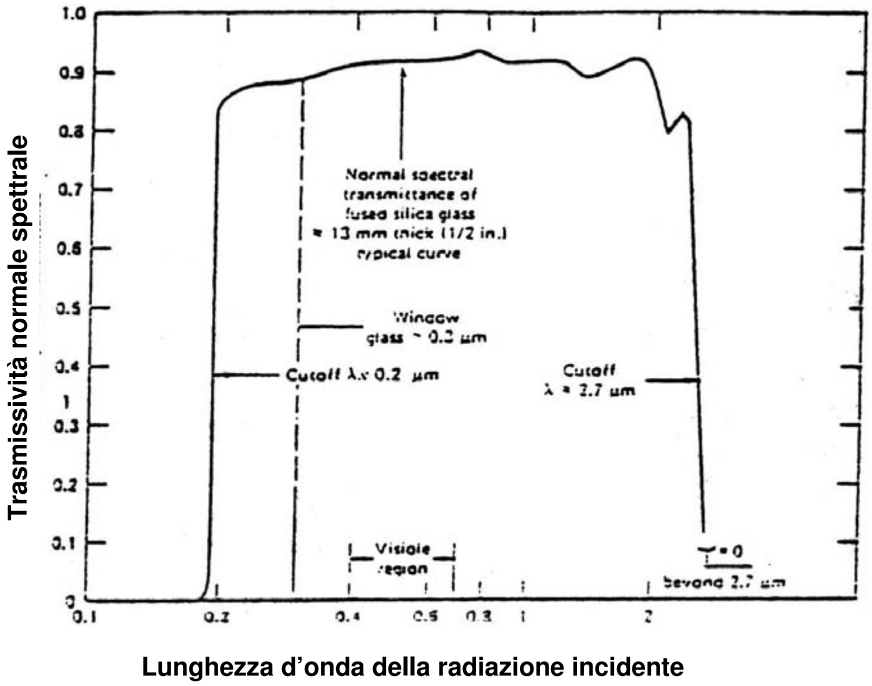

Transmissivity of a single (standard) glass depends on radiation wavelength.

Standard glass is "transparent" in the range 0.2 to 2.7μm

Radiant properties(II)

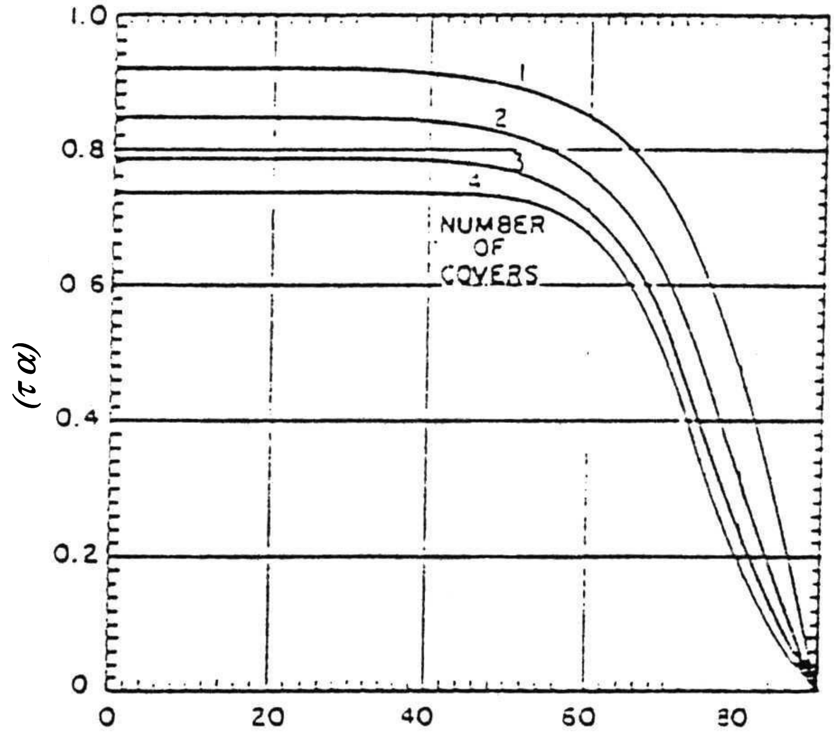

Angolo della radiazione incidente

Transmissivity depends on incidence angle of sun rays

Up to some 60° transmissivity values are close to normal incidence ones

<u>If the glass covers are more than one, transmissivity decreases even more, even if convection heat losses are reduced</u>

New technologies have been developed for increasing τ as high inc. angles (chem, etching, special coatings)

Radiant properties (III)

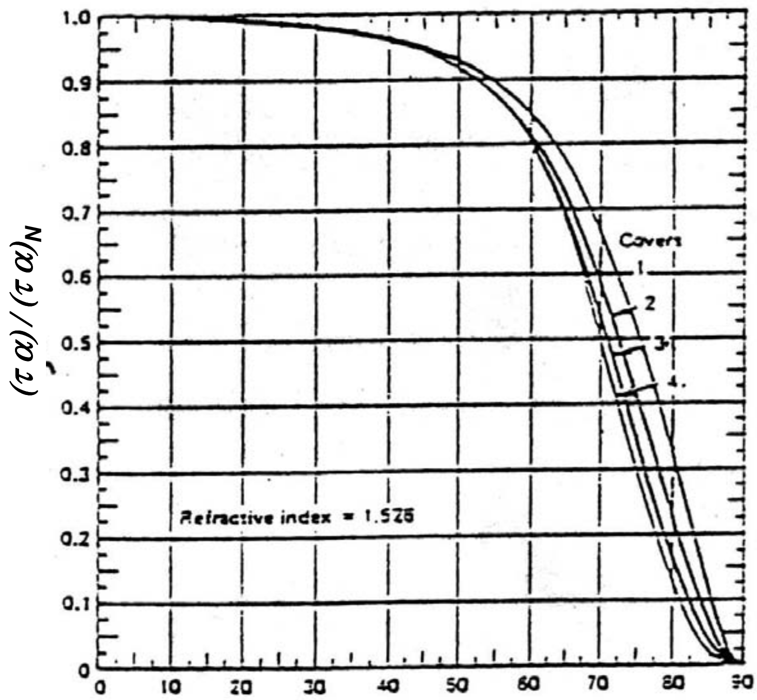

Angolo di incidenza dei raggi solari al collettore, θ_w

Multiple covers affect the transmissivity behavior with the incidence angle (zenith angle of surface) different from normal

The y ratio is also referred as INCIDENCE ANGLE MODIFIER, IAM

Incidence angle modifier (I)

The effects of glass transmissivity as a function of the incidence angle can be accounted for also in terms of the IAM, incidence angle modifier parameter.

IAM (K_θ) is defined flat for plate collectors as the ratio of $(\tau\alpha)_n$ at some incident angle θ_w to $(\tau\alpha)_n$ at normal incidence

For flat plate collectors IAM is well described by a linear function of the group ($1/\cos\theta_W$ -1). An example of correlation is the following, where b_0 typically is 0.10-0.12

$$K_\theta = \frac{(\tau\alpha)}{(\tau\alpha)_n} = 1 - b_o\left[\frac{1}{\cos(\theta)_W} - 1\right]$$

Collector efficiency expression will be accordingly modified as

$$\eta = F_R(\tau\alpha)_n K_\theta - c_1 \frac{(T_i - T_a)}{G_t}$$

C_1=F_R K"

Absorption and emission (I)

The perfect solar absorber should capture all the incoming solar radiation while minimizing the heat losses by long wave emission. This requires high absorbances in the near visible region and low emissivity in the medium infrared range.

Selective surfaces can accomplish this double task. In such a case some coating (metal oxides or dielectric metal compounds, Cermets) is applied onto the copper surface of the absorber

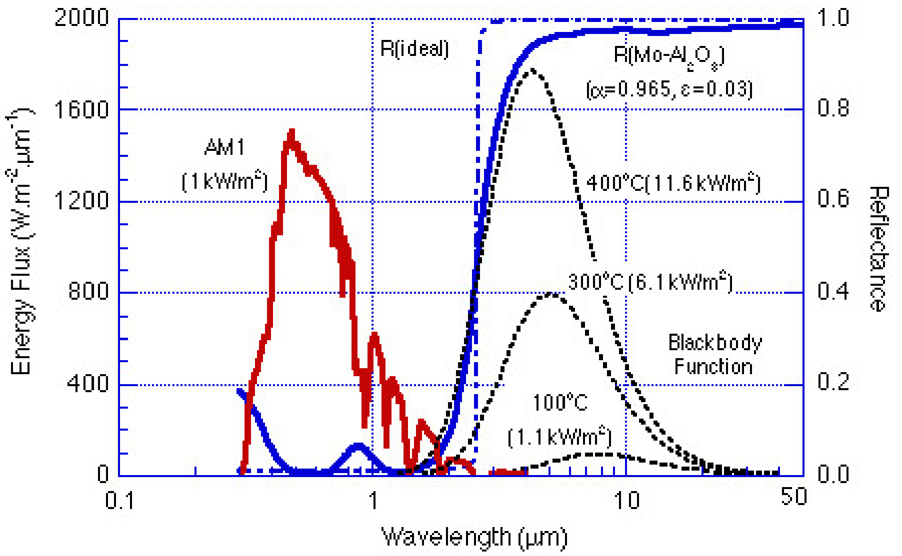

Absorption and emission (II)

DC reactively sputtered stainless steel-carbon (SS-C) coating

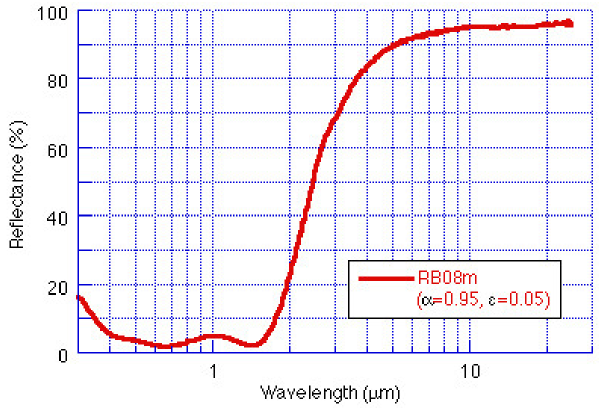

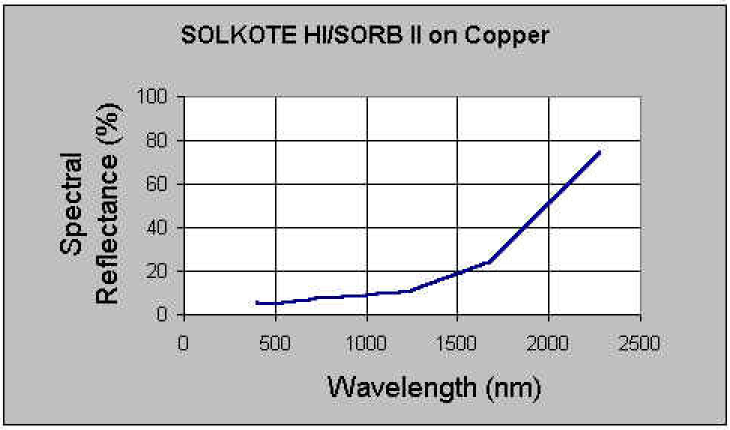

Here at the side some examples of selective radiation properties of solar coatings

When radiation losses are minimized the following task is to reduce the convetion between the absorber and the glass cover

A possible solution: a Vacuum enclosure

Collector Energy Balance

Collector Energy Balance (I)

$G''_{inc} = G''_{direct} + G''_{diff}$

K'' is the overall heat transfer coeff. with reference to Absorber surface temperature

$G''_u = G''_a - G''_{disp}$

$G''_u = G''_a - K'' (T_{p, ave} - T_a)$

$G''_a = G''_{inc} (\tau\alpha)_{ave}$

$(T_{p, ave} - T_{fluid, ave}) = G''_u / h_{fluid}$

$T_{p, ave} = G''_u / h_{fluid} + T_{fluid, ave}$

$G''_u (1 + K''/ h_{fluid}) = G''_a - K'' (T_{fluid, ave} - T_a)$

$G''_u = F'[G''_a - K'' (T_{fluid, ave} - T_a)]$

$F' = h_{fluid} / (K'' + h_{fluid})$ Efficiency factor

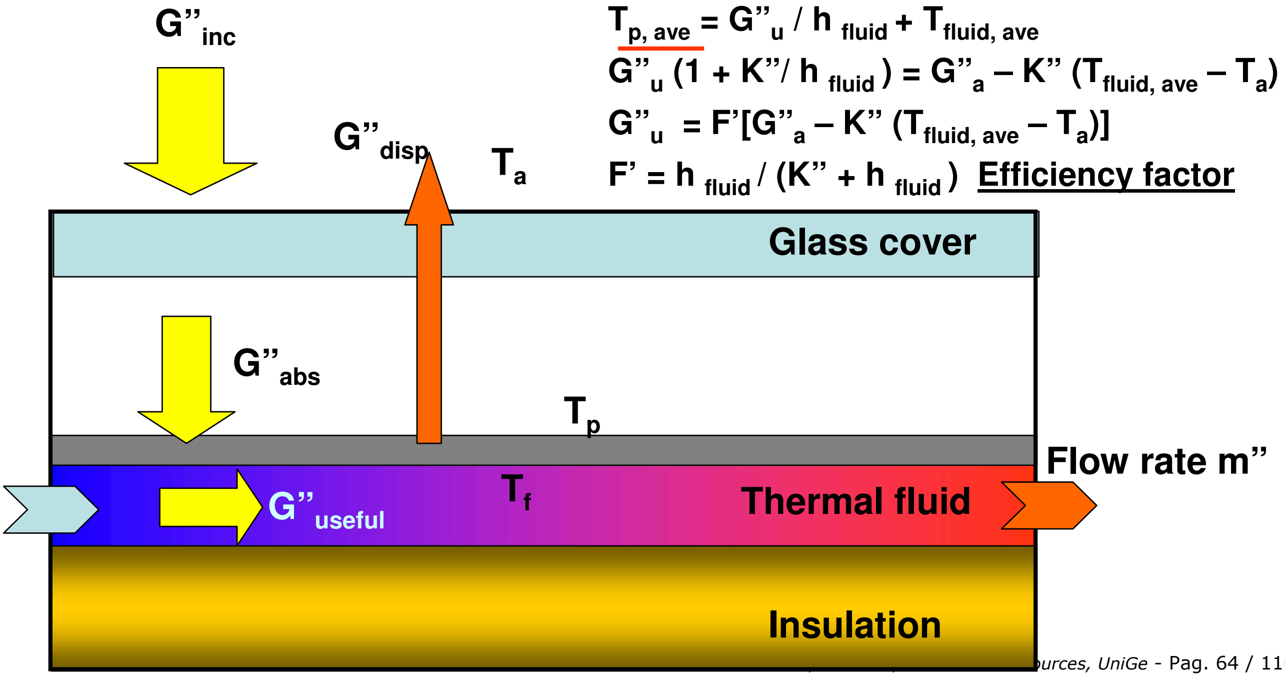

Collector Energy Balance (IIIb)

Collector heat balance can be written in terms of fluid inlet temperature

In such a case the Heat Removal Factor F_R is introduced

$G''_u = F'[G''_a - K'' (T_{fluid, ave} - T_a)]$

$G''_u = F_R[G''_a - K'' (T_{fluid, in} - T_a)]$

$$F_R / F' = (1 - \exp[-F'K''/(m''c)])(m''c)/K''/ F'$$

$F' = h\ fluid / (K'' + h\ fluid)$

$F_R = (1 - \exp[-F'K''/(m''c)])(m''c)/K''$

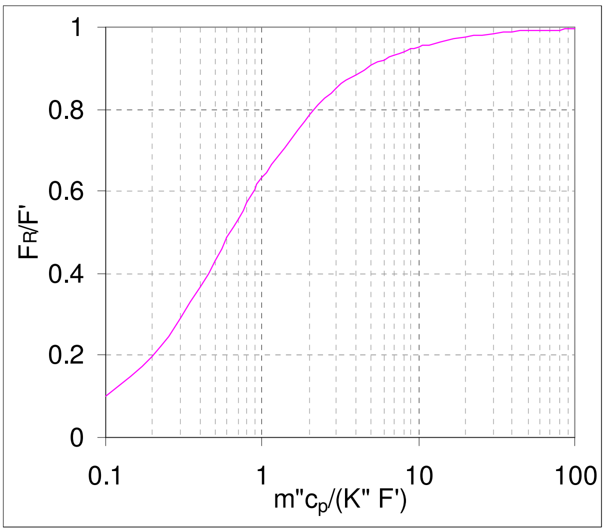

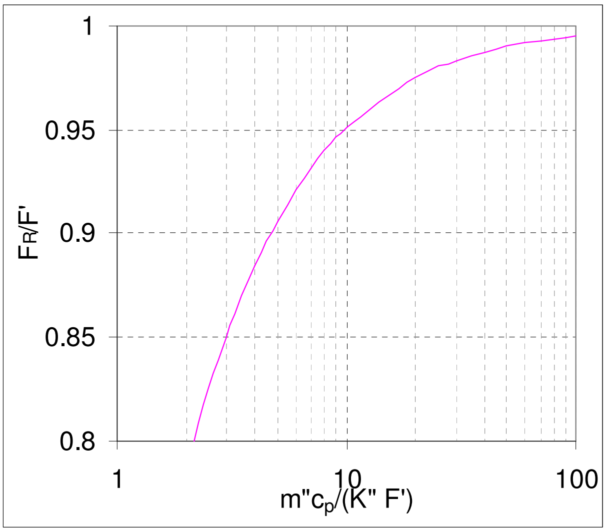

Collector Energy Balance (IV)

$G''_u = F_R[G''_a - K'' (T_{fluid, in} - T_a)]$ (Bliss equation)

$G''_a = G''_{inc} (\tau\alpha)$

$E_a = E_{inc, ave} (\tau\alpha)_{ave}$ [J/m² day] (on a daily basis, monthly ave)

Collector efficiency η is defined as: $\eta = G''_u / G''_{inc}$

$\eta = F_R [G''_a - K'' (T_{fluid, in} - T_a)] / G''_{inc}$

$\eta_{ave} = F_R [E_a - K'' (T_{fluid, in} - T_{a, ave}) \Delta\tau] / E_{inc}$ (on a daily basis, monthly ave)

$E_a = E_{inc} (\tau\alpha)_{ave}$

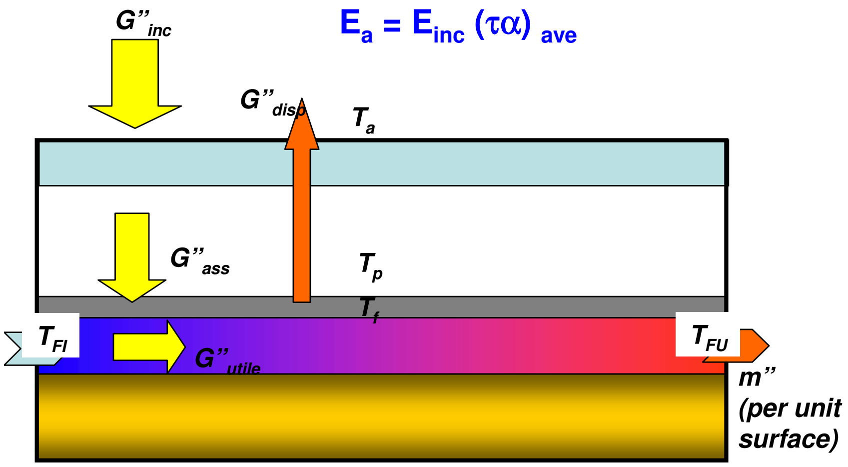

$E_{inc} = E_T$

E_T = Overall insolation on tilted surface

Collector Efficiency, two definitions

$\eta_{ave} = F_R (\tau\alpha) - F_R K'' [(T_{fluid, in} - T_a)] / G''_{inc}$

$\eta_{ave} = F' (\tau\alpha) - F_R K'' [(T_{fluid, ave} - T_a)] / G''_{inc}$

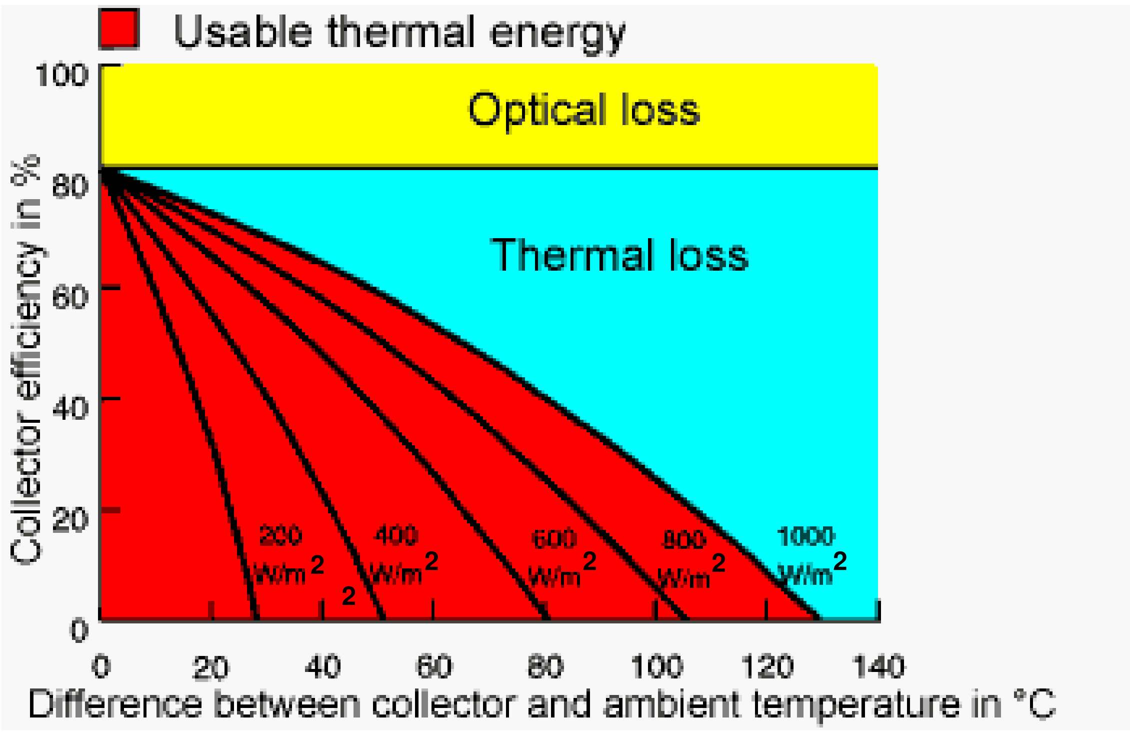

Collector Efficiency (II)

$\eta = F_R(\tau\alpha) - F_R K'' [(T_{fluid, in} - T_a)] / G''_{inc}$

$\eta = a + bx$

Notice:
1) Sometimes $F_R(\tau\alpha)$ is written as η_0
2) Sometimes $\eta = a + b_1 x + b_2 x^2$

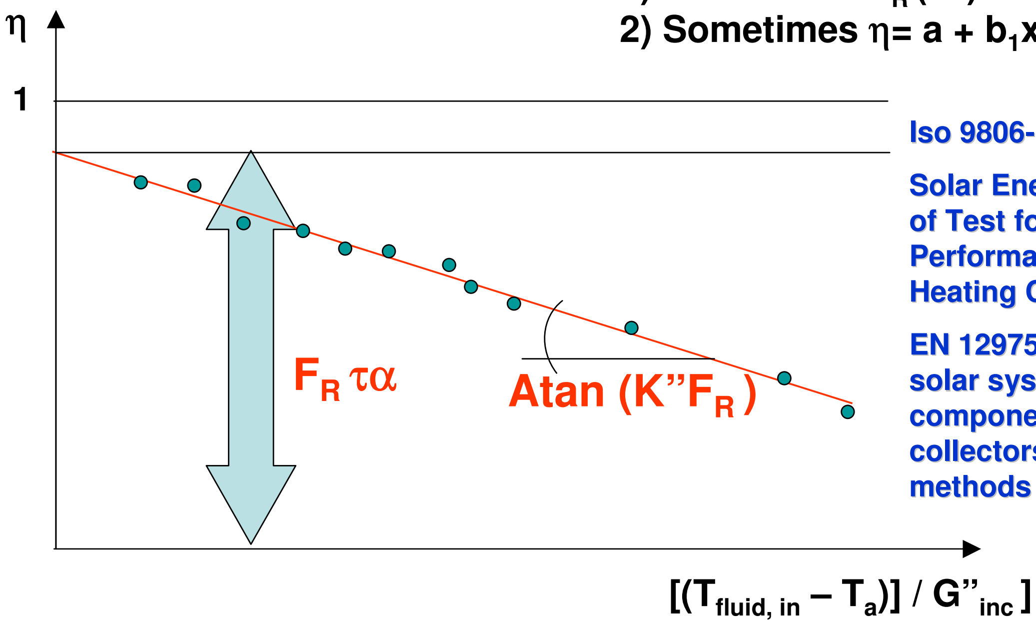

Iso 9806-1

Solar Energy – Methods of Test for the Thermal Performance of Liquid Heating Collectors

EN 12975-2:2006 Thermal solar systems and components – Solar collectors – Part 2: Test methods

Collector Efficiency Tests

ISO 9806 procedure

- Solar radiation greater than 800 W/m2.
- Wind speed between 2 and 4 m/s.
- Angle of incidence of direct radiation is within 2% of the normal incident angle.
- Fluid flow rate 0.02 kg/s-m2 (unless specified by manufacturer) and stable within1%
- Min Temperature rise at collector 1.5K
- Data points: minimum of four fluid inlet temperatures, from ambient temperature ((within 3K) to 70°C

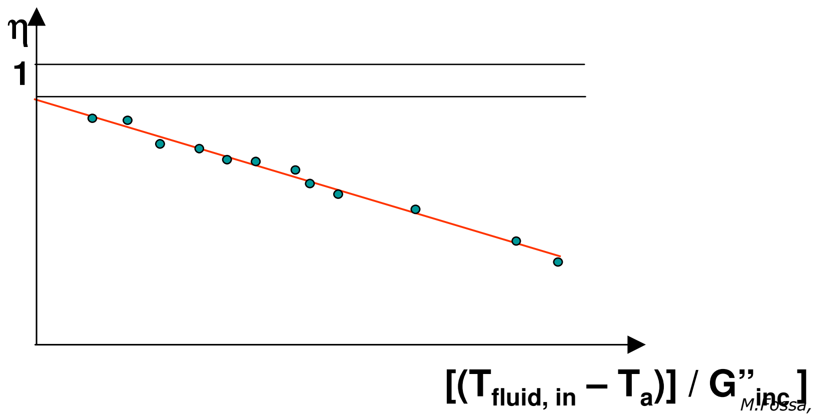

Iso 9806-1

Solar Energy – Methods of Test for the Thermal Performance of Liquid Heating Collectors

Collector Efficiency (III)

EN 12975
Indoor Test

The lamps capable of producing a mean irradiance over the collector aperture of at least 700 W/m^2. Values in the range 300 to 1000 W/m^2 can be used for special tests.
The irradiance at a point on the collector aperture shall not differ from the mean irradiance over the aperture by more than ±15 %
The spectral distribution of the simulated solar radiation shall be approximately equivalent

Solar collector types

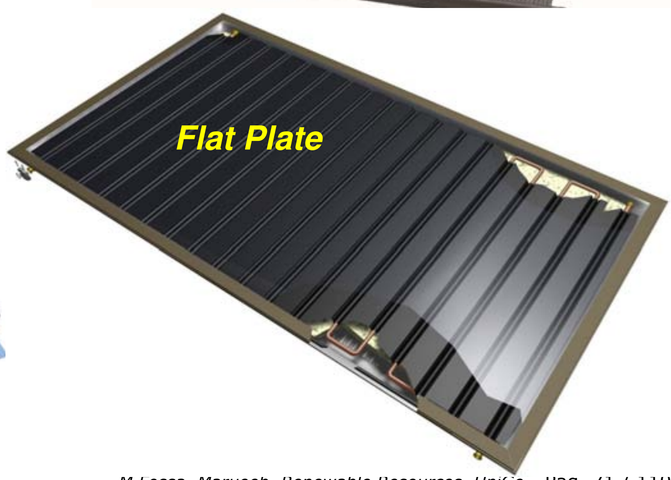

Collector Efficiency, different collectors

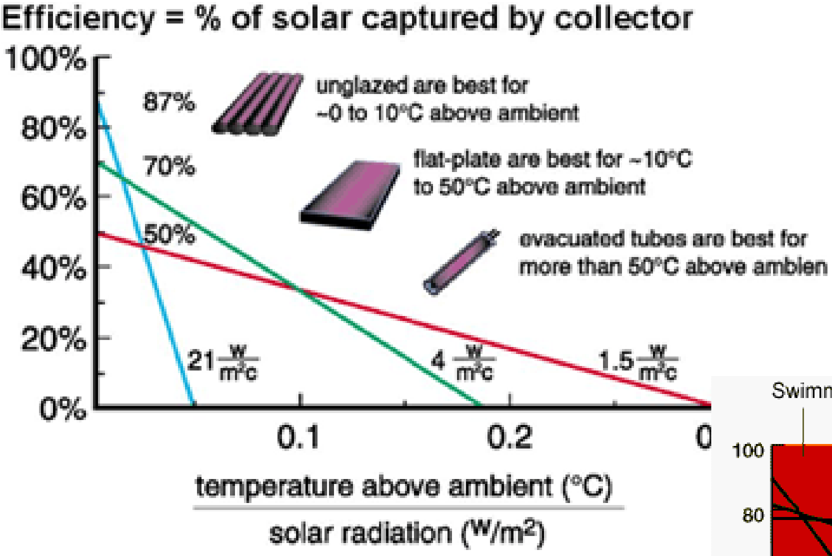

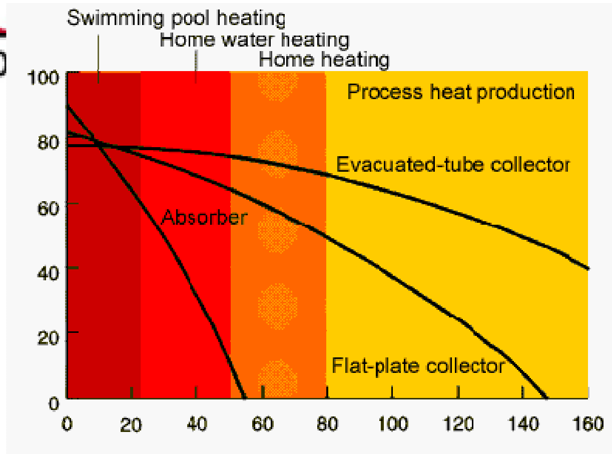

Collector Efficiency(VI)

Reference Area

Very important is to know Efficiency to which Area is referred to.

A_{gross}, $A_{aperture}$, $A_{absorber}$

Technical Data

Model		SP3 2m²
Number of tubes		20
Gross area	ft.² / m²	31 / 2.88
Absorber surface area	ft.² / m²	22 / 2.05
Aperture area *1	ft.² / m²	22.7 / 2.11
	inches	55 ¾
	mm	1418
	inches	80
	mm	2031
	inches	5 ½
	mm	143
	%	81.5
	W/(m²·K)	1.43
	W/(m²·K²)	0.0076
	kJ(m²·K)	5.4
	lbs / kg	112 / 51

...er surface area. (As tested by ISFH in Europe)

Technical Data

Model - Vitosol 200-F		SV2
Total surface area	ft.² / m²	27.0 / 2.51
Absorber surface area	ft.² / m²	25.0 / 2.32
Aperture *1	ft.² / m²	25.1 / 2.33
Dimensions *2		
Width	inches	41 ¾
	mm	1056
Height	inches	93 ¾
	mm	2380
Depth	inches	3 ½
	mm	90
Optical efficiency *3	%	79.3
Heat loss coefficient U_1	W/(m²·K)	3.95
U_2	W/(m²·K²)	0.0122
Thermal capacity	kJ(m²·K)	6.4
Weight	lb / kg	115 / 52
Fluid capacity	USG	0.48
(heat transfer medium)	ltr	1.83
Maximum working pressure *4	psig	87
	bar	6
Maximum stagnation temperature *5	°F / °	221
Connection	inche	¾
	mm	22
Requirements for installation surface and anchorage		equate lo

*1 *Important for system design considerations.*
*2 *Dimensions rounded to the nearest ¼ inch.*
*3 *Based on absorber surface area.*

Flate plate collectors (I)

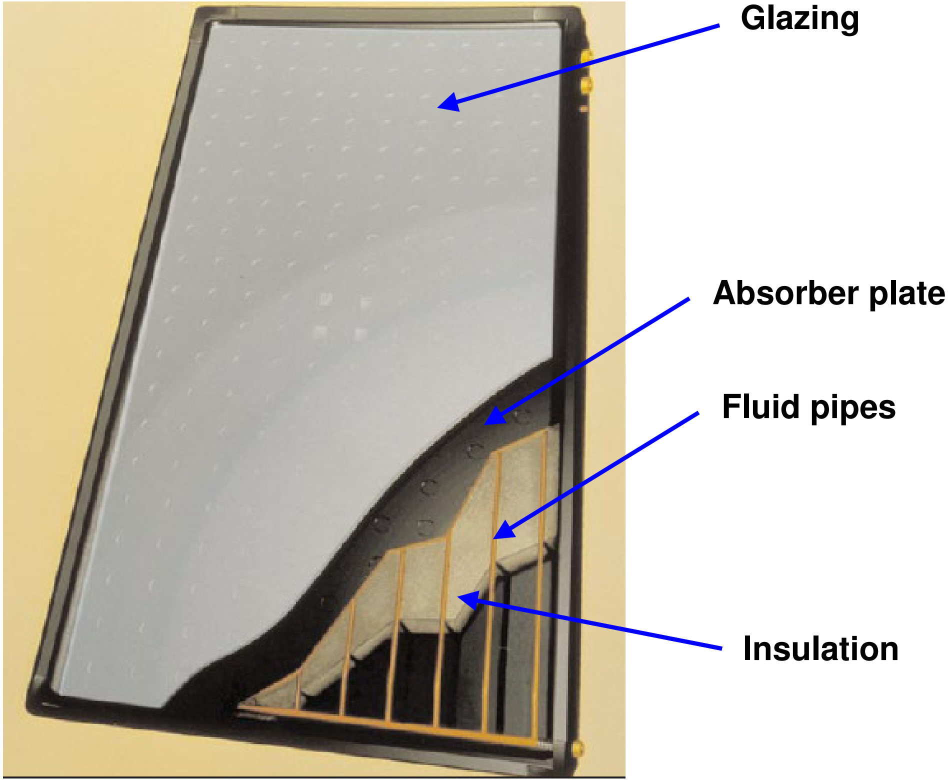

Evacuated Tube collectors (I)

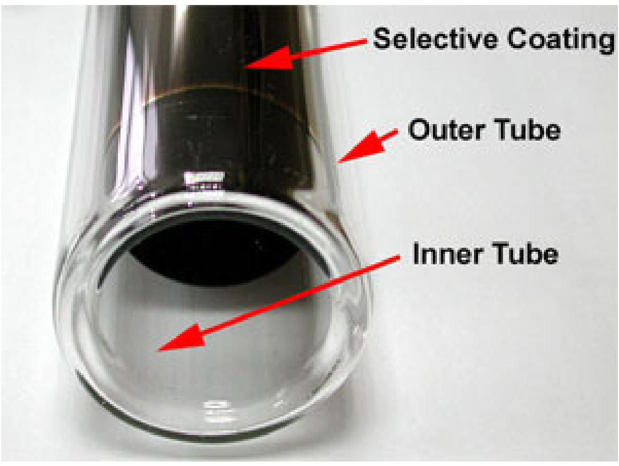

In ET collectors the heat losses are reduced thanks to a double glazing with vacuum in between. Glass curvature is often beneficitial to incoming sun beams. The glass configuration is similar to a thermos bottle, and an absorbing coating can be present of internal cylinder.

Inside the inner tube a flat or tubular fin is attached to a U-pipe or coaxial one where the carrier fluid is circulated

In some cases, a Heat Pipe is present as additional medium for transferring the heat from the evacuated pipe to the carrier fluid at collector top header

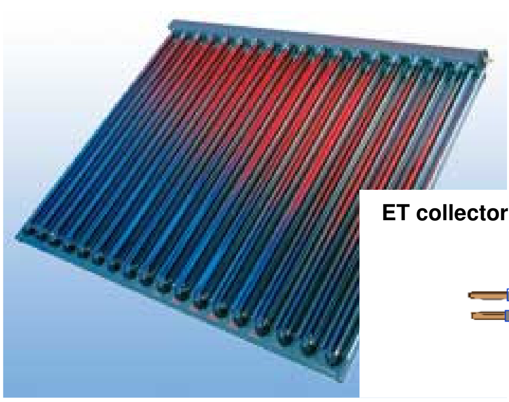

ET collector with flat absorber

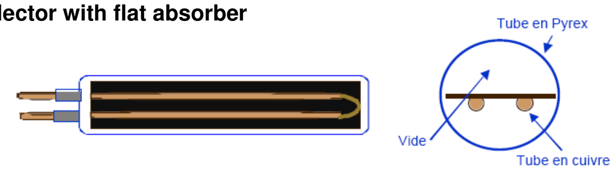

Coupe d'un capteur sous vide

Evacuated tube collectors (Ib)

"Each evacuated tube consists of two glass tubes made from extremely strong borosilicate glass. The inner tube can be coated with a selective absorbing layer (e.g aluminum nitride Al-N/Al).

During the manufacturing process, the air contained in the space between the two layers of glass is pumped out, while the top of the tubes are exposed to high temperatures. This fuses the two tubes together into a single evacuated tube.

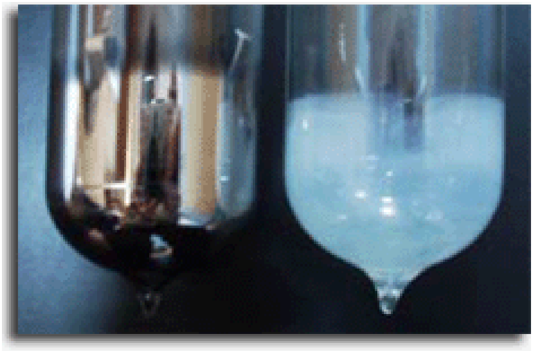

In order to maintain the vacuum (typically 10^{-3}Pa) between the two glass layers, sometimes a barium getter is used (as in old television tubes).

Barium layers actively absorbs any CO, CO2, N2, O2, H2O and H2 out-gassed from the evacuated tube during it's lifetime and increases the longevity of the vacuum. This barium layer also provides a clear visual indication of the vacuum status; the silver barium layer turns white if the vacuum is lost making it easy to identify

(Source: Apricus.com).

Evacuated vs flat plate

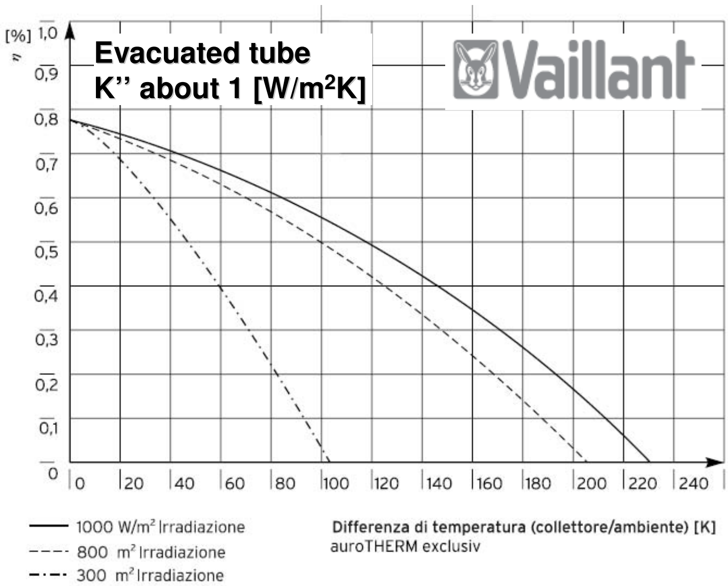

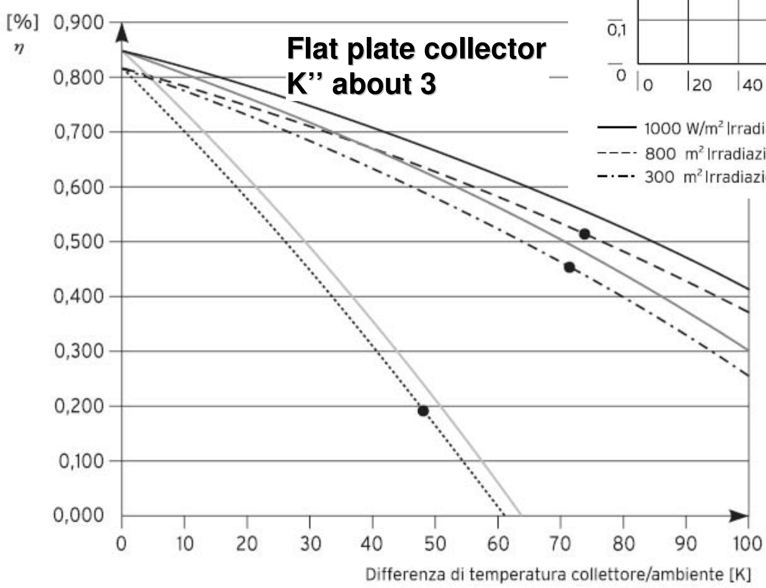

DHW solar systems (natural circulation)

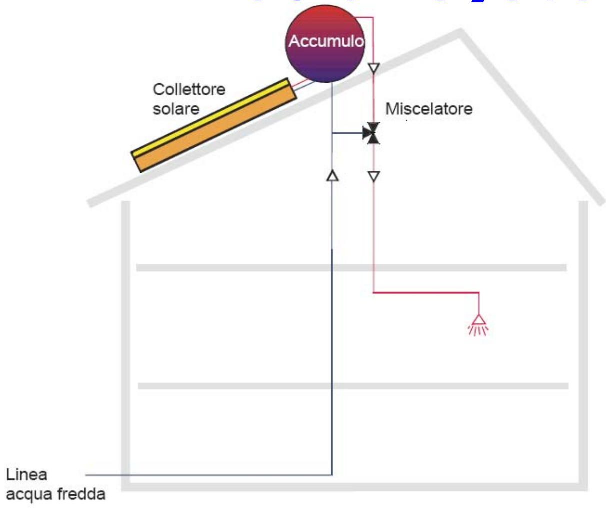

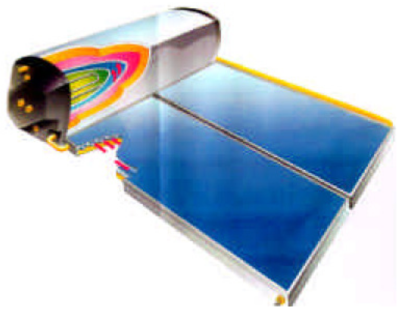

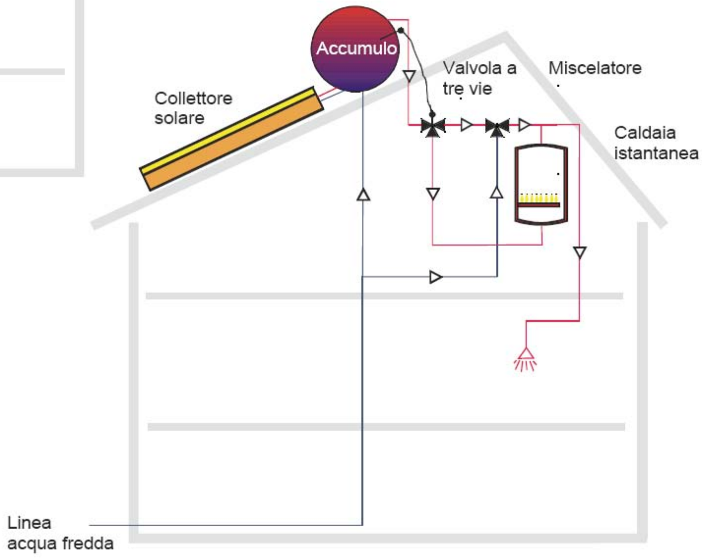

DHW solar systems (forced circulation)

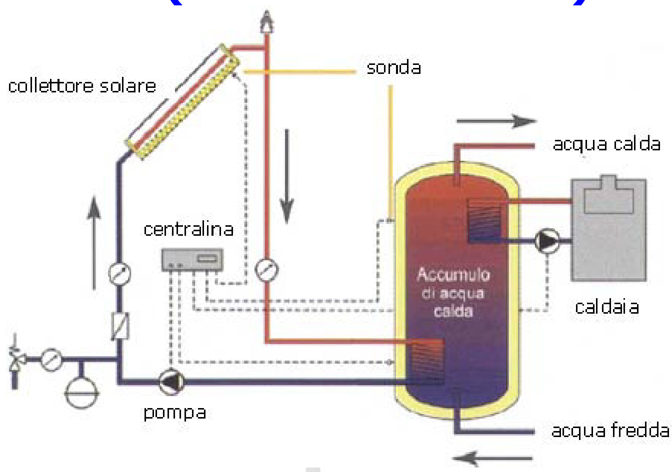

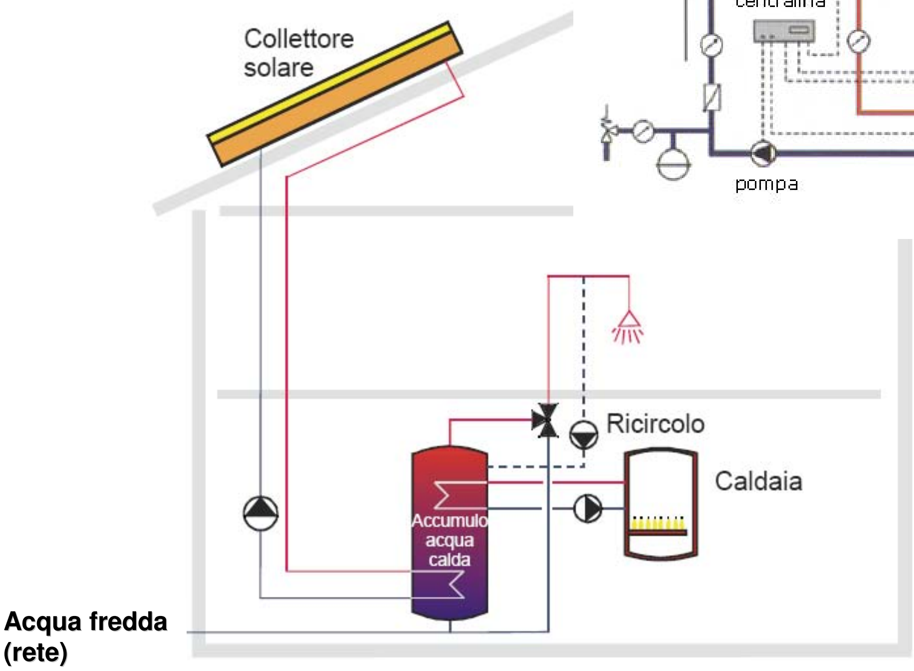

Heat Exchangers in solar systems

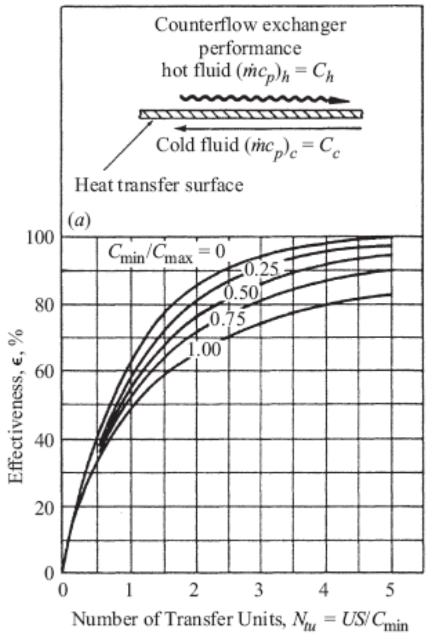

Plate heat exchangers are the most efficient ones. Spiral HE are an economic solution which avoid additional pumps Effectiveness is usually between 0.6 e 0.8 and the Overall Heat Transfer coefficient must be at least 100W/K per square meter of collector

$Ntu = A_{ex}K''_{ex} / C_{min}$

Storage tank should be about 50-80 liters per square meter of collector

Collectors, back of the envelope economic analysis

Flat collectors: 300-400euro/m² (++)
Solar tank (300 liters): 600-800 euros (++)
Condensation gas burner, with integrated solar tank (24kW): 1500-3000euros

Modello	Alt./Prof./Largh. in mm del collettore	Peso collettore in Kg	Superficie collettore lorda/netta in m²	Assorbimento assorbitore α (%)	Emissione assorbitore ε (%)	Grado di rendimento η_0 (%)	Coefficiente di dispersione k_1 [W/m²K]	Coefficiente di dispersione k_2 [W/m²K²]	Codice nr.	Prezzo in Euro
	collettore solare piano a circolazione forzata									
VFK 990/1	1930/ 110/ 1160	43	2,24/2,02	95 ± 2,0	5 ± 2	85,4	3,37	0,0104	302383	764,00

DHW cost for different fuels (VAT included)

Diesel*	**1,190 €/l**	**0,140 € /kWh**
LPG**	**1,650 € /kg**	**0,122 € /kWh**
Natural Gas***	**0,95 € /m³**	**0,100 € /kWh**

Heat for 1 kg of water from 15°C to is about 125kJ or 0.035kWh.

Heating 50x4x365=73000 liters/years of DHW with burner efficiency of 90% means 2500 kWh, or 255€

*** Heating value 11.3kWh/kg, density (liq.) 820 kg/m³,** **(1kWh=3.6MJ)**
**** Heating value 12.7kWh/kg, density (liq.) 510 kg/m³,**
***** Heating value 9.5kWh/m³, or 13.3kWh/kg, density 0.71 kg/m³**
++ 4 m² + tank , 2000 euros (2016, turn on key)

F-Chart Method

The F-Chart method is a world accepted procedure for the design of active and passive solar heating systems, especially for selecting the size and type of solar collectors supplying the DHW and heating loads.

F is the the fraction of hot water (air) demand provided by the solar system

It was originally developed as part of the Dr. Sanford Klein's Ph.D. thesis, entitled "A Design Procedure for Solar Heating Systems" (1976),Klein et al. (1976a, 1977).

The F-Chart method consists of correlations of the results of a large number of

detailed simulations using TRNSYS, a transient systems simulation program by Klein et al. (1973).

The first publication regarding the F-Chart method was first published one year after Klein's Ph.D. thesis in the book by Beckman, Klein, and Duffie (1977),entitled "Solar Heating Design by the F-Chart Method."

The F-Chart method is a carefully constructed correlation that is based on 1,000s (spellout) of simulations with a streamlined version of the TRNSYS program, developed by the University of Wisconsin. Therefore, an assessment of the accuracy of the F-Chart method should include an assessment of the accuracy of the TRNSYS program.

F-Chart Method (II)

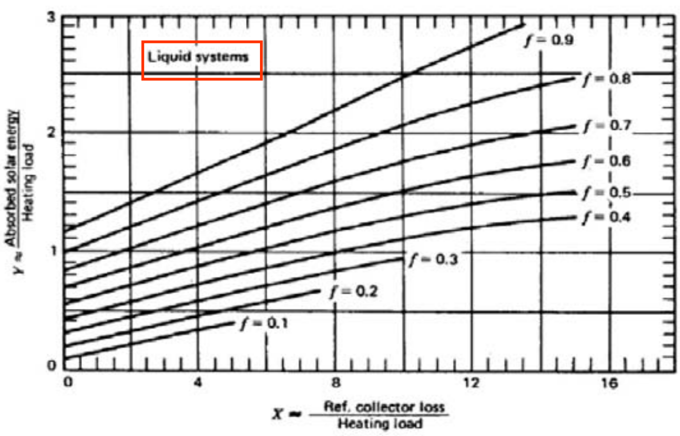

$\overline{H}_T$ = Monthly averaged, daily radiation
L = Monthly total heating load

$$X = F_R U_L \times \frac{F'_R}{F_R} \times (T_{ref} - \overline{T}_a) \times \Delta\tau \times \frac{A_c}{L}$$ **Xc**

$$Y = F_R (\tau\alpha)_n \times \frac{F'_R}{F_R} \times \frac{\overline{(\tau\alpha)}}{(\tau\alpha)_n} \times \overline{H}_T N \times \frac{A_c}{L}$$

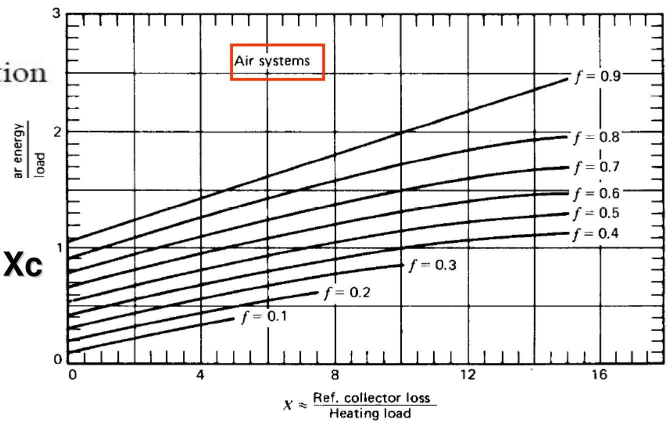

Concentration vs non concentrated

	Tfluid [°C]	Concentration Ratio	Beam	Diffuse	Reflected
Concentration, Tower	500-700	100-1000	X	0	0
Concentration, Parabolic trough	400-500	50-500	X	0	0
Concentration, Fresnel	250-300	50-250	X	0	0
Non concentrating, Flate Plate	40-100	1	X	X	X
Non concentrating, Evacuated	40-150	1	X	X	X

Concentration ratio

Concentration ratio C is defined as the ration of aperture area to receiver area. For flate plate collectors, C=1

$$C = \frac{A_a}{A_r}$$

Which is ,maximum Concentration ratio C ?

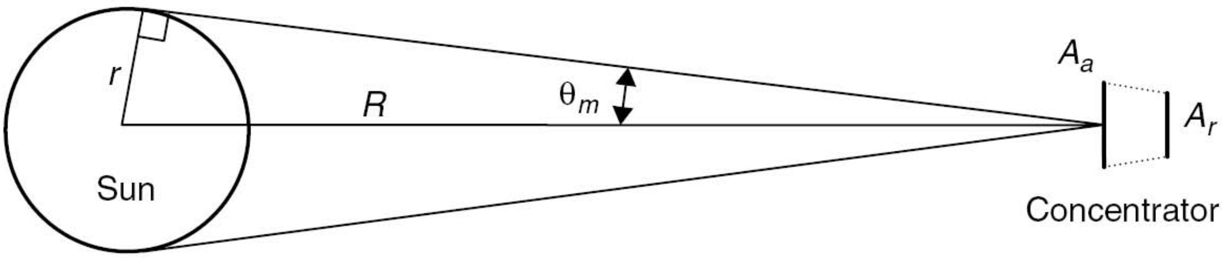

$$Q_s = (4\pi r^2)\sigma T_s^4$$

$$F_{s-r} = \frac{A_a}{4\pi R^2}$$

Qs is overall heat transfer rate from sun to the universe

A fraction can be intercepted by the solar concentrating device

Concentration ratio

Heat power received by collector

$$Q_{s-r} = A_a \frac{4\pi r^2}{4\pi R^2} \sigma T_s^4 = A_a \frac{r^2}{R^2} \sigma T_s^4$$

If receiver acts as a blackbody, it re-irradiates toward sun according to:

$$Q_{r-s} = A_r F_{r-s} \sigma T_r^4$$

Maximum receiver temperature must be equal to the sun one (II law of Thermodynamics)

$$\frac{A_a}{A_r} = \frac{R^2}{r^2} F_{r-s}$$

$$Q_{r-s} = Q_{s-r}$$

Concentration ratio

Since maximum view factor value is 1, say $F_{r\text{-}s}$=1

The maximum concentration ratio C is (3D concentrator)

$$C_{max} = \frac{A_a}{A_r} = \frac{R^2}{r^2} = \frac{1}{\sin^2(\theta_m)}$$

A similar analysis for linear (1D) concentrators gives:

$$C_{max} = \frac{1}{\sin(\theta_m)}$$

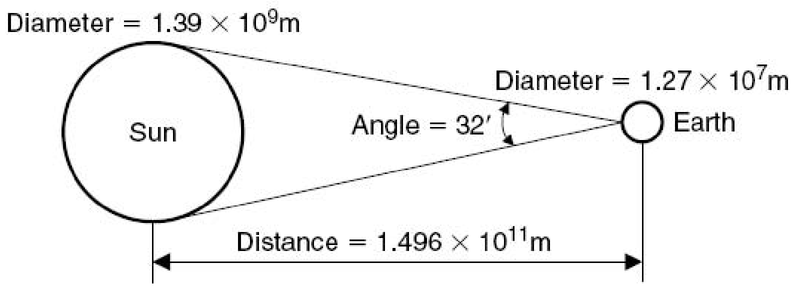

Concentration ratio

For single-axis tracking, $C_{max} = 1/\sin(16') = 216$.
For full tracking, $C_{max} = 1/\sin^2(16') = 46{,}747$.

Notice: the half accepting angle θ_m defines the relationship between concentration ratio and viewing angle of the collector (portion of the sky viewed by the collector)

Thermal analysis of concentraing collector, Q in [W]

$$\eta = \frac{\dot{Q}_u}{A_a G_t}$$

$$\dot{Q}_u = F_R[SA_a - A_r K''(T_i - T_a)]$$

$$S = G''_{inc}\,(\rho\tau\alpha)_{\text{mirror, glass cover if any, absorber}}$$

S is the overall transmitted radiation flux by mirrors/lenses of concentrating collector times the receiver absorption factor

Concentration, heliostats (2 axis tracking)

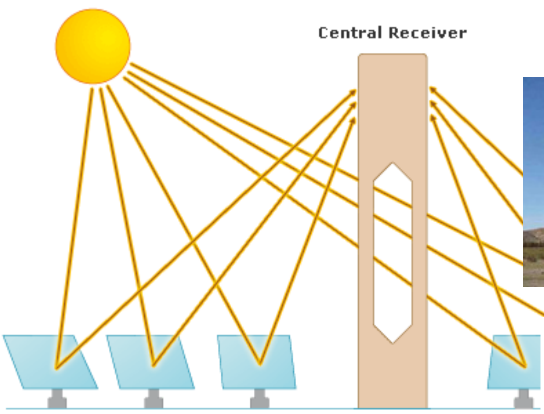

Fonte: Albengoa Solar

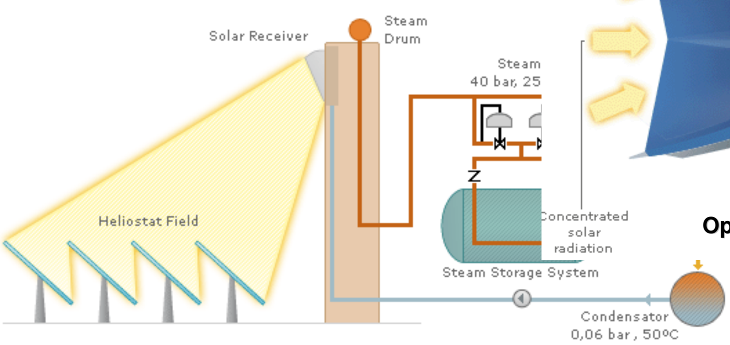

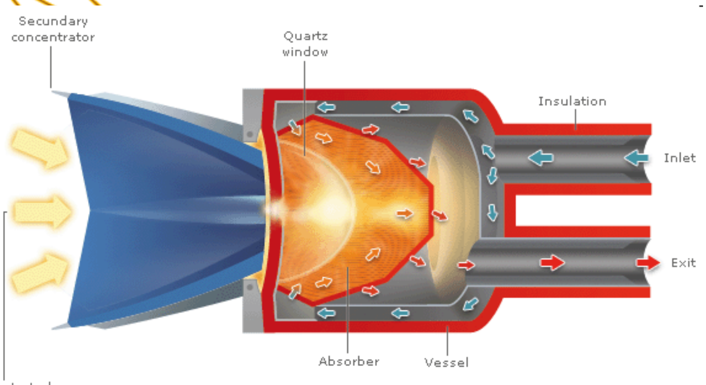

Operating scheme for a pressurized air receiver

Concentration, heliostats (II)

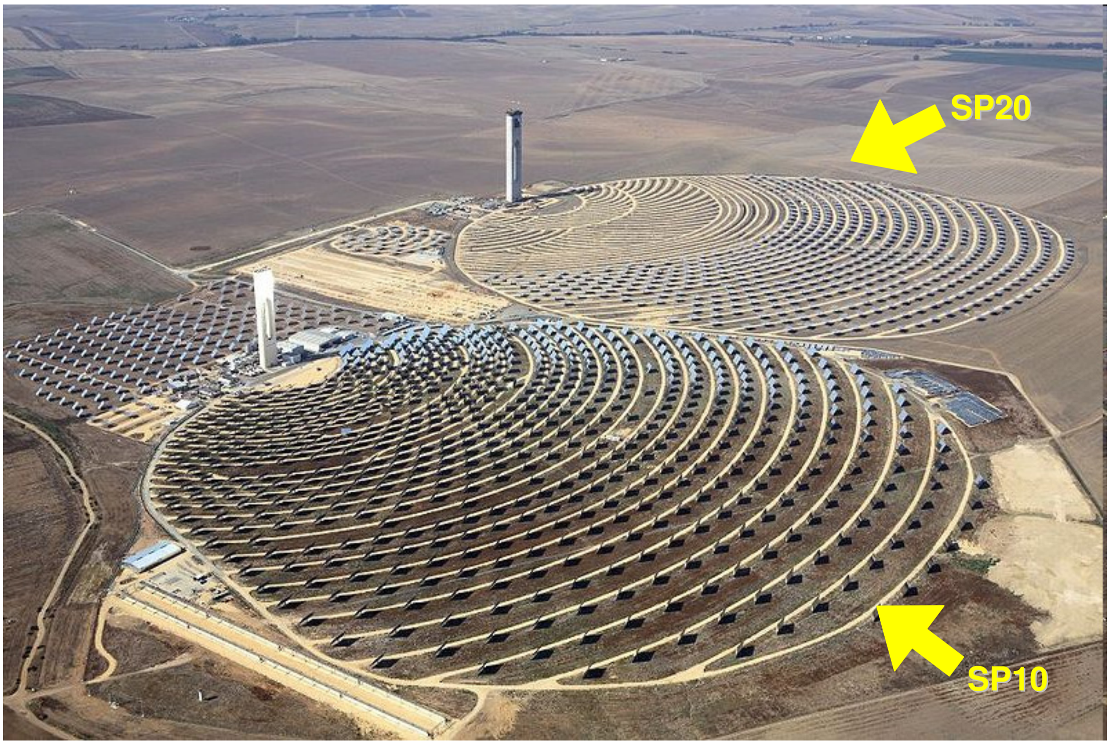

Concentration, heliostats (III)

SP10

Technology:	Power tower
Status:	Operational
Country:	Spain
City:	Sevilla
Region:	Sanlúcar la Mayor
Lat/Long Location:	37°26′ 30.97″ North, 6°14′ 59.98″ West
Land Area:	55 hectares
Solar Resource:	2,012 kWh/m^2/yr
Source of Solar Resource:	Abengoa Solar
Nominal Power	11MW$_e$
Electricity Generation:	23,400 MWh/yr (Expected/Planned)
Generation Data Explanation:	Gross generation

(0.02 kWe/ m^2)

Concentration, linear parabolic

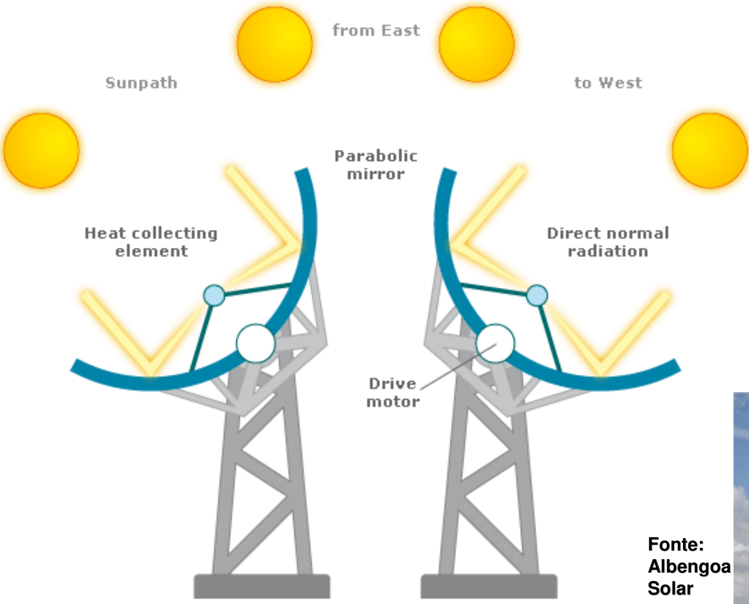

Fonte: Albengoa Solar

Concentrazione, parabolic, single axis (I)

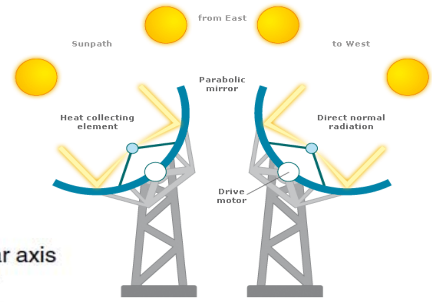

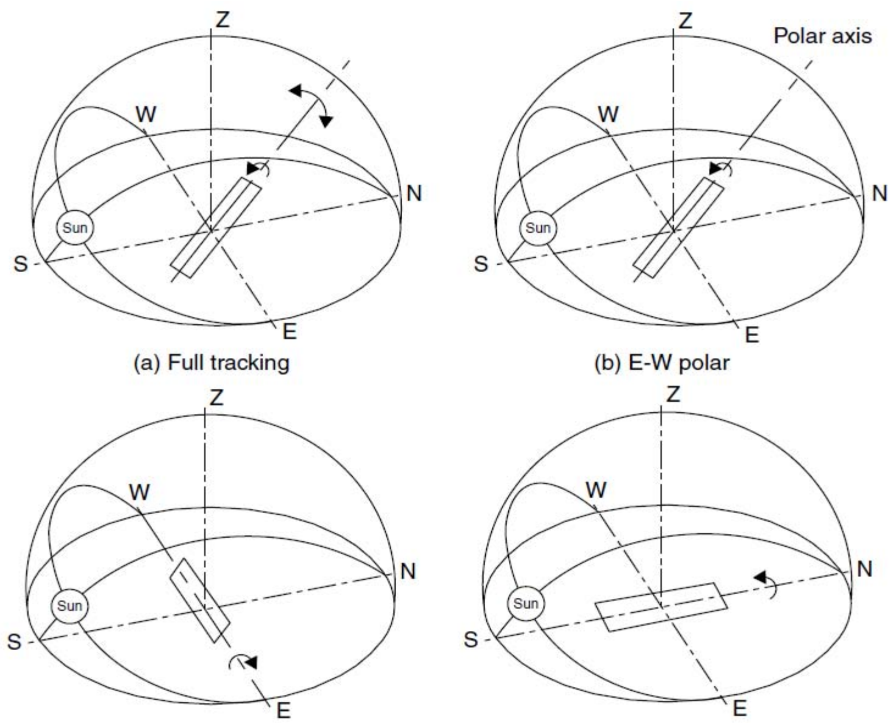

(a) Full tracking

(b) E-W polar

(c) N-S horizontal

(d) E-W horizontal

Concentration, parabolic, single axis (II)

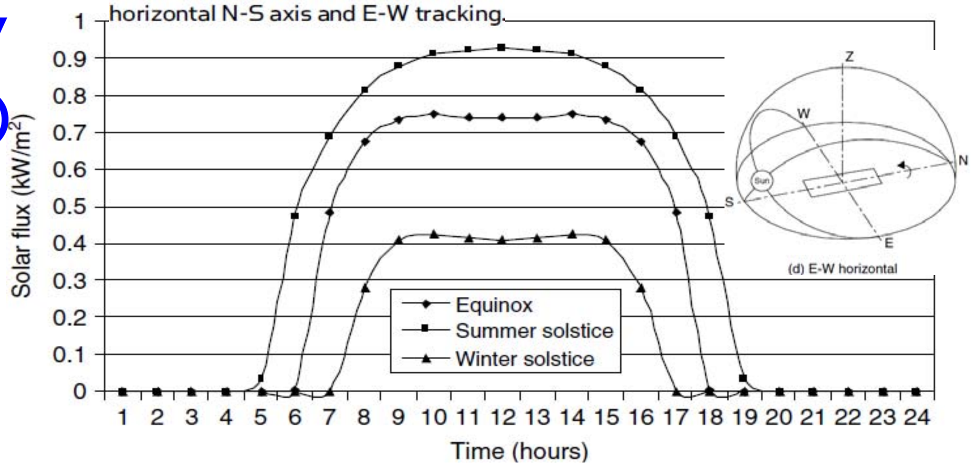

Daily variation of solar flux: horizontal E-W axis with N-S tracking.

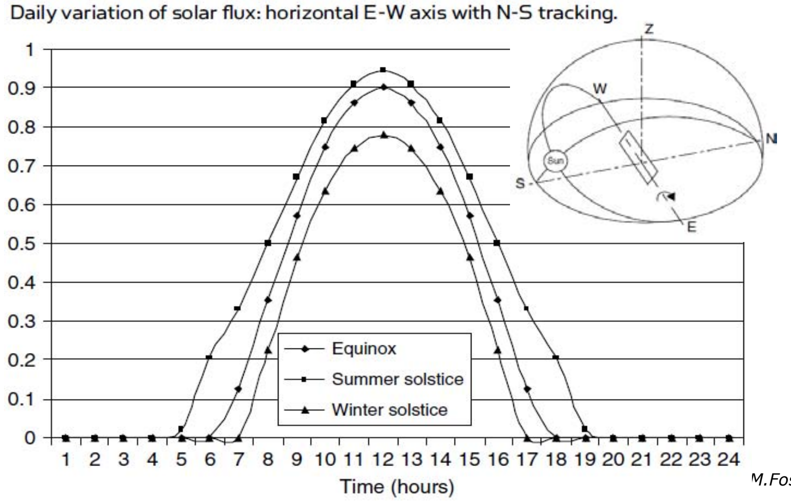

Tracking Axis	Percentage to full tracking		
	E	SS	WS
Full tracking	100	100	100
E-W polar	100	91.7	91.7
N-S horizontal	89.1	97.7	60.9
E-W horizontal	73.8	74.0	86.2

E = equinoxes, SS = summer solstice
WS = winter solstice.

Renewable Energies
Energy from the sun, Photovoltaic Modules

Photovoltaic Effect (I)

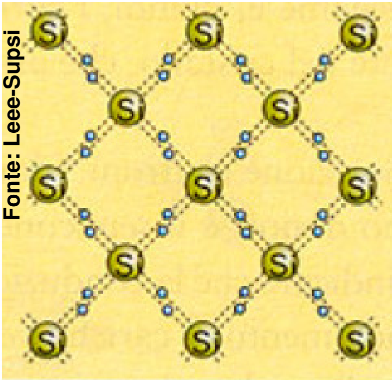

Semiconductors. There are two main semiconductor materials: germanium (Ge) and silicon (Si). This one is the most employed in the electronic industry, thanks to the abundancy of silica on earth

A semiconductor is an insulator at low temperatures. Covalent bonds in the silicon crystal (diamon lattice disposition) do not make available any charge (electron) for current flow.

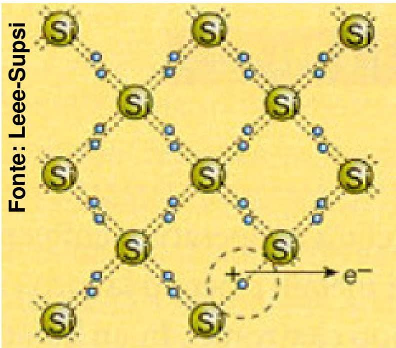

At high enough temperatures, or for <u>photon absorption</u>, some <u>electrons</u> in the valence band can move to the conduction band, leaving holes (positive charges) in the valence band.

Both conduction electrons or valence holes are charges able to carry the electric current

Blackbody emission and photon flux

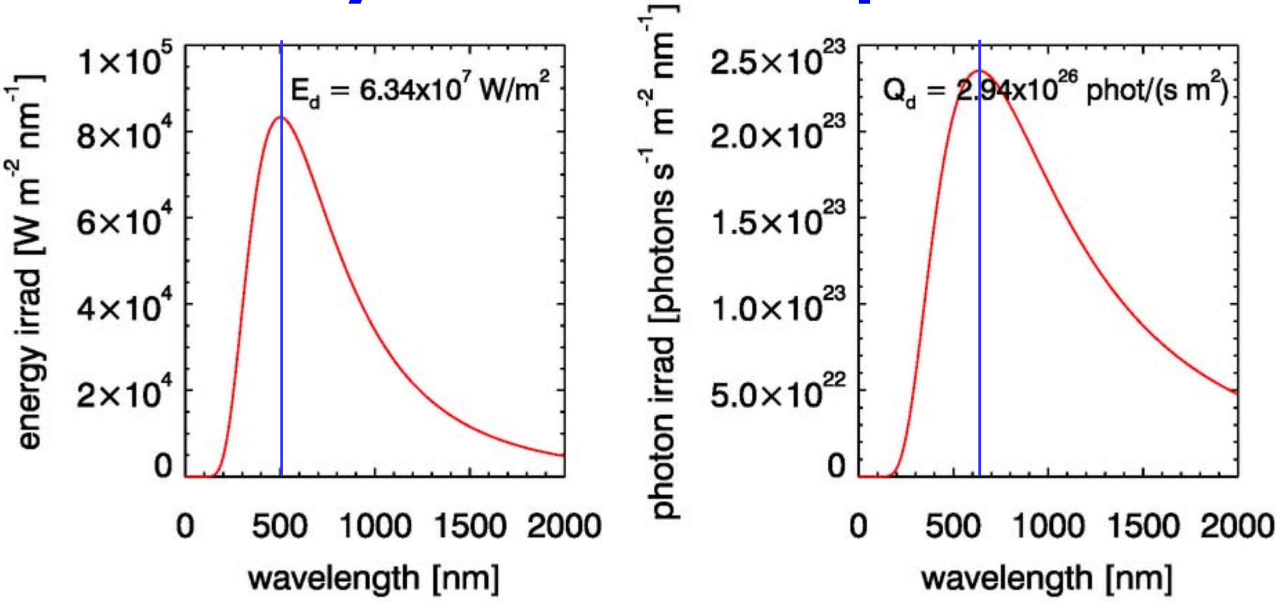

$$Q_b(\lambda,T) = \frac{E_b(\lambda,T)}{hc/\lambda} = \frac{2\pi c}{\lambda^4}\frac{1}{e^{hc/\lambda KT}-1}$$

[photons/(s m^2 m)]

Blackbody spectral energy and photon irradiances, at a temperature of 5780 K

Photovoltaic Effect (III)

Solid state electronics and photovoltaic technology arise from the unique properties of <u>(crystal) silicon</u> and germanium, each of which has four <u>valence electrons</u> and which form diamond type lattices since valence electrodes are shared with surrounding atoms (<u>covalent bonds</u>). Substitution atoms (dopants) can dramatically change the electrical properties of the <u>intrinsic semicondutor.</u>
An energy input can rise the valence electrons to their conduction state (<u>conduction band</u>) For crystal silicon such an energy is equal to 1.2 [eV]

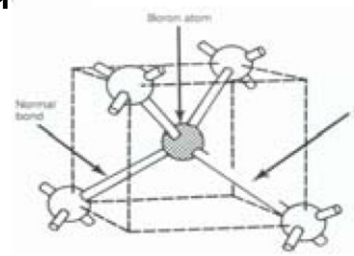

This energy input can be given by a suitable photon. :
$E_{ph} = 1.24/\lambda$ [eV/μm]
Based on the above relationship only photons with wavelength lower than 1.1 [μm] have enough energy for electron activation to the conduction band

Once an electron leaves its valence band it can move in the crystal lattice as done in metals.
At each conduction electron corresponds a hole in the valence band that behaves like a free positive charge able to move

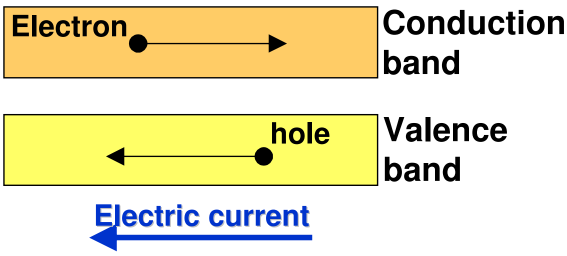

Photovoltaic Effect (IIIb)

When a semiconductor is taken out of thermal equilibrium, for instance by illumination and/or injection of current, the concentrations of electrons (*n*) and holes (*p*) tend to relax back toward their equilibrium values through a process called <u>*recombination*</u> in which an electron falls from the conduction band to the valence band, thereby eliminating a valence-band hole. There are several recombination mechanisms.

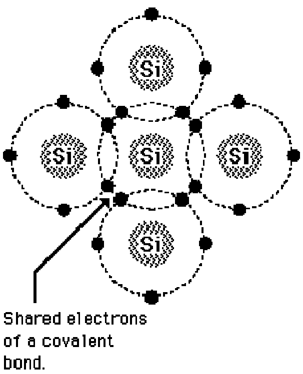

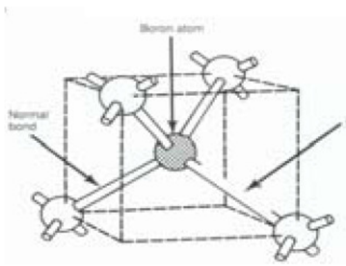

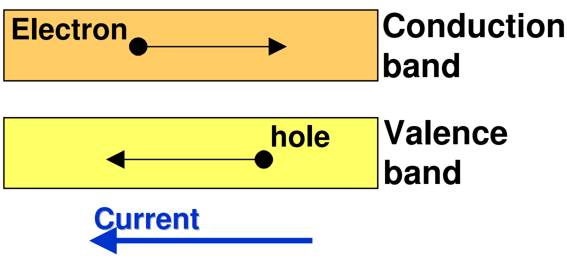

Photovoltaic Effect (II)

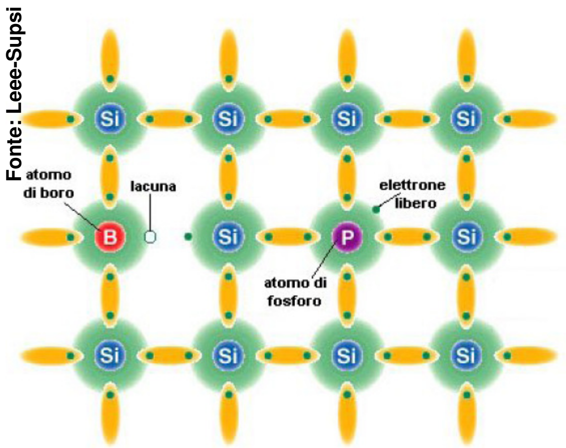

Doping
when semiconductor silicon is doped with phosphorous (<u>donor atom</u>), one electron is donated to the conduction band for each atom of phosphorous introduced. phosphorous is has five valence electrons. Silicon is now of <u>type N</u>

Dopant concentration is usually very low ($5 \cdot 10^{22}$ Si atomscm^{-3} vs dopant concentrations ranging from 10^{13} cm^{-3} to 10^{18}

If silicon is doped with boron (valency of three, <u>acceptor atom</u>), each boron atom accepts an electron from the valence band, leaving behind a hole.
Silicon is now of <u>type P</u>

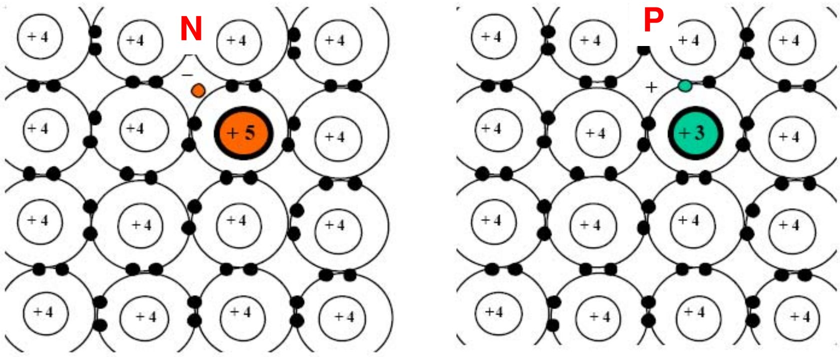

Photovoltaic Effect (V)

Where an *n*-type semiconductor comes into contact with a *p*-type semiconductor, a *pn* junction is formed. In thermal equilibrium there is no net current flow

Since there is a concentration difference of holes and electrons between the two types of semiconductors, holes diffuse from the *p*type region into the *n*-type region and, similarly, electrons from the *n*-type material diffuse into the *p*-type region. As the carriers diffuse, an electric field (or electrostatic potential difference) is produced, which limits the diffusion of further holes and electrons.

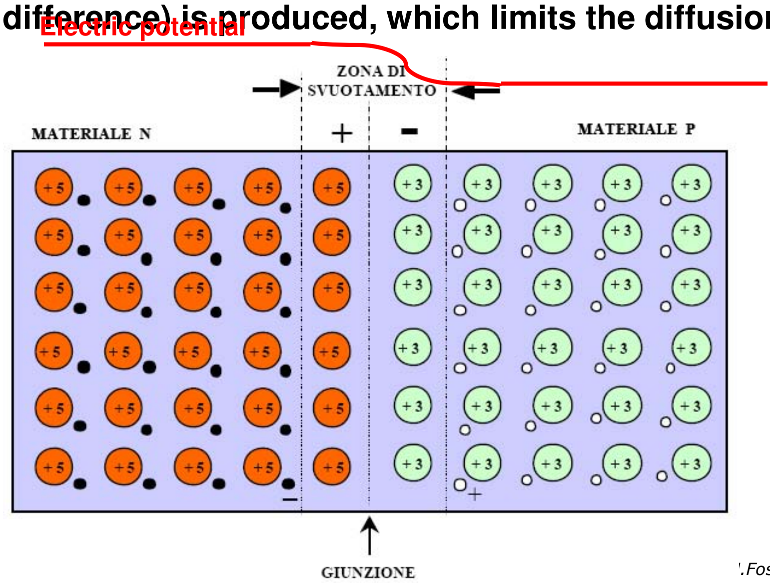

Depletion zone *(<u>zona di svuotamento</u>)*

The Junction (IV)

The electric potential originating at the junction is able to prevent charge recombination is a charge pair (electron/hole) is created due to a photon energy input. This is the basic working principle of the <u>Photovoltaic effect</u>.

Electrodes move toward the higher potential (emitter zone) while holes moves toward the base at lower electric potential.

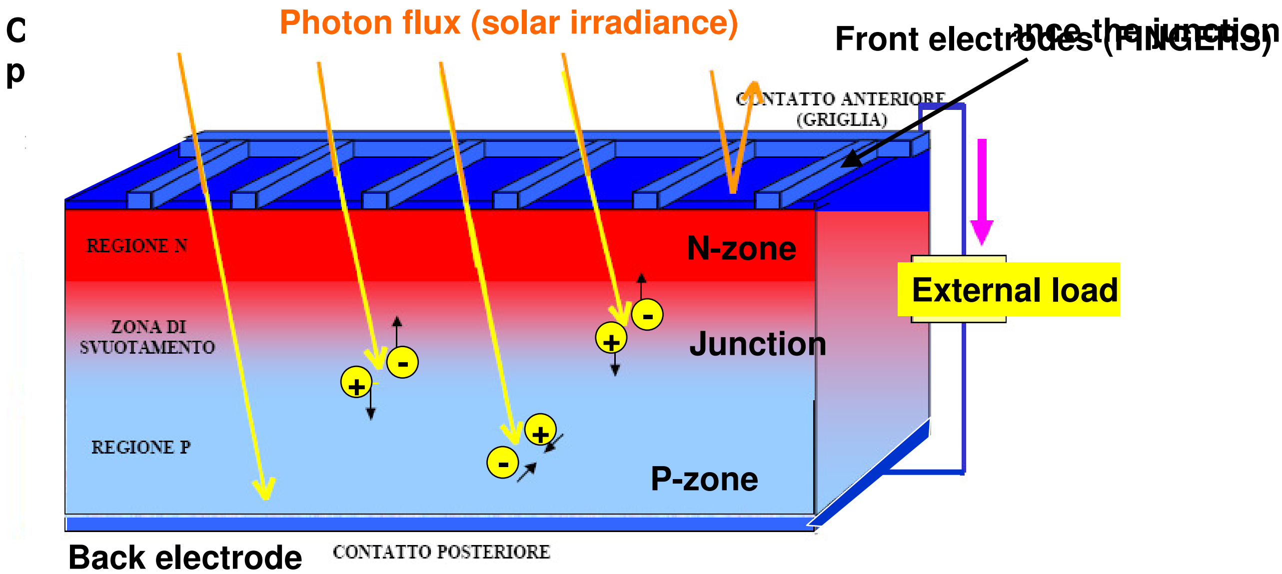

PV Conversion (I)

Photons able to generate charges in the silicon semiconductor needs wavelengths lower than 1.1µm. The solar spectrum on earth (AM =1.5) contains 75% of its energy below that wavelength.

But this 75% energy availability cannot exploited since:

- The excess of photon energy with respect to the energy gap value is necessarely converted into heat
- Not all photons are absorbed due to reflections and shading by electrode fingers
- Electrode/hole recombinations without photocurrent
- Internal photocurrent flow (shunt resistance)
- Photocurrent energy is lost as Joule effect (series resistance and electrode/connection resistances)

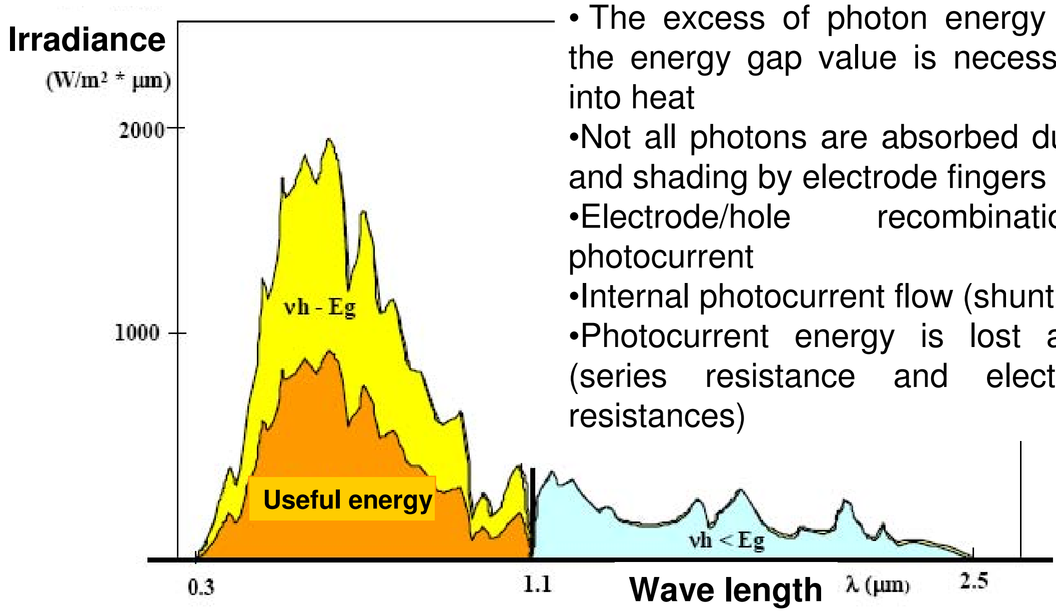

PV Conversion (III)

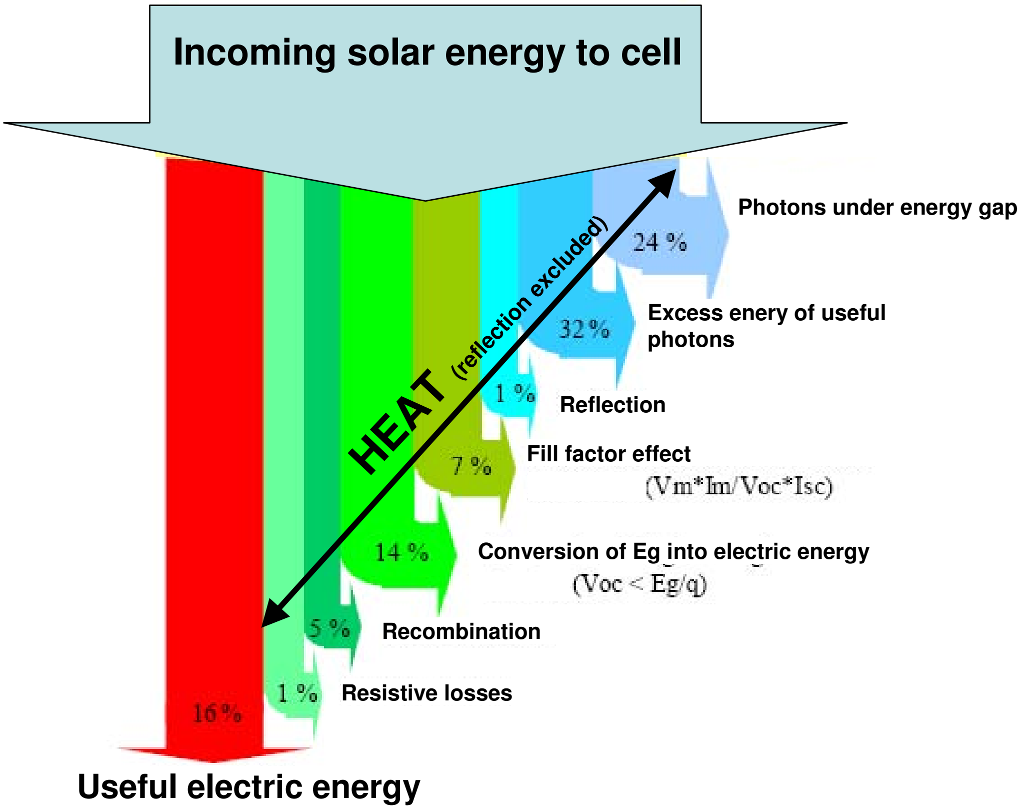

Cell behaviour

In "dark" conditions, the cell behaves as a diode.
The diode characteristic curve is described by an exponential law. The simplest description of the diode behaviour is stepwise linear function, with an activation voltage of about 0.6-0.7V. Best description is an exponential law as below:

When the cell is illuminated, its response is the one of current generator, usually depicted in the 4th quadrant of the I-V plane

$$I_D = I_0\left(\exp(\frac{V_D}{V_T}) - 1\right)$$

$$V_T = KT/q$$

V_T Thermal Voltage

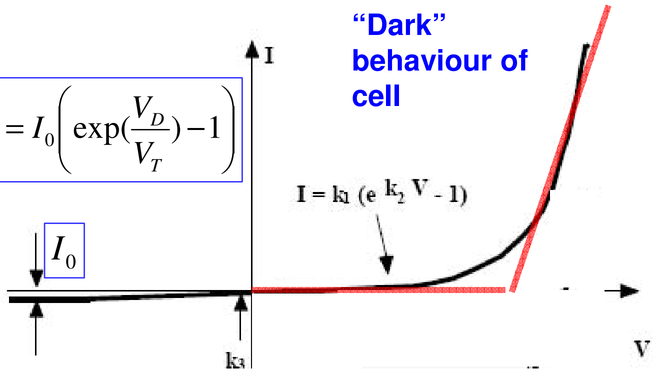

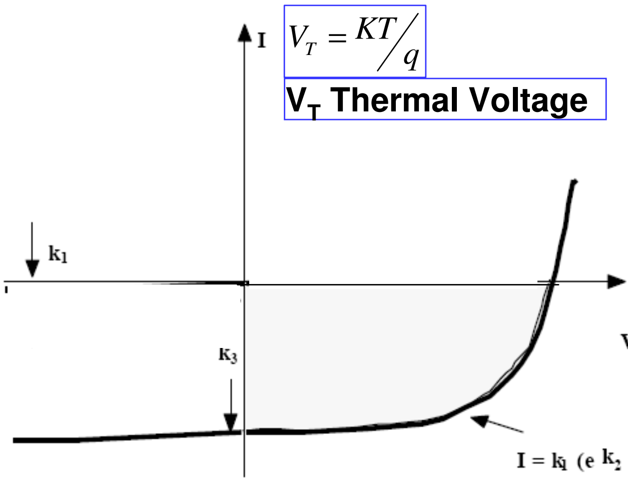

I = k1 (e k2 V - 1) - k3

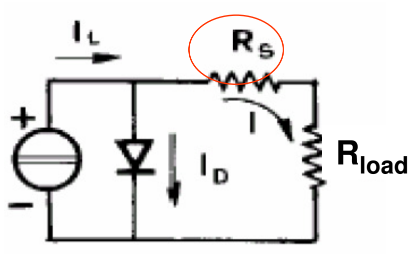

$I_D = I_{Dark}$

Cell behaviour (II)

The characteristic cell curve (as a generator) can be described as a function of a number of key parameters.
I_{sc} = short circuit current
V_{oc} = Open circuit voltage
I_m = Current at the maximum power P_{max} V_m = Voltage at the maximum power

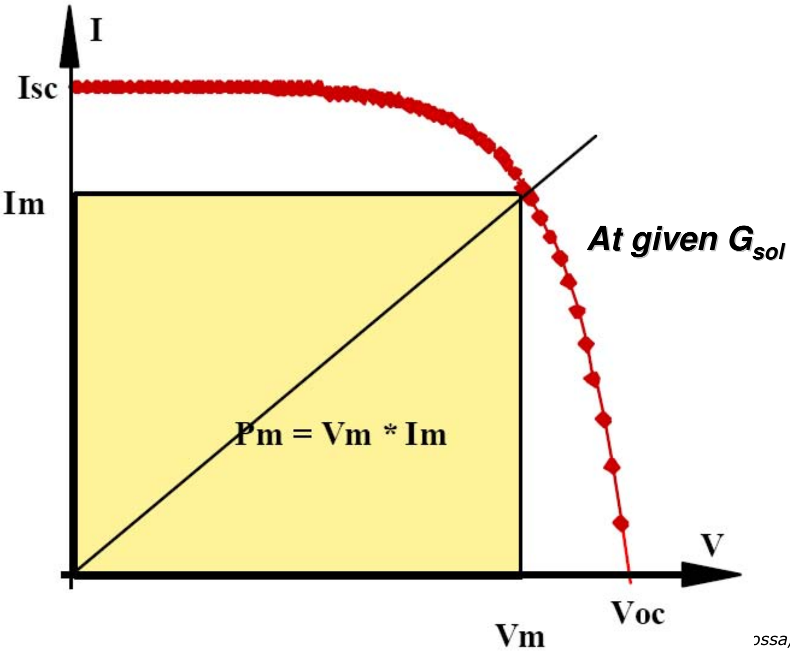

Cell behaviour (II)

it is clear that an efficient solar cell will have a high short-circuit current, I_{SC}, a high open-circuit voltage, V_{OC}, and a fill factor, *FF*, as close as possible to 1.

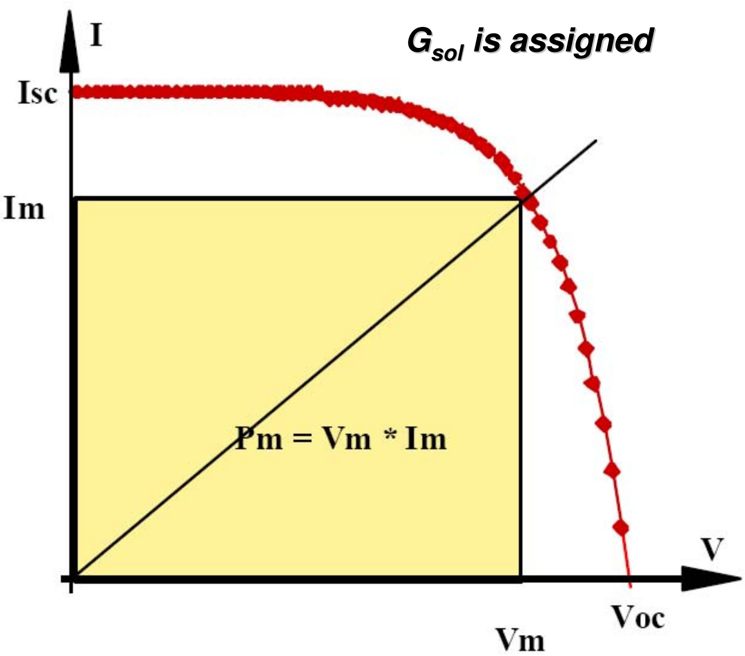

The following paramemeters can be definined:

FF (Fill Factor)

$FF = P_{max} / (I_{sc} V_{oc})$

Efficiency η

$\eta = P_{max} / P_{solare\ incidente}$

Cell behaviour (III)

Generally Speaking cell characteristic curve depends on Irradiance, temperature and semiconductor type

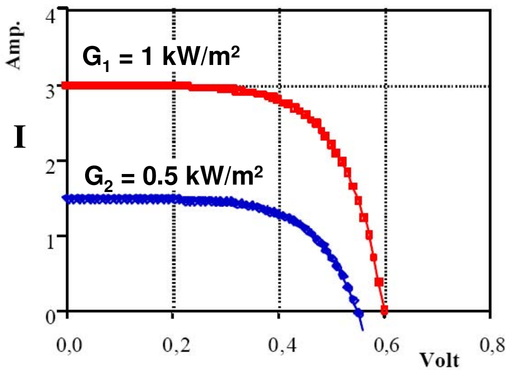

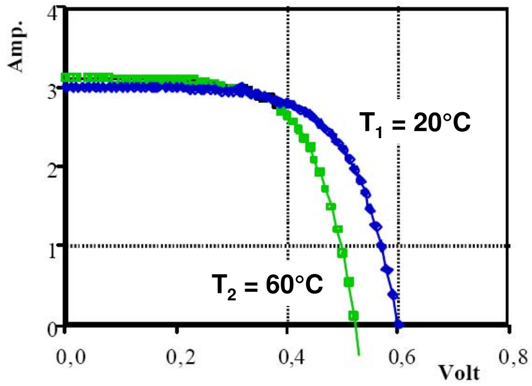

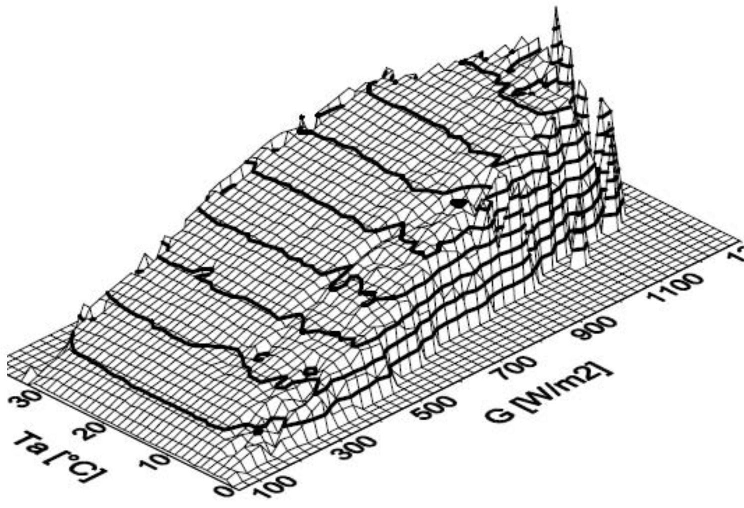

Fonte: Leee-Supsi

Cell behaviour (IV)

Temperature does not affect significantly the short circuit current while it reduces OC voltage

$I_L = I_{sc} = f(G) \sim const \cdot G$

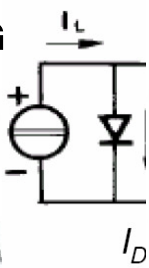

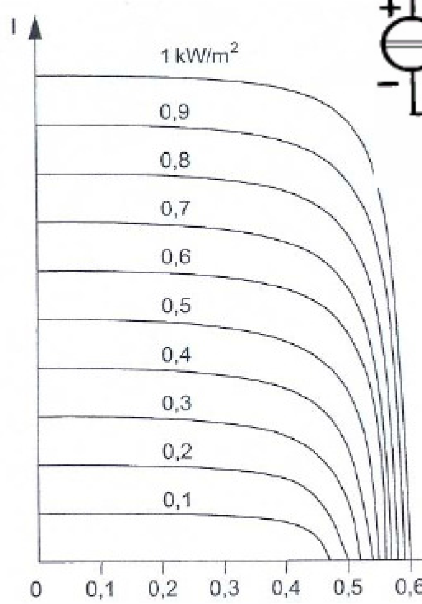

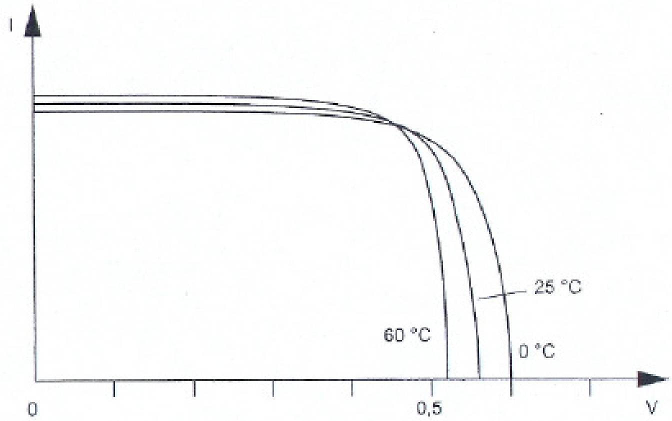

Irradiance levels act on current, while the effects on voltage are less important

Efficiency reduction with temperature is around 0.4 - 0.6 [%/°C] (for silicon cells)

Cell behaviour (V)

Decrease in conversion efficiency with temperature (crystalline cells) is around 0.4 - 0.6 [%/°C]

Reference temperature (also the test temperature) is 25°C.

Reference irradiance is 1000W/m²

Crystalline silicon (more performing) is more affected by temperature effects than amorphous silicon (less performing)

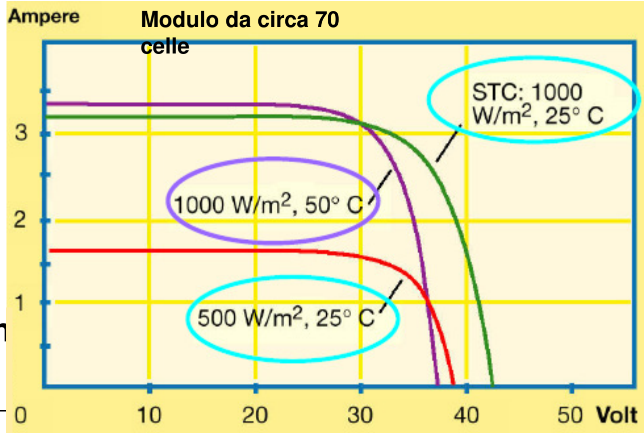

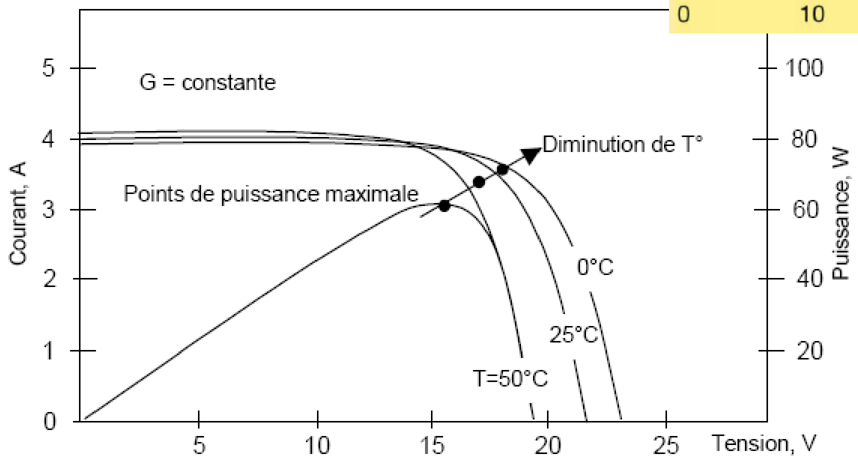

Cell test

Standard PV cell Test is done at irradiance equal to 1000W/m², with spectrum having the AM=1.5 distribution (Cei-EN 60904-1, 60904-3 standards). During the test the cell is maintained at T=25°C, while being illuminated for a very short period. A reference cell is devoted to measure the real irradiance on target

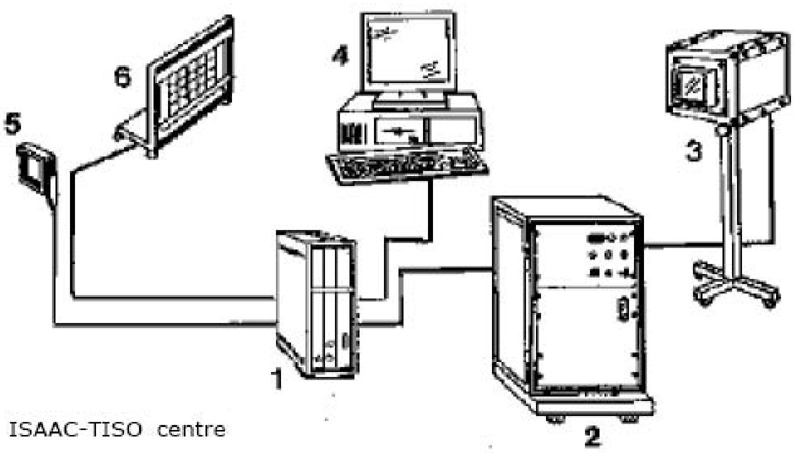

ISAAC-TISO centre

1. Electronic load
2. Flash generator
3. Light box and flashbulb
4. Data processing and printer
5. Reference cell
6. Module holder

NOCT, Normal operating Cell Temperature, temperatura effettiva di lavoro per G=800W/m², T_a=20°C, w_{wind} = 1 m/s

Cell test (II)

The conventional approach to flash testing, has been described by several authors (e.g. Mueller, 1993). The method is based on maintaining a nearly constant light intensity while rapidly changing the bias voltage on the cell to sweep out the I-V curve. <u>Typically about 1000 I-V data points are acquired during a 2-10ms test</u>. For solar simulators in PV industry xenon light sources are normally used. The spectral irradiance of this lamp type differs considerably from AM1.5 spectral irradiance and corrections are needed. Uniform illumination is needed to avoid performance losses and test errors

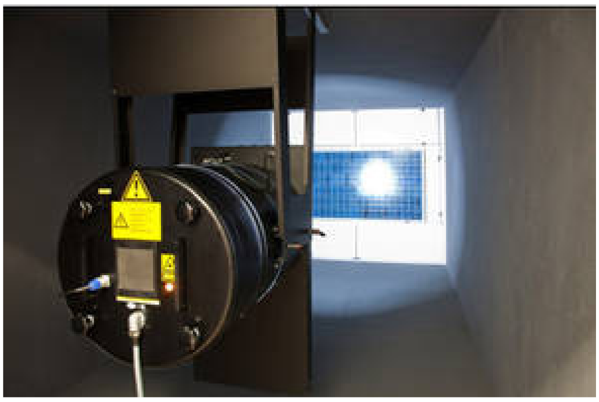

The spectral mismatch caused by the differences of the simulator spectrum to the standard spectrum in conjunction with different spectral responses of reference and test cell is potentially significant error source for all devices.

Cell test (III)

Quality indicator	Methode	Classification A	Classification B	Classification C
Non-uniformity of ir radiance	Monitoring of irradiance distribution in the test area. Calculation from measured Min/Max values of irradiance	<2 %	<5%	<10%
Spectral match to AM 1.5 reference spectral Irradiance (IEC 60904-3)	Ratio of irradiance contributions of 6 wavelength ranges (400-500-600-700-800-900-1100): Solar simulator/AM 1.5 reference	0.75 to 1.25	0.6 to 1.4	0.4 to 2.0
Temporal stability of emitted light (LTI = Long Term Instability)	Monitoring of irradiance at a fixed position in the test area. Calculation from Min/Max values during I-V data acquisition time	<0.5%	<2 %	<10%

Quality of Solar Simulator is of fundamental importance in PV testing

During the I-V data acquisition sweep irradiance is normally not completely stable
but subject to fluctuations. As the photocurrent generation of cells follows these fluctuations, an irradiance correction of each I-V data point to the target irradiance level is required.

Cells and modules (I)

Singol cells are typically electrically connected in series to constitute a module.

Typical modules are constituted by 60-90 cells in series and module dimensions are often around 1x1.6m. First modules for off grid generation required at least some 20-30 cells in order to have as a series enough voltage to recharge lead accumulators.

The cell has typical size of 100cm^2 and rectangular or esagonal shape. In nominal condition the silicon cell delivers (irradiance 1000 W/m^2) 3A at 0.5V hence with a rated power of 1.5W

CELLS

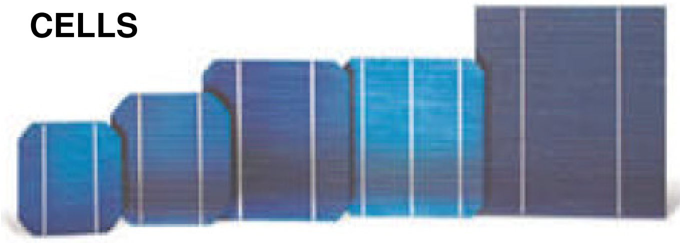

Cells and modules (II)

Mono crystal cells (c-Si) employs high purity semiconductors with theoretical lattice disposition. Monocrystal ingots (dia around 15cm) are grown according to a complicated and expensive procedure at the end of which thin 200-300μm wafers are obtained.

The production of polycrystalline cells is less demanding: in this case the pure silicon is solidificated into a multi crystal/ multy orientation ingot. Due to the presence of defects at crystal boundaries, the efficiency is lower than monocrystal cells.

Amorphous silicon (a-Si) and other thin film cells based on other semiconductors (e.g. cadmium telluride CdTe, copper indium diselenide CIS and CIGS with gallium) have very thin thicknesses and can be deposited onto different substrates like glass or plastic, even on non flat surfaces. A-Si cost per kWp is ... re 10% max

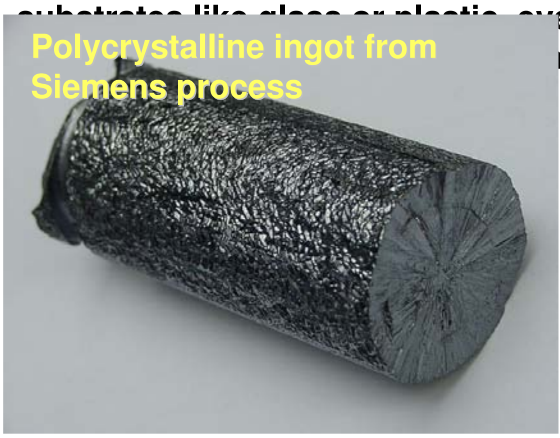

Best CdTe cells achieved (2014) efficiencies close to 20% and these cells have the shortest energy payback time

CIGS demonstrated to be able to work with concentration at 30% efficiency otherwise close to 20% at 1 sun

Cells and modules (IIb)

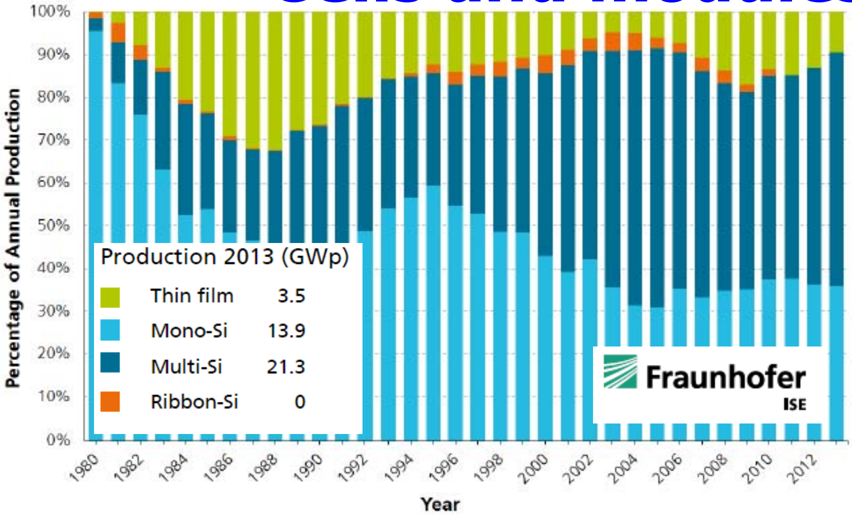

Multi and mono Silicon technology still accounted for about 90% of the total production in 2013.

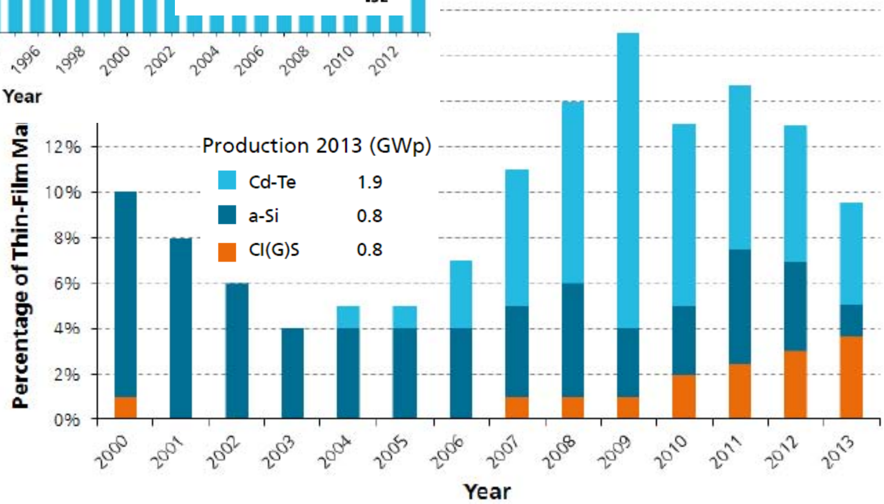

Cells and modules (III)

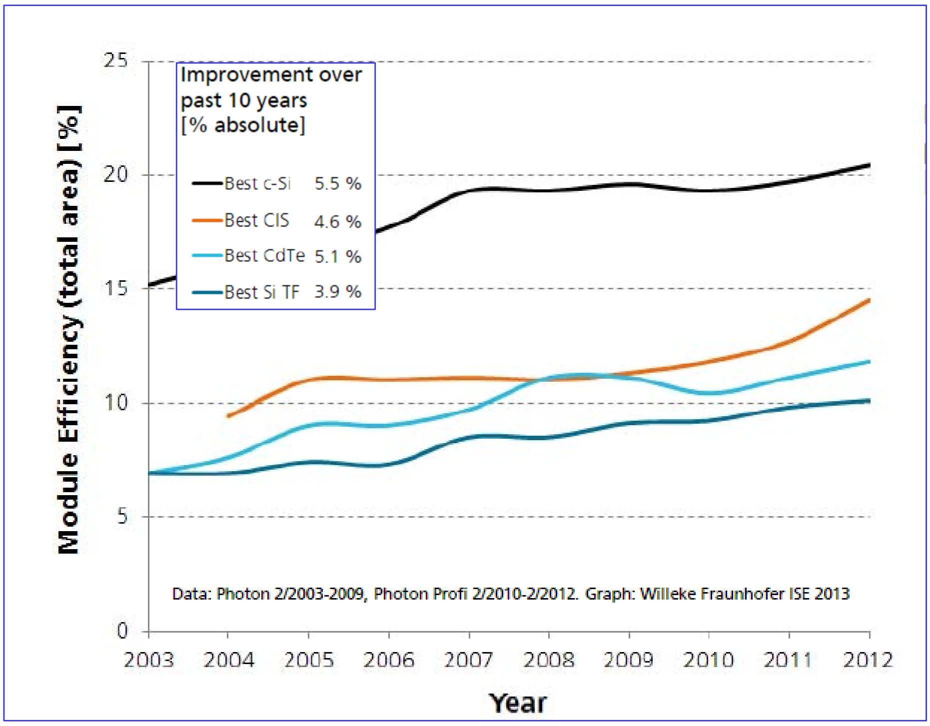

Cells and modules (IIIB)

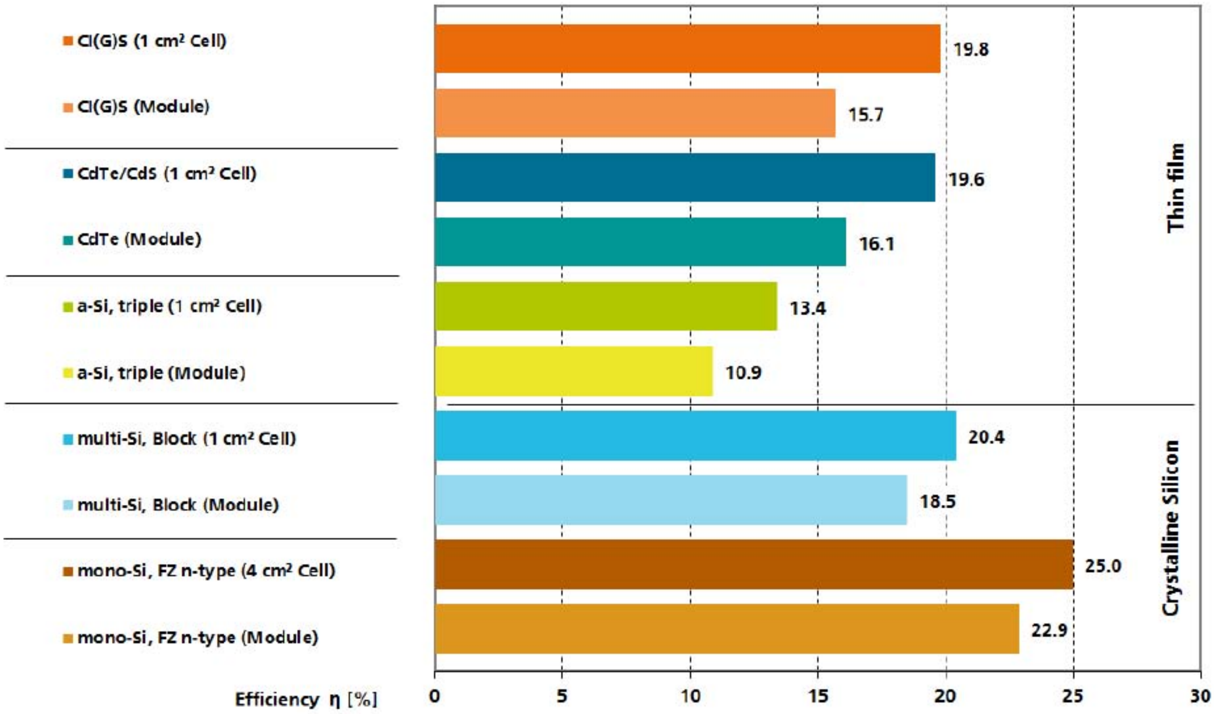

Data: Green et al.: Solar Cell Efficiency Tables,(Version 1-43), Progress in PV: Research and Applications 2014. Graph: PSE AG 2014

Cells and modules (IV)

Metallurgical grade silicon: purity 99% (2N)

Base material is quartz silica

Electronic grade silicon : Purity 99,9999 (6N)

Electronic grade Si EG-Si

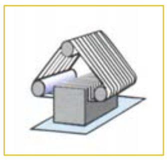

Solar grade Silicon: purity 99,99 (4N)

Ingots and Wafers

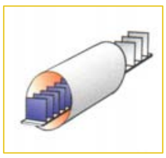

PV cell

Silicon process

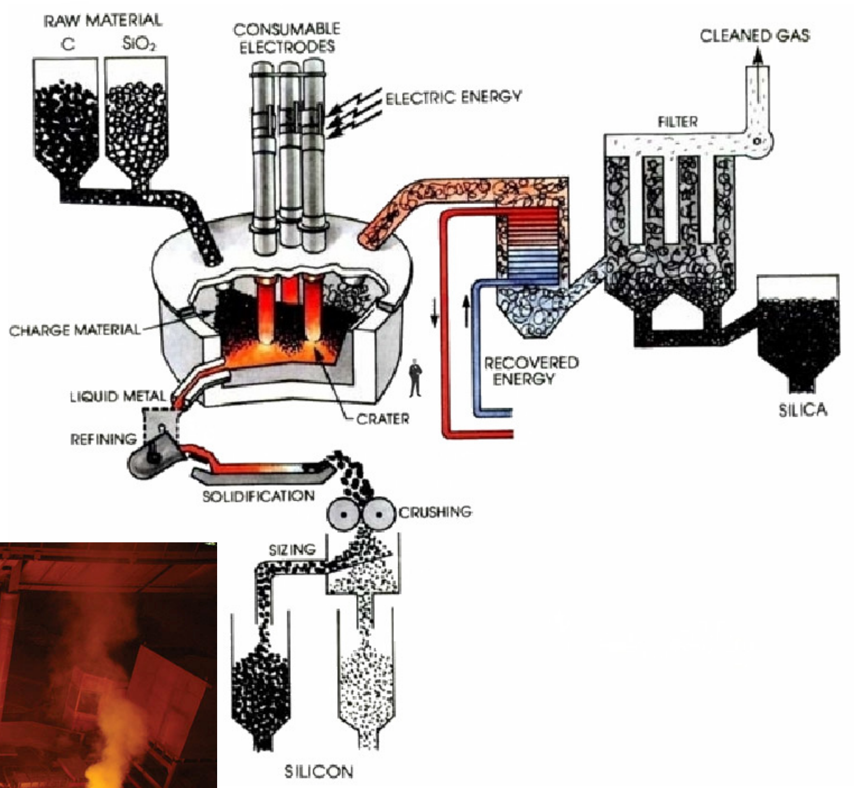

Schematics and picture of a metallurgical grade silicon production plant (Source Elkem Silicon, Norway)

Silicon process (IIb)

Czochralski (CZ) Process for (mono) crystal growth

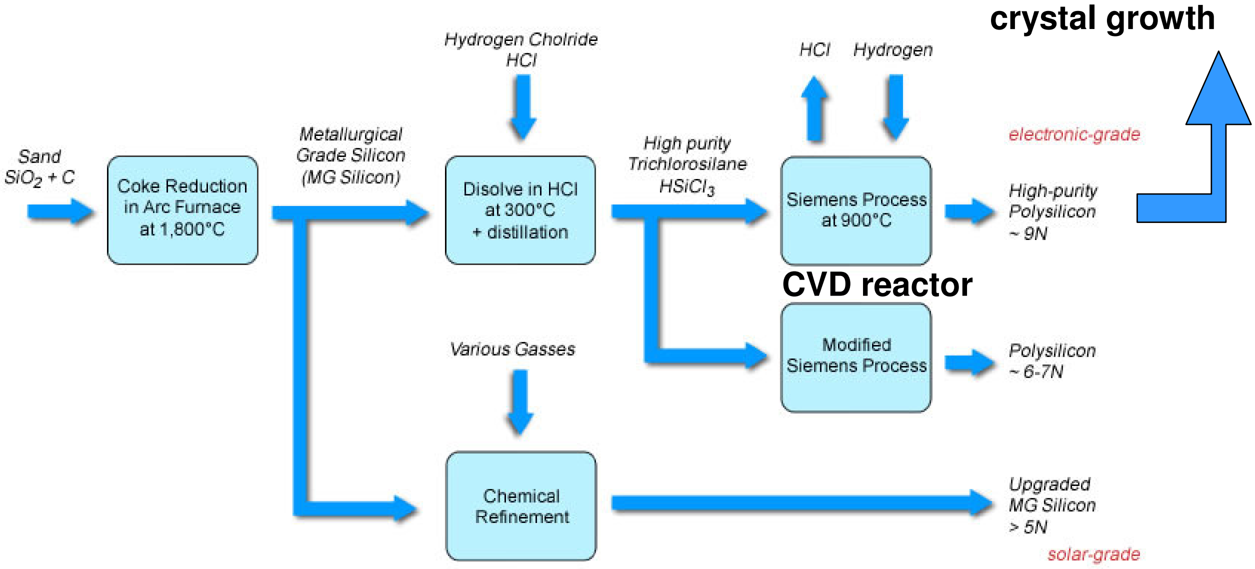

Silicon process (IV)

Czochralski Process (CZ)
Silicon with a single, continuous crystal structure is grown from a small seed crystal that is slowly pulled out of a polysilicon melt into a cylindrical shaped ingot (Czochralski process).
Process is run under inert gas atmosphere (Ar, CO e SiO). Molten Si is kept at 1420°C in a quartz crucible

Il processo si basa su una camera a vuoto (o contenente gas inerti come per croglioli di grande dimensione) dove polisilicio di opportuna pezzatura viene fuso in un crogiolo di quarzo alla temperatura di circa 1420°C.
Quando il polisilicio è completamente fuso ed amalgamato, un monocristallo di inseminazione (seed crystal) viene calato nel crogiolo fino a toccare la parte liquida e subire la parziale fusione della parte terminale. Il cristallo di inseminazione viene mantenuto in lento movimento di rotazione e successivamente sollevato, per dar luogo ad un lingotto avente la forma di un solido di rotazione, che cristallizza in maniera ordinata (monocristallo).

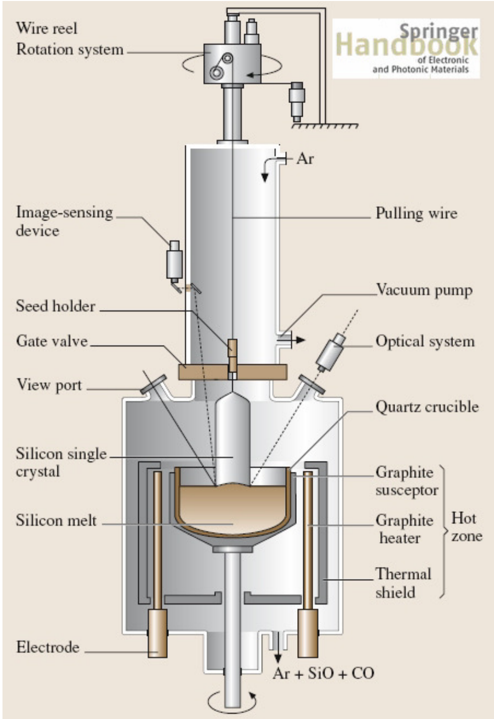

Cell wafering

The Ingot is cut by the way of wire saws. Cutting action is done by a slurry carrying abrasive material (silicon carbide 5~30 μm Dia). Wire diameter is around 120-160microns. Wafer thickness is about 200microns

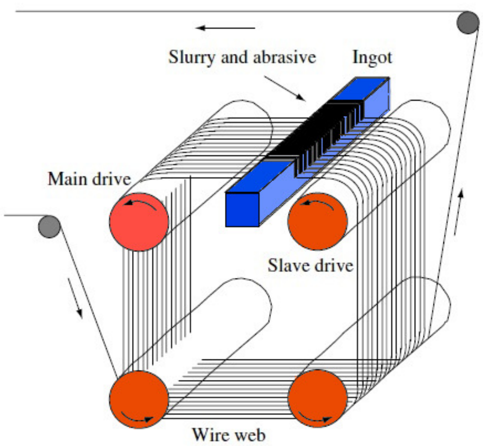

Taglio del lingotto
Il taglio del lingotto in sottili strati (wafer) è preceduto in genere dalla *squadratura* del lingotto medesimo, con una taglia standard 10x10 cm^2. Il taglio del lingotto in strati sottili è effettuato con macchine multifili, dove fino a 700 fili metallici, guidati da rulli scanalati, eseguono il taglio grazie all'apporto di materiale abrasivo.

L'abrasivo utilizzato per il taglio è polvere di carburo di silicio (dimensioni 5~30 μm), miscelata in un liquido (*slurry*) che solitamente è glicole polietilenico (PEG). La dimensione dei fili (in acciaio inossidabile, spesso rivestito da ottone) è in genere compresa tra 120 e 160 μm.

Negli ultimi anni si è assistito alla riduzione dello spessore del wafer da 325 a circa 200 μm.

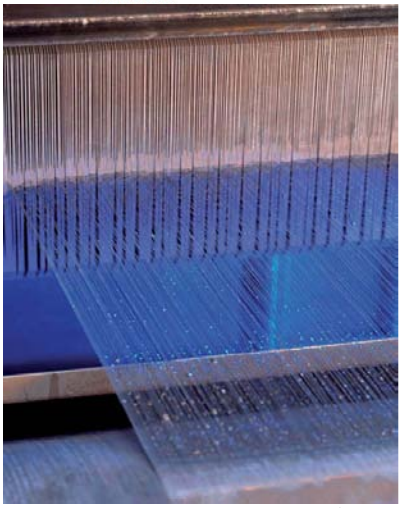

Top Commercial modules

SIGNATURE™ BLACK
X21 - 335 PANEL

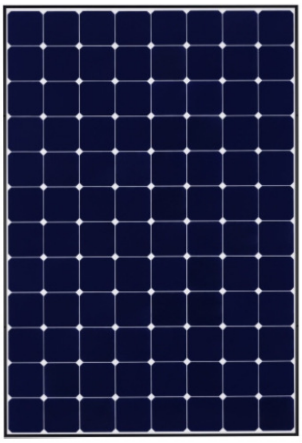

X21 - 345 PANEL

ELECTRICAL DATA	X21-335-BLK	X21-345
Nominal Power[12] (Pnom)	335 W	345 W
Power Tolerance	+5/−0%	+5/−0%
Avg. Panel Efficiency[13]	21.1%	21.5%
Rated Voltage (Vmpp)	57.3 V	57.3 V
Rated Current (Impp)	5.85 A	6.02 A
Open-Circuit Voltage (Voc)	67.9 V	68.2 V
Short-Circuit Current (Isc)	6.23 A	6.39 A
Maximum System Voltage	600 V UL ; 1000 V IEC	
Maximum Series Fuse	20 A	
Power Temp Coef. (Pmpp)	−0.30% / °C	
Voltage Temp Coef. (Voc)	−167.4 mV / °C	
Current Temp Coef. (Isc)	3.5 mA / °C	

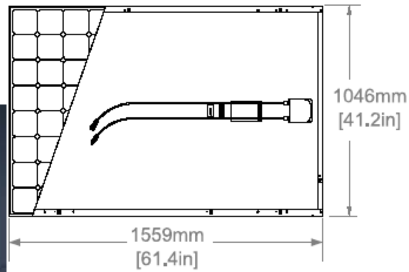

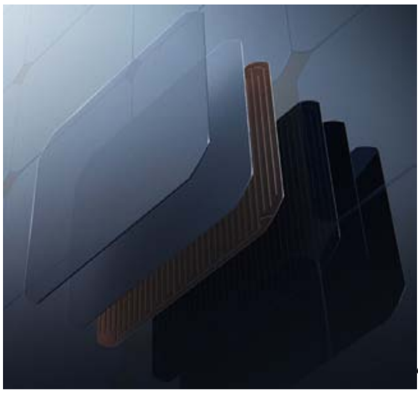

Fingerless technology front electrode and back copper electrode

Cells, Energy Payback period

“To calculate payback, Dutch researcher Alsema reviewed previous energy analyses and did not include the energy that originally went into crystallizing microelectronics scrap. His best estimates of electricity used to make nearfuture, frameless PV were 600 kWh/m2 for single-crystalsilicon modules and 420 kWh/m2 for multi-crystalline silicon.

Assuming 12% conversion efficiency (standard conditions) and 1,700 kWh/m2 per year of available sunlight energy (the U.S. average is 1,800), Alsema calculated a payback of about 4 years for current multicrystallinesilicon PV systems.

Projecting 10 years into the future, he assumes a solar-grade silicon feedstock and 14% efficiency, dropping energy payback to about 2 years.”

U.S. Department of Energy
Energy Efficiency and Renewable Energy

Figure 1. Energy Payback for Rooftop PV Systems

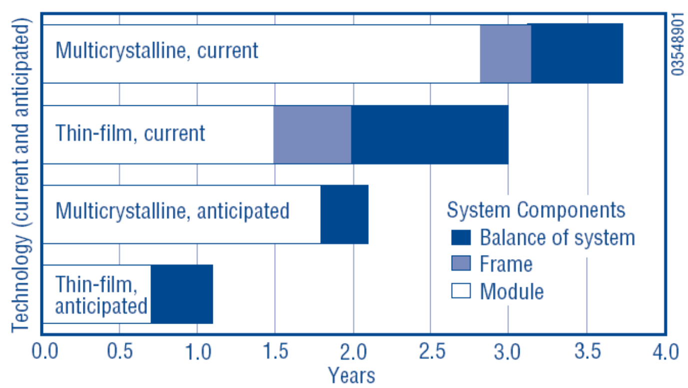

Reaping the environmental benefits of solar energy requires spending energy to make the PV system. But as this graphic shows, the investment is small. Assuming 30-year system life, PV systems will provide a net gain of 26 to 29 years of pollution-free and greenhouse-gas-free electrical generation.

Figure 2. Cumulative Net Clean Energy Payoff

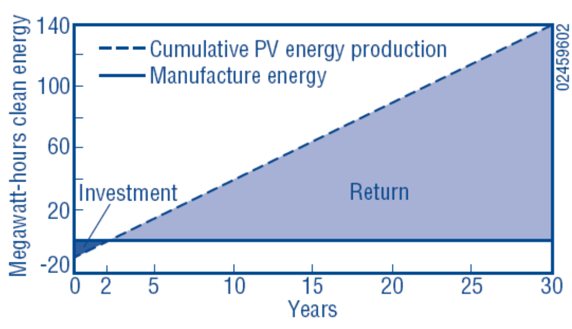

Cells, Energy Payback period

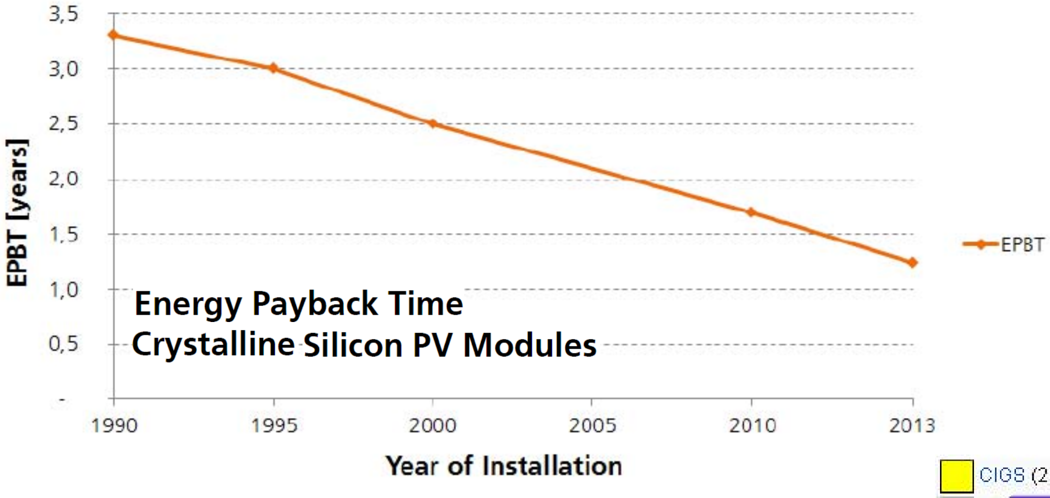

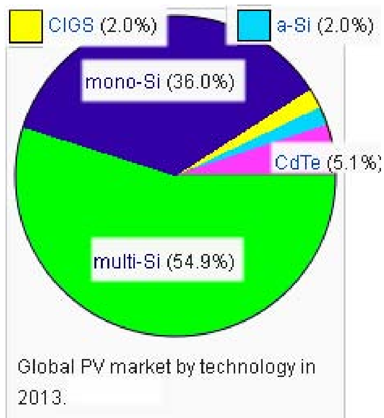

Global PV market by technology in 2013.

Elettronics (IV)

Module strings connected in parallel

The inverter system convert DC to AC current and provide the proper load for allowing the modules to work at their MPP

This control is named Max Power Point Tracking (MPPT)

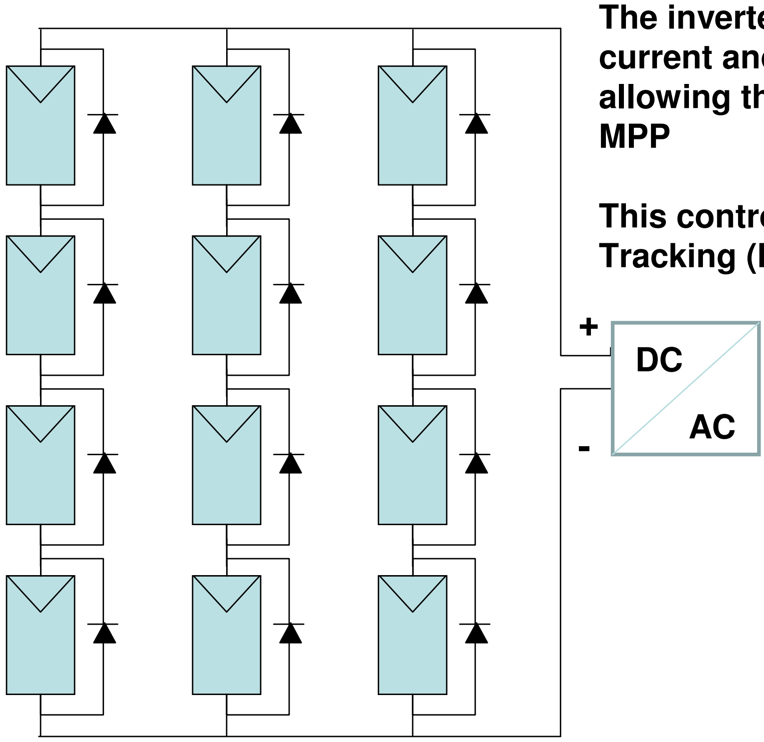

Inverter/converter market

Inverter / Converter	Power	Efficiency	Market Share (Estimated)	Remarks
String Inverters	Up to 100 kWp	98%	~ 50%	• ~ 15 €-cents /Wp • Easy to replace
Central Inverters	More than 100 kWp	Up to 98.5%	~ 48 %	• ~ 10 €-cents /Wp • High reliability • Often sold only together with service contract
Micro-Inverters	Module Power Range	90%-95%	~ 1.5 %	• ~ 40 €-cents /Wp • Ease-of-replacement concerns
DC / DC Converters (Power Optimizer)	Module Power Range	Up to 98.8%	n.a.	• ~ 40 €-cents /Wp • Ease-of-replacement concerns • Output is DC with optimized current • Still a DC / AC inverter is needed • ~ 0.75 GWp installed in 2013

Fraunhofer ISE

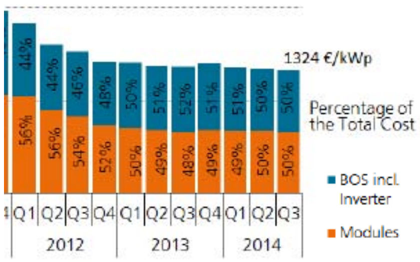

Data: BSW-Solar. Graph: PSE AG 2014

Elettronics (IX)

$$0.8 \times P_{PV} < P_{INV\,DC} < 1.2 \times P_{PV}$$

Field/string Power (PV) and Inverter power (INV DC)

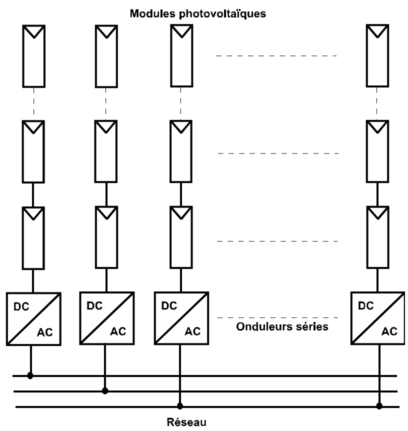

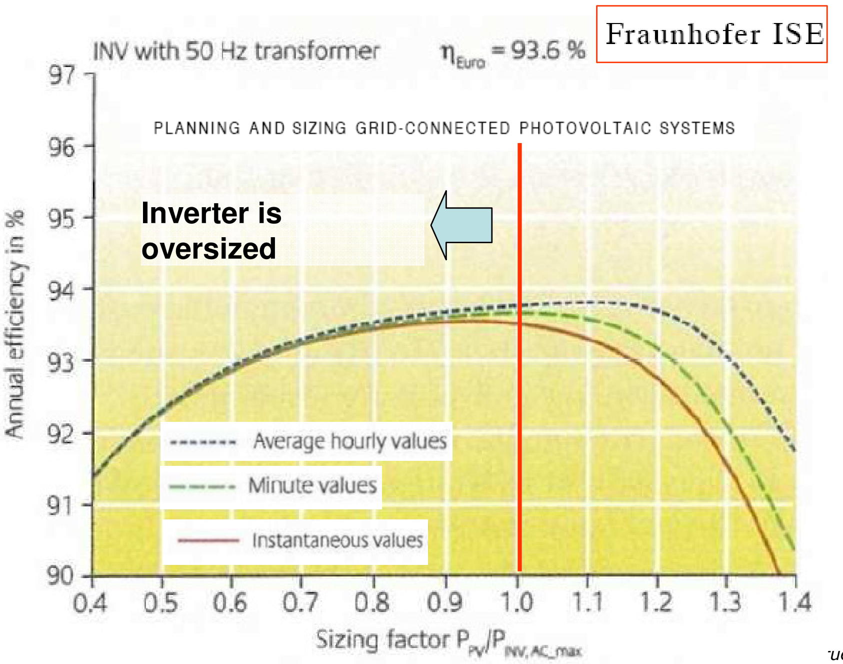

$$c_{INV} = \frac{P_{PV}}{P_{INV\,AC}}$$

Sizing factor

$$0.83 < c_{INV} < 1.25$$

Costs, module trend

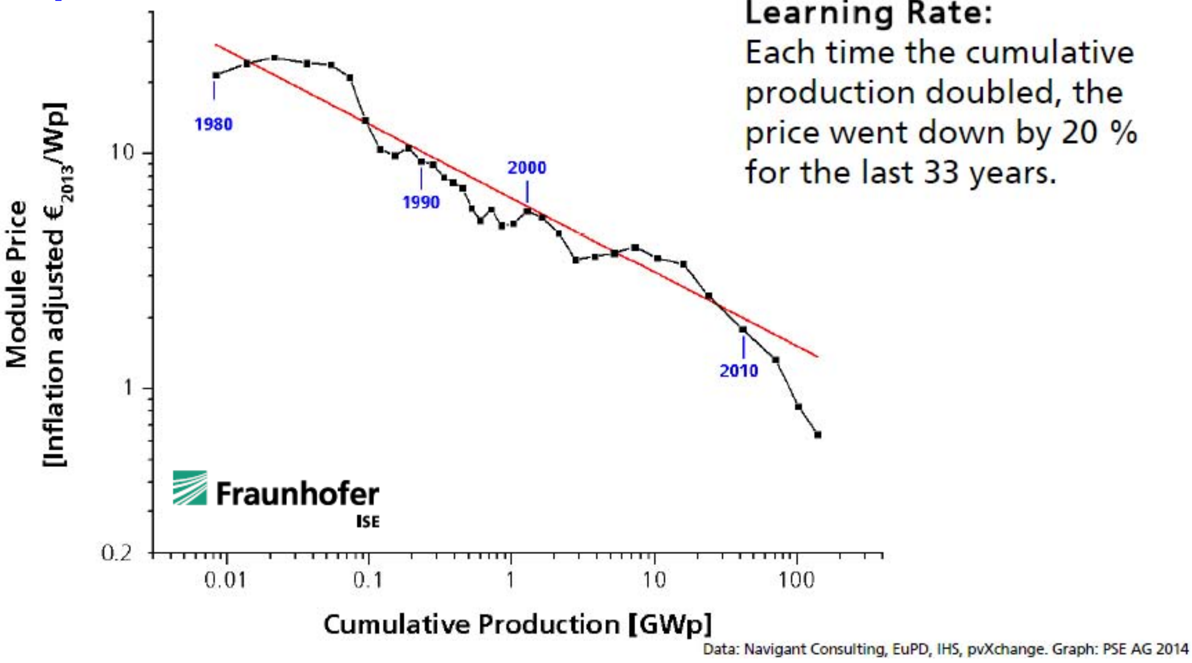

Learning Rate:
Each time the cumulative production doubled, the price went down by 20 % for the last 33 years.

Costs, small rooftop systems (in Germany)

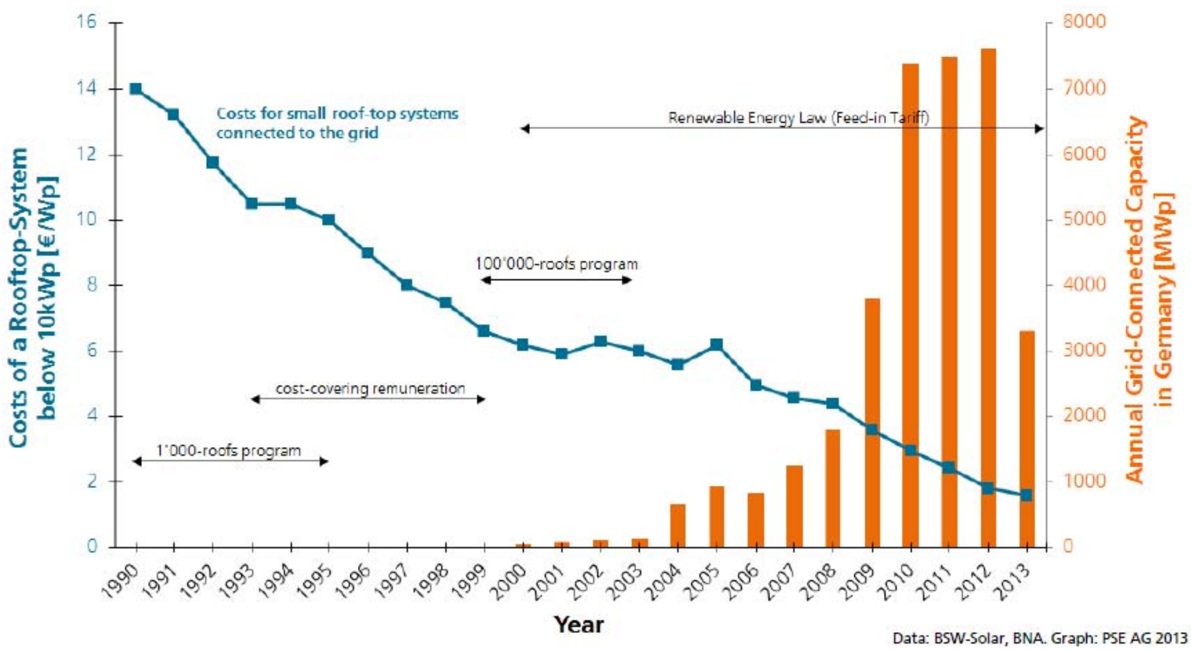

Costs, medium size systems (in Germany)

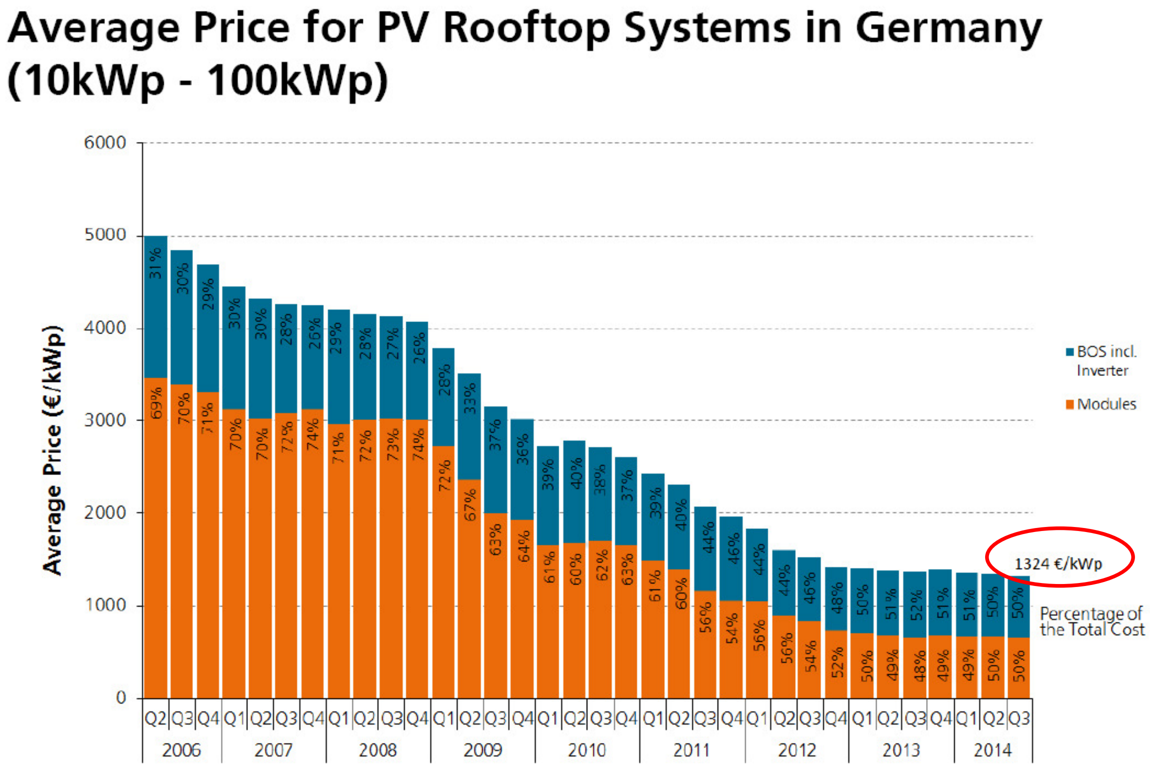

Renewable Energies

Energy from the earth, Geothermal Heat Pumps

Heat from Earth (I)

More than 99% of earth mass has a temperature greater than 1000 °C. Only 0.1% of earth mass is cooler than 100 °C

The type of geothermal application depends on the temperature level of the geothermal reservoir. For a normal geothermal temperature gradient (about 3 °C per 100 m), the type of application is related to the depth :

- 0 – 1000 m heating with heat pumps;
- 1000 – 3500 m heating without heat pumps (aquifers);
- 3500 – 6000 m hot dry rock systems, heat and power production.

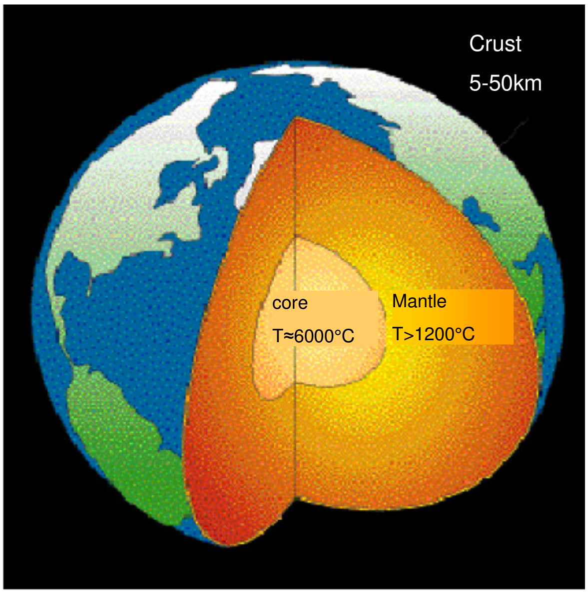

Geothermal systems

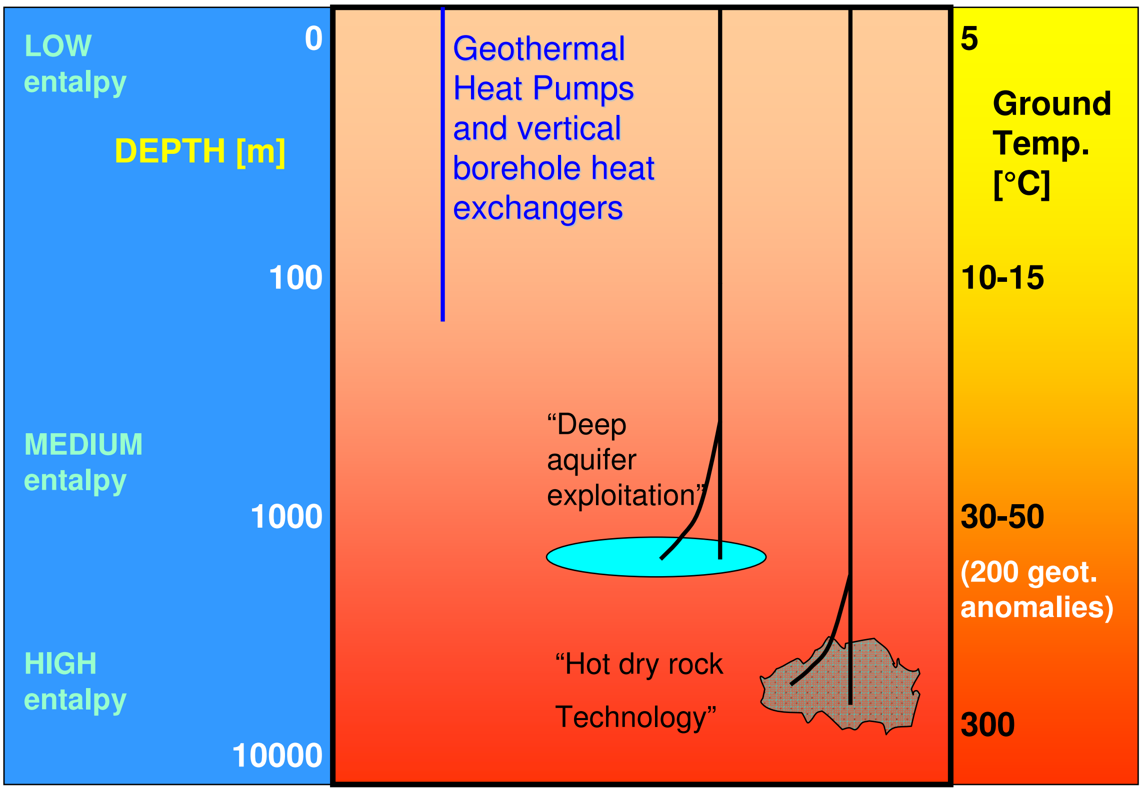

Country	Power (MWe)		Energy yield per year (GWh/anno)		ΔProduz. 2010-2012
	2010 (a)	2012 (a)	2010 (b)	2012 (c)	(GWh/anno)
USA	3005	3152	15.219	~ 16.000	+ 781
Filippine	1966	1966	9929	9900	(-29)
Indonesia	1197	1307	9357	10.250	+ 893
Messico	958	983	6618	6800	+182
Italia	882	875	5340	5590	+ 250
Nuova Zelanda	731	731	5833	5830	(-3)
Islanda	575	664	4465	5160	+ 695
Giappone	536	536	2632	2620	(-12)
Kenia	170	216	1453	1900	+ 447
Costa Rica	164	207	1176	1480	+ 304
El Salvador	204	204	1525	1520	(-5)
Nicaragua	90	159	302	~ 600	+ 298
Turchia	94	94	668	650	(-18)
Russia	82	82	505	500	(-5)
Papua-N.Guinea	56	56	400	395	(-5)
Guatemala	40	49	271	330	+59
Cina	24	24	162	160	(-2)
Portogallo	25	23	197	180	(- 17)
Francia	16	16	110	108	(-2)
Etiopia	7,3	7,3	18	17	(-1)
Germania	6,6	6,6	28	27	(-1)
Austria	1,4	1,4	~ 1	~ 1	circa 0
Tailandia	0,3	0,3	~ 2	~ 2	circa 0
Australia	0,1	0,1	~ 1	~ 1	circa 0
TOTALE	10.830	~ 11.360	66.212	~ 70.023	3811

Heat from Earth

High temperature and electricity production

UGI bullettin 2013)

Heat from Earth, HDR

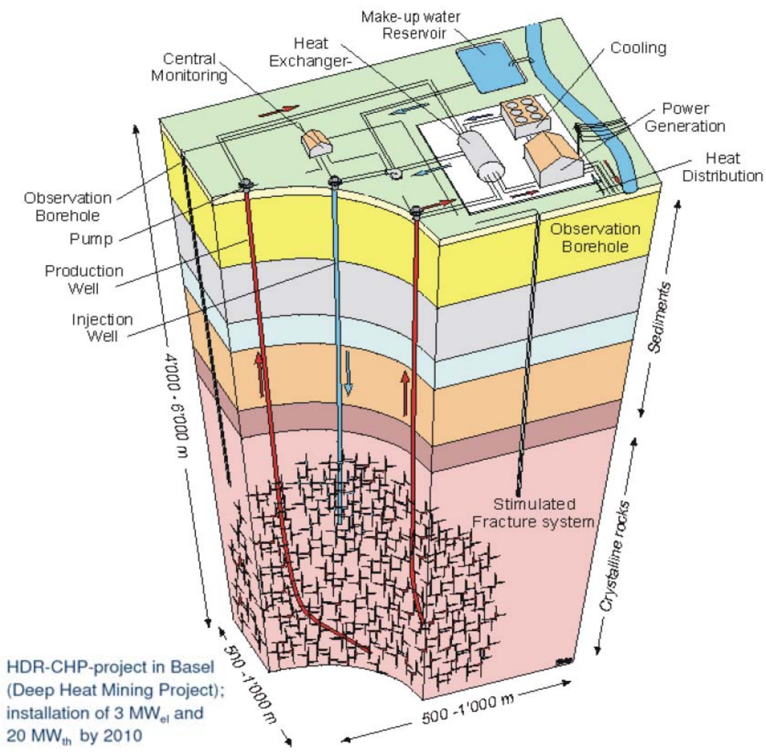

Hot Dry Rock è technology is expected to make available high temperature geothermal heat to be available in most areas.

Drilling to deep layers (4000-6000m) should allow to reach high temperature rocks, where, in principle, articially induced fracturing and water pumping would be able to provide steam for a Rankine cycle

Several technical and ecomimical issues are still to be properly addressed

Heat from Earth, Deep aquifers

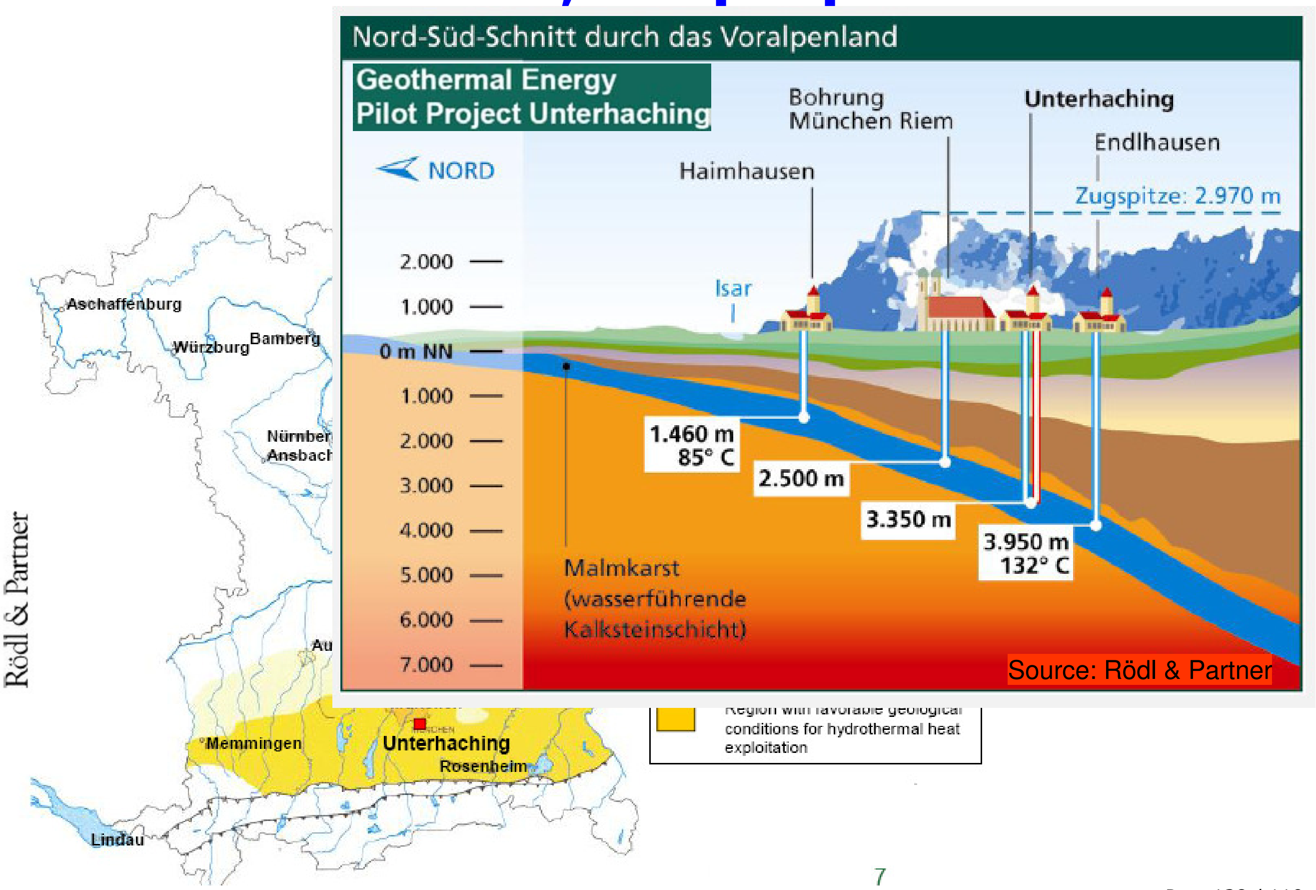

Heat from Earth, Deep aquifers (II)

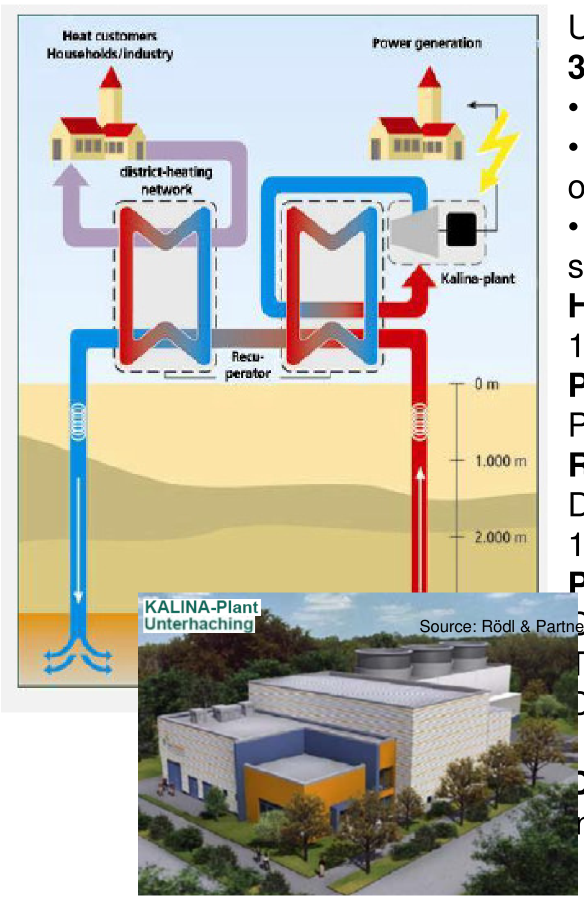

Utilization of **thermal water** from a depth of **3,350 m**

• production of up to **38 MWt**

• installation of a power plant with the capacity of **3.36 MW_{el}**

• first construction phase **28 MWt,** second construction phase **40 MWt**

Heat Exchanger:
1 x Heat supply, 1 x Electricity supply

Pump and Turbine Installations:
Pilot pump, at technical limit actually

Reinjection Well:
Drilling plan: depth: 3,300 m, Diameter casing: 16 inch

Production Well:
Depth: 3,350 m, Production rate: 150 l/s, Temperature 122°C; Thermal Water Pipeline / District Heating: Length: 3.6 km app. 10 km

District supply of Unterhaching (22,000 inhabitants) in the long run (70 MW)

High Temperatures Geothermal Heat, Italy (I)

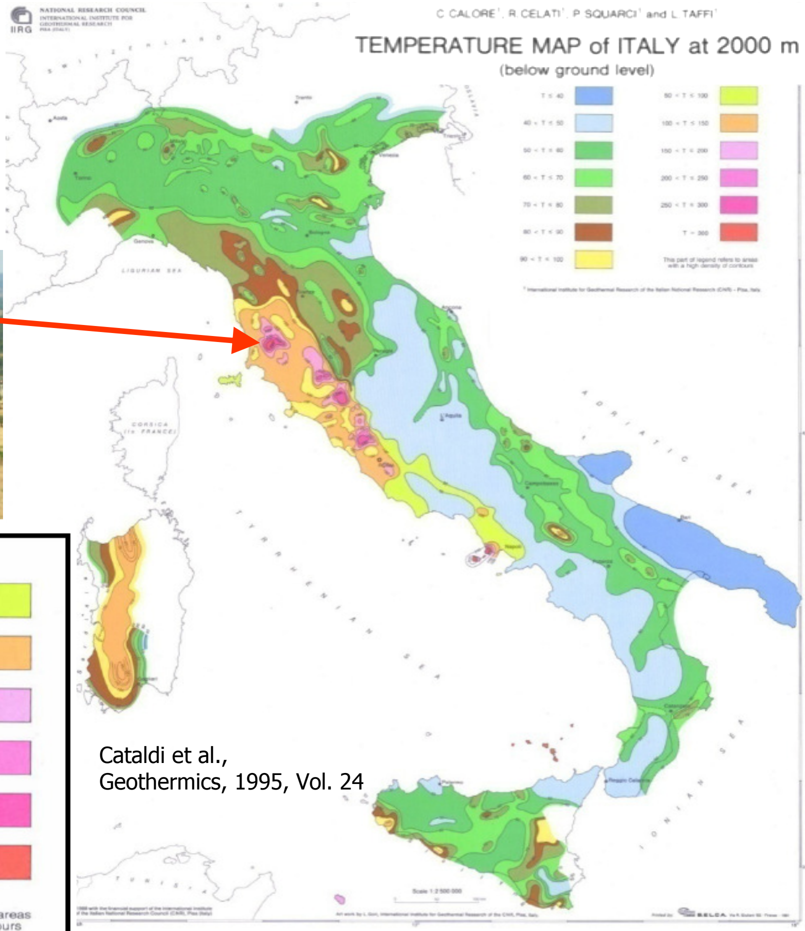

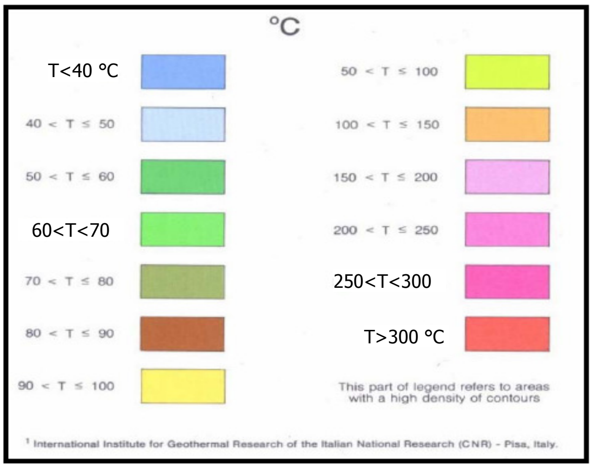

Cataldi et al., Geothermics, 1995, Vol. 24

Geothermal Heat, Italy (Larderello)

• Potenza geotermoelettrica installata complessiva	MW 810,5
• Produzione netta complessiva nell'anno 2006	TWh 5,2

Fig. 5 - Un pozzo di vapore ed il vapordotto che alimenta una centrale elettrica nell'area di Larderello, Toscana. In primo piano l'impianto di boccapozzo (valvole di intercettazione, di misura e campionamento).

Medium temperature Geothermal Heat, Italy

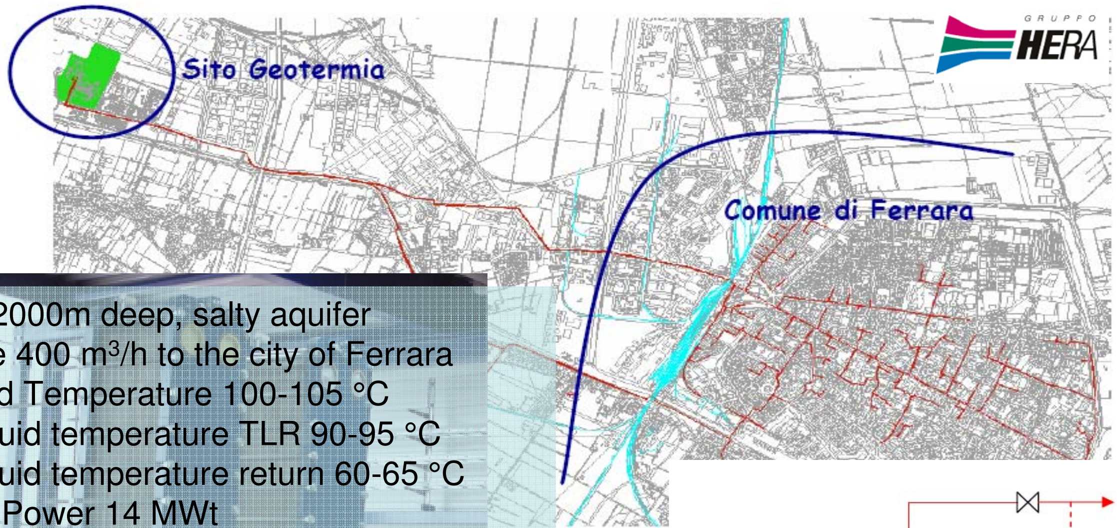

- 2 wells, 2000m deep, salty aquifer
- Flow rate 400 m^3/h to the city of Ferrara
- Geo Fluid Temperature 100-105 °C
- Carrier fluid temperature TLR 90-95 °C
- Carrier fluid temperature return 60-65 °C
- Thermal Power 14 MWt
- Continuous operation for Domestic Heating

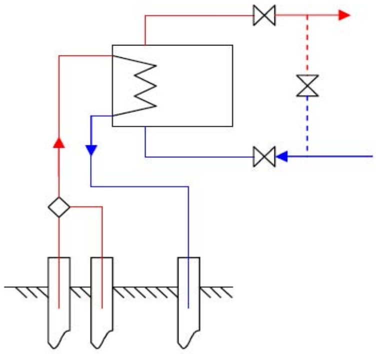

Extraction wells Inject. well

Low Entalpy Geothermal systems: Ground Source Heat Pumps

Geothermal Heat Pumps (GSHP) are systems able to exploit the favorable ground temperatures for building heating and cooling. When they employ vertical borehole heat exchangers (BHE) they work in closed loop mode (Ground Coupled Heat Pumps, GCHP)

Closed Loop
(Ground heat exchangers)

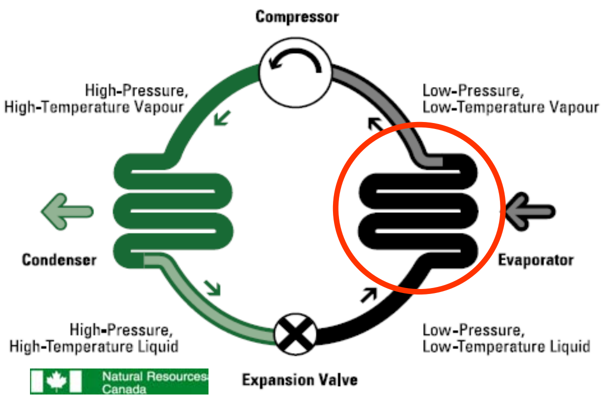

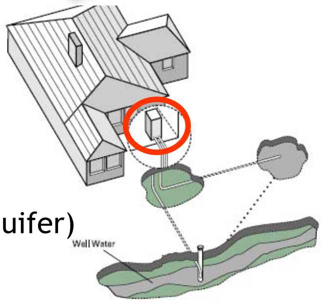

Open Loop (aquifer)

CO_2 Emissions (UE data):
- 0.53 kg/kWh Electric Heater
- 0.26 kg/kWh Gas Burner
- **0.13** kg/kWh **GCHP** with COP= 4

Heat Pumps

Performance of HP are measured in terms of **Coefficient of Performance COP**

In winter operating mode (heat pumps mode)

COP_{pdc}=Heat at high temp. Source (Condenser)/(Mech. Energy, compressor)

In summer operating mode (cooling mode)

COP_{c}=Heat at low temp. Source (evap.)/(Mech. Energy, compressor)

Geothermal HP = Lower temp. Source is ground or aquifer

Scroll compressor

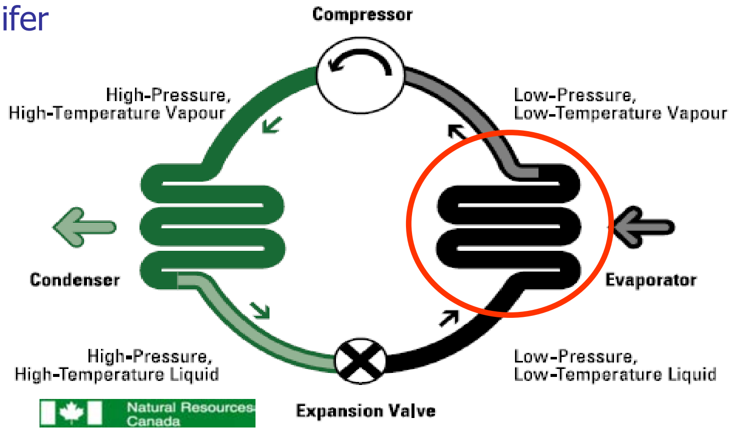

Heat from:
- Air
- Ground (closed loop circuit)
- Aquifers (open loop circuit)

Why GCHP ? (GCHP vs ASHP)

Energy Demand from buildings inevitably increases with decreasing external temperatures. In this condition the efficiency of air source heat pump (ASHP) decreases as well for second law reasons. On the other hand the stable ground temperatures allow the GCHP to be less influenced by building energy demand and they can work at high efficiency even at low external air temperatures

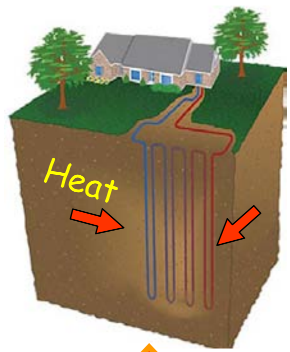

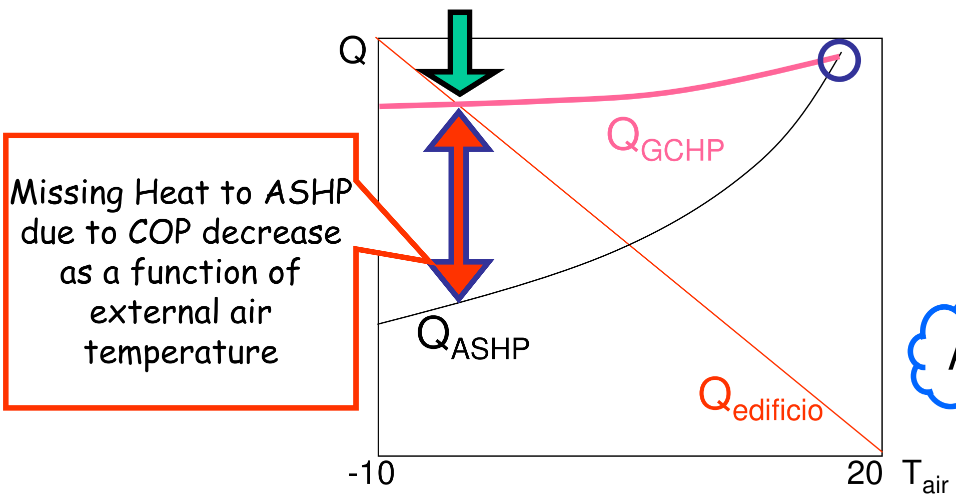

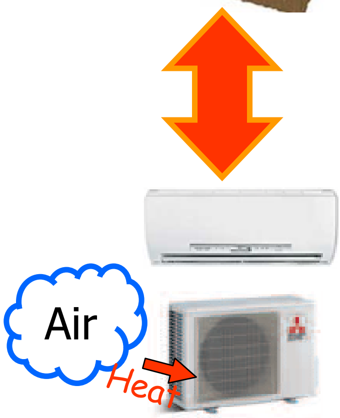

GCHP vs ASHP (air source HP)

$Q_{ground} = Q_{build}(COP-1)/(COP)$ **Winter Mode**

$Q_{ground} = Q_{build}(COP+1)/(COP)$ **Summer Mode**

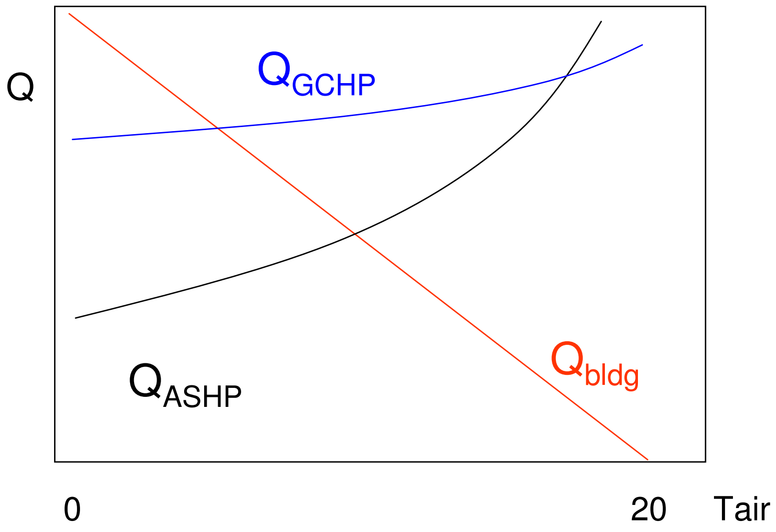

Ground water HP (2012, Lombaria Building, Milano, Italy)

Extraction wells	8	-
Well depth	50	m
Water Flow rate	320	liters/s
Water temperature (from/to)	15 // 6	°C
Water temp. (cooling mode)	15 // 22	°C
Heat pumps number	3	-
Heating power	3x2150	kW
COP, winter mode	4.5	-
COP, summer mode	6	-

Horizontal ground heat exchangers

Borehole (vertical) Heat Exchangers, BHE

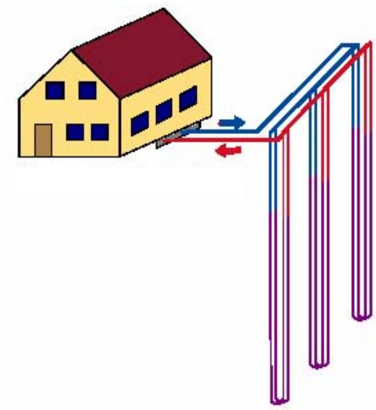

BHE - types

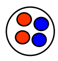

Single BHE

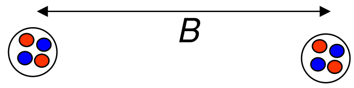

Double BHE

BHE resi stance [K/W m] – BHE Diameter 0.11 m, Tubo PE DN 25 PN10 – Typical values for turbulent pipe flow					
Pipe Spacing [mm]	BHE type	Grout conductivity [W/m K]			
		0.7	1	1.5	2.0
70	Single U	0.134	0.109	0.0893	0.0785
70	Double U	0.0762	0.0627	0.0515	0.0454
50	Single U	0.182	0.142	0.110	0.0936
50	Double U	0.127	0.0995	0.0774	0.0659

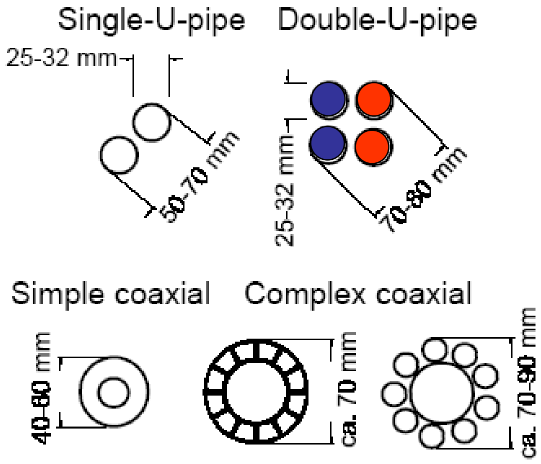

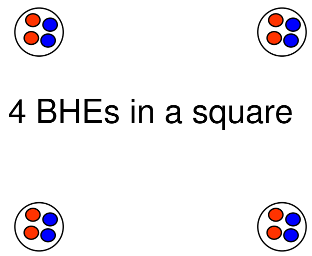

BHE components

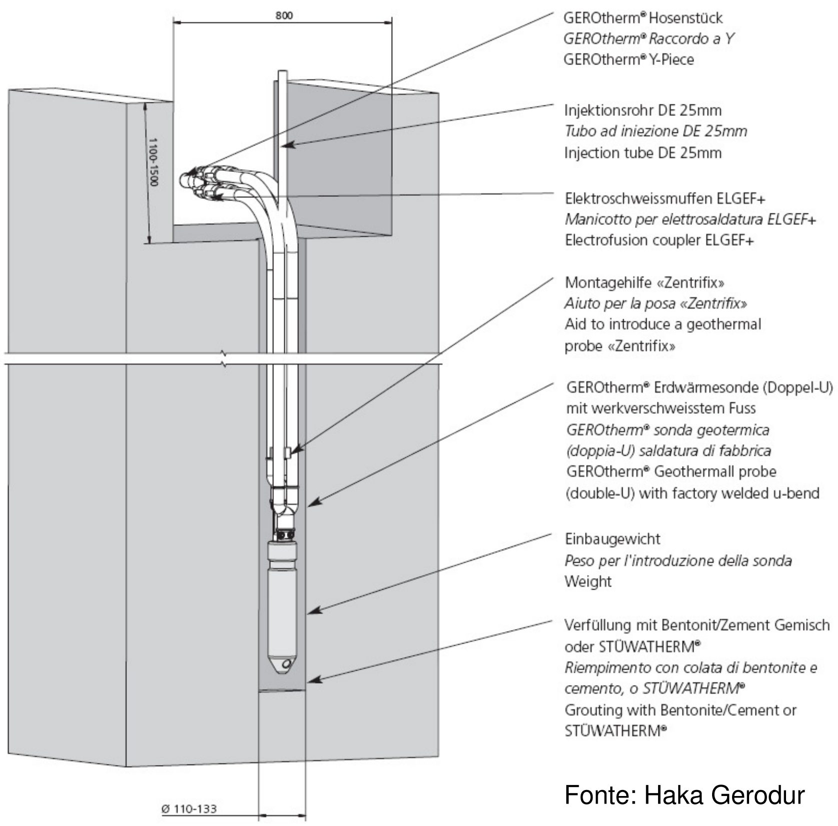

Fonte: Haka Gerodur

BHE components (II)

HAKA.GERODUR AG
Giessenstrasse 3
CH-8717 Benken SG

Telefon +41 (0)55 293 25 25
Telefax +41 (0)55 293 25 26

sekretariat@hakagerodur.ch
http://www.hakagerodur.ch

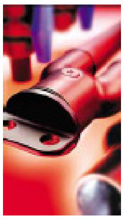

Distanziatore per sonde geotermiche

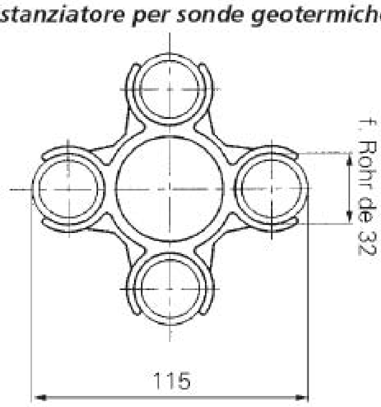

Drilling and installing BHEs

GeoPiles for structural and thermal purposes

Dock Midfield, 300 geopiles

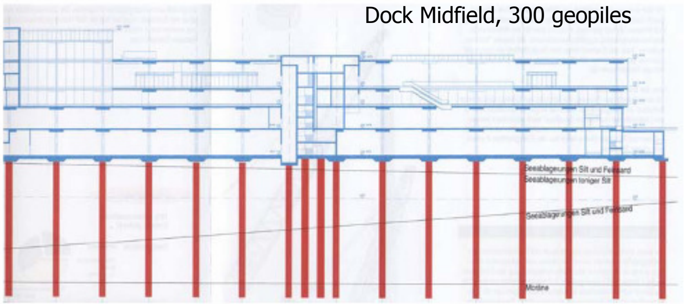

Dock Midfield, Zurigo airport (Ref. D.Pahud, www.isaac.supsi.ch)

free cooling, no compressor power (Dock Midfield, 58000m2, year 2006, 580 MWh/yr)

GHP in Europe

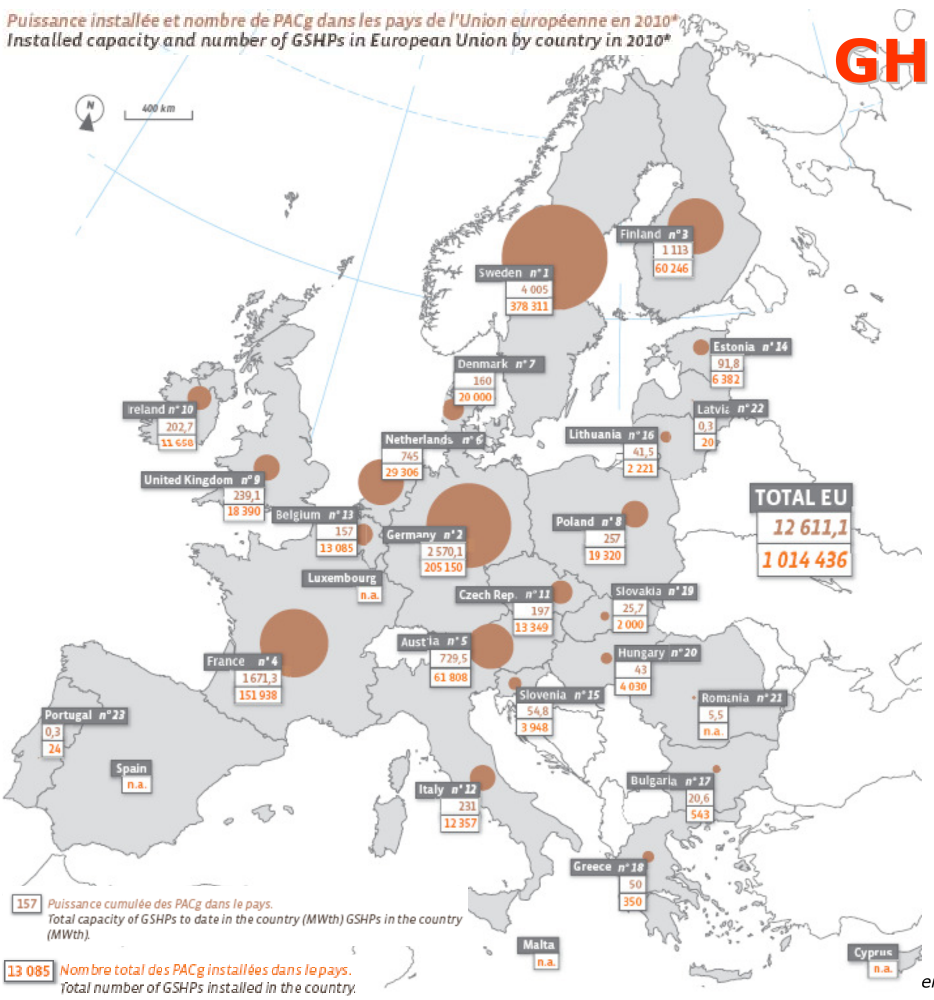

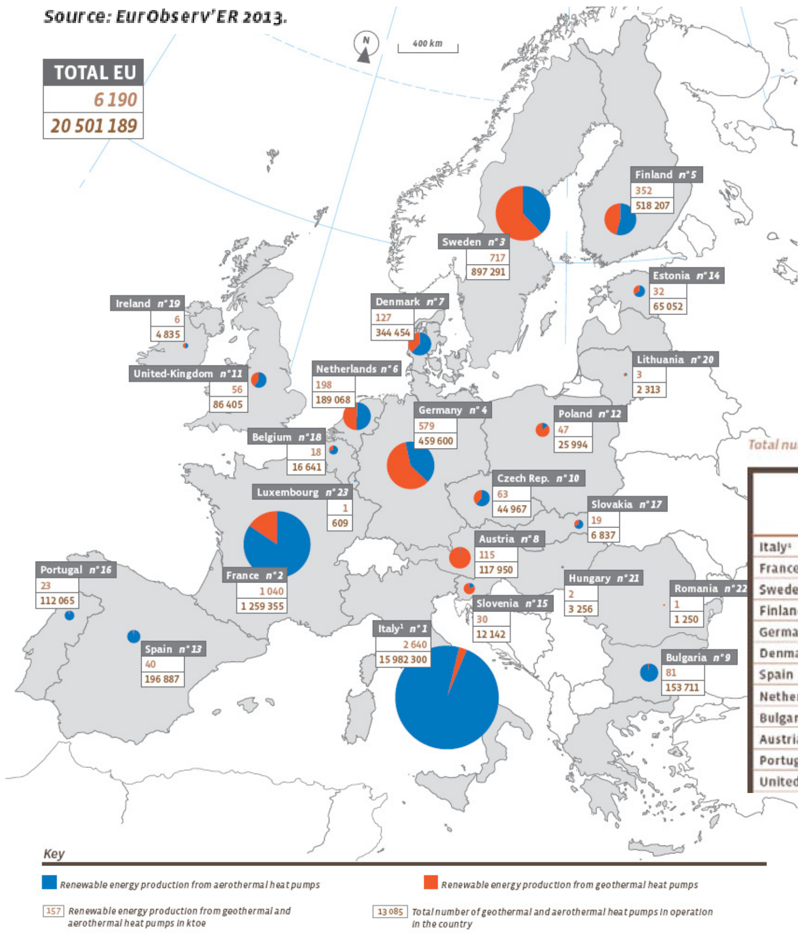

GSHP and ASHP in Europe

Total number of heat pumps in operation in 2012 in the European Union and associated rene

	Aerothermal HP	Renewable heat aerothermal (ktoe)	Geothermal HP	Renewable heat geothermal (ktoe)
Italy¹	15 972 000	2 580	10 300	61
France	1 136 310	879	123 045	161
Sweden	654 233	274	243 058	442
Finland	445 787	212	72 420	140
Germany	194 800	235	264 800	344
Denmark	308 119	79	36 335	48
Spain	195 989	39	898	1
Netherlands	147 815	100	41 253	98
Bulgaria	149 962	79	3 749	2
Austria	4 317	1	113 633	114
Portugal	111 374	22	691	1
United Kingdom	68 645	34	17 760	23

GHP in Sweden

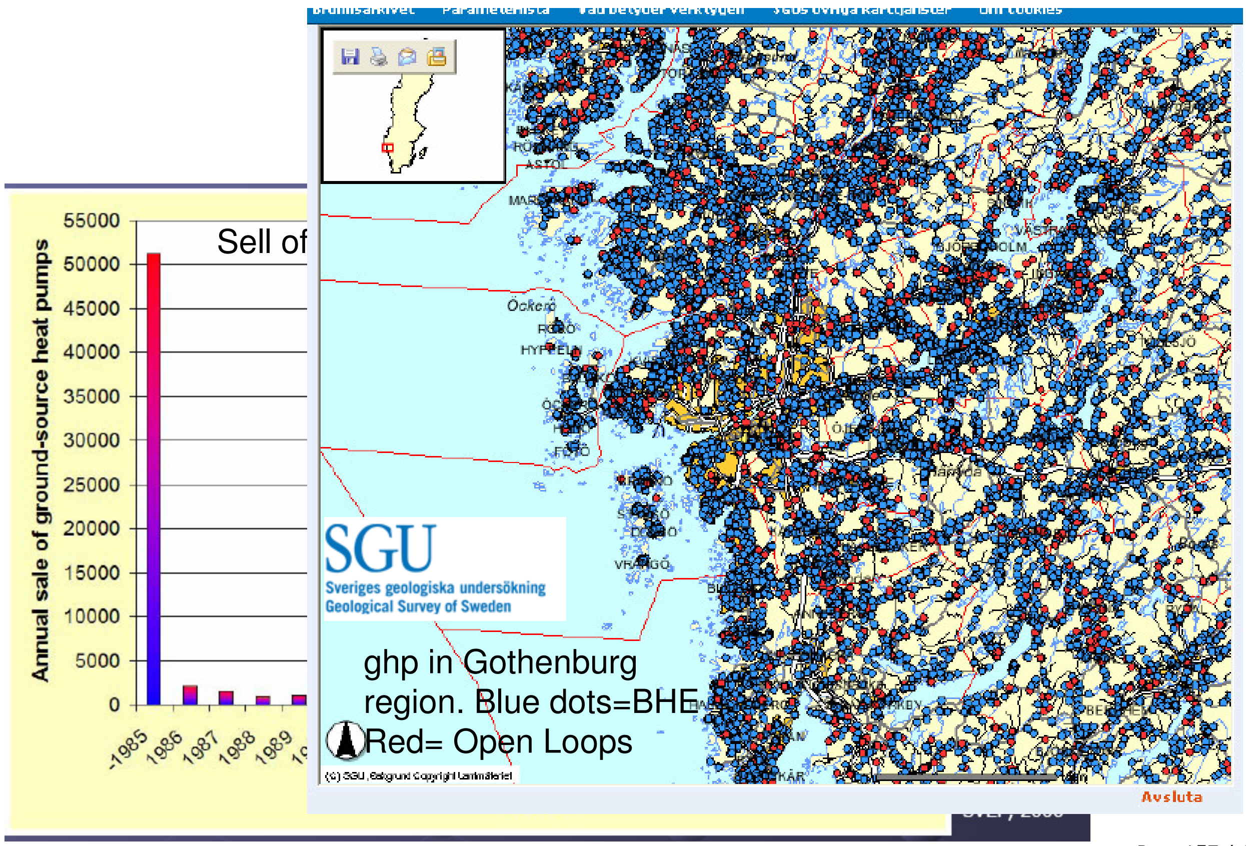

Ground temperature vs depth and season (I)

Reliable Ground temperature measurements started in the XVIII century. In Paris observatory cellar (depth 28m) Lavoisier started the measurements in 1782

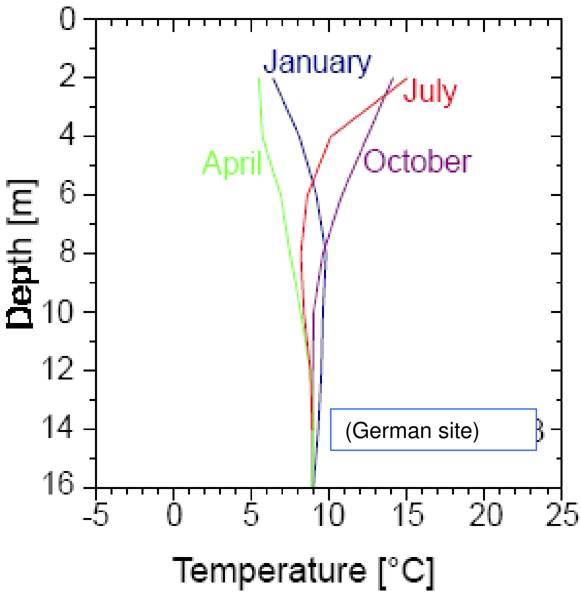

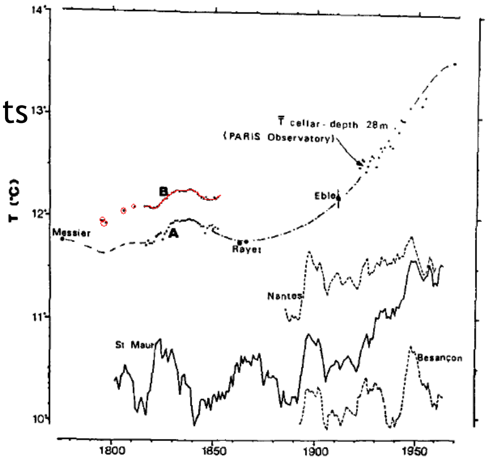

FIG. 1. Temperatures of the Paris Observatory cellar (A, annual mean of Gay-Lussac's thermometer; B, annual mean of Lavoisier's thermometer; dashed-dotted curve, probable secular evolution of temperature; and 10-year running means of annual air temperatures at three selected stations.

Ground temperature vs depth and season (II)

UNDISTURBED GROUND TEMPERATURE

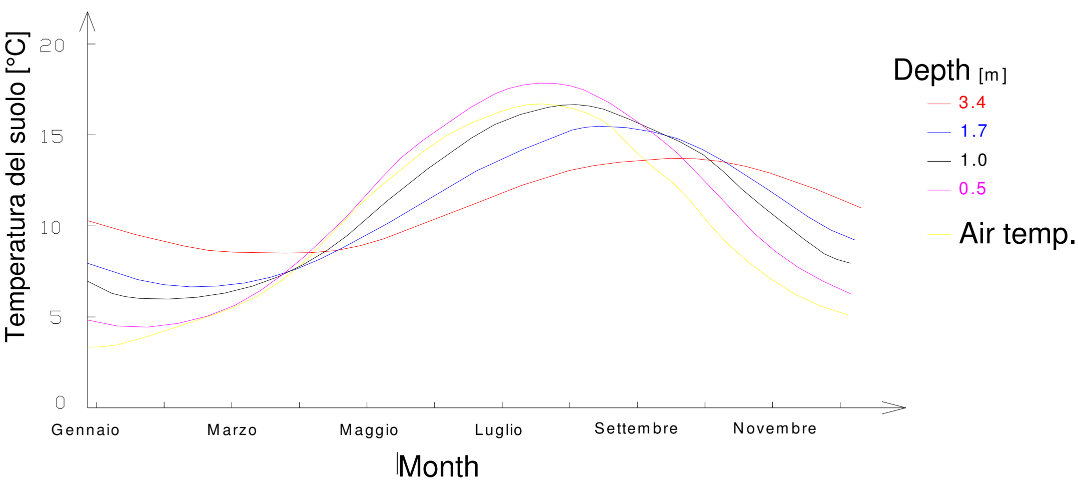

Ground (and air) temperature close to surface vs time

Ground Temperatures during Heat Extraction (I)

Extracted heat from BHEs in the early and medium period satisfies an Energy Balance which mainly accounts for the ground heat capacity and the phenomenon is a fully transient one.
In the long term the exctracted heat is balanced by surrounding ground heat conduction, top surface heat gains (insolation, rain percolation, air heat transfer), eventually aquifer heat transfer.

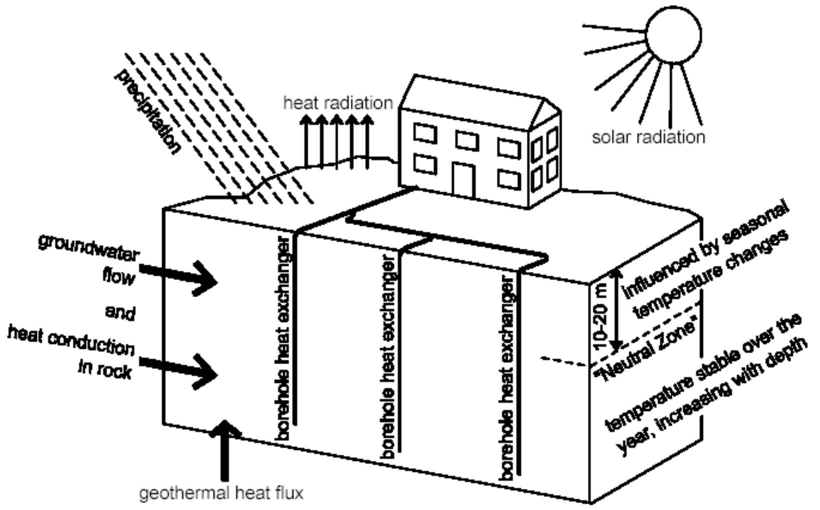

BHE field design must take into consideration the transient nature of the heat exctraction mechanisms in order not to reach unsuitable ground temperatures for high COPs. Ground thermal regeneration (heat injection, as possible in summer working mode) mitigates the ground temperature decrease

Ground Temperatures and Heat Extraction (II)

The next pictures show a fundamental experiments in GCHP research of 20 yrs ago (Elgg, near Zurich). Ground Temperatures have been measured close to a 105m deep BHE at a radial distance of 0.5 and 1m and at different depths (1, 2, 5, 10, 20, 35, 50, 65, 85, and 105 m).

The experiment lasted 5 yrs and showed typical short (on/off cycles) and long term behaviour of the ground volume to the repeated sequences of heat extraction

Si può osservare che nel caso di una sonda singola, dopo qualche anno il processo di raffreddamento si esaurisce e il profilo di temperatura del terreno raggiunge un andamento stabile.
Gli andamenti di temperatura del terreno su scale temporali più brevi (ciclo di funzionamento orario, "attacca e stacca") sono decisamente diversi e mostrano gradienti di temperatura molto forti e differenze di temperatura tra zona indisturbata (far field) e strati immediamente adiacenti alla sonda fino a 5-10°C. Durante il ciclo di prelievo termico ha luogo infatti un notevole raffreddamento degli strati del suolo prossimi alla sonda, con una zona radiale interessata al fenomeno dell'ordine delle decine di centimetri. Questa medesima regione, durante le ore in cui la pompa di calore è inattiva ed il prelievo termico è azzerato, è sede di una risalita della temperatura (ciclo orario).

Ground temperature before and after heat extraction

Ground temperature profile 1m from BHE (Rybach e Eugster, 1997)

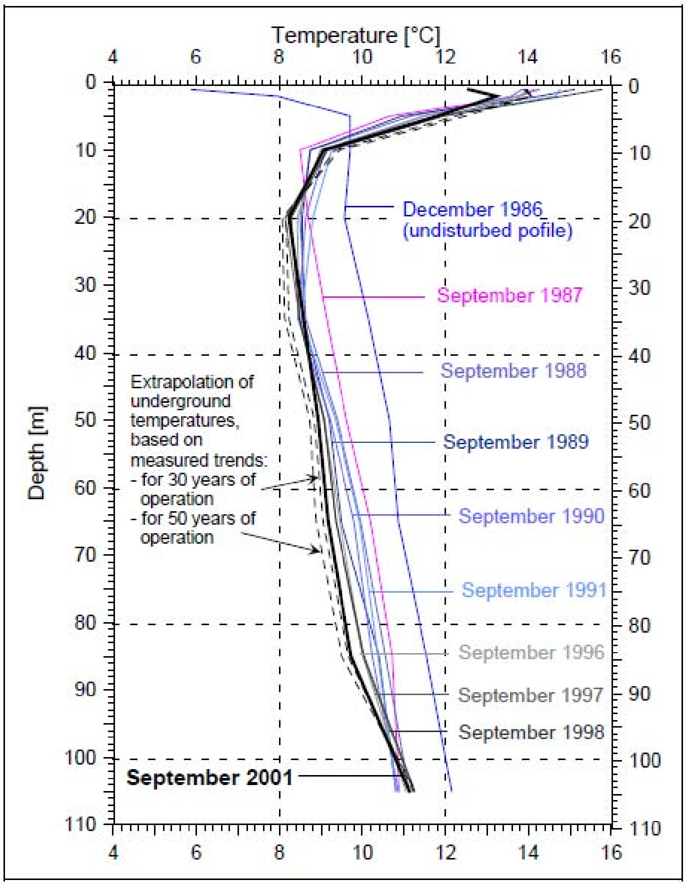

Ground temperature before, <u>during</u> and after heat extraction

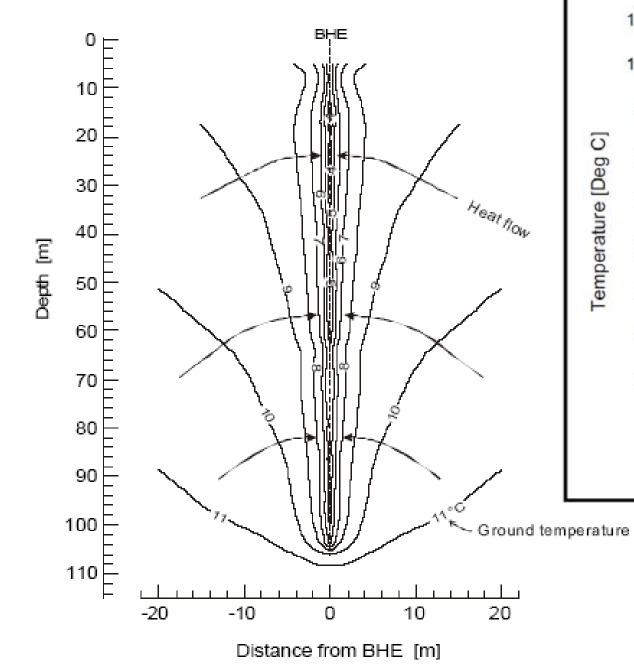

Isothermal profiles around a single BHE, 105m deep. Elgg, Zurich, (Source: Rybach e Eugster, 1997)

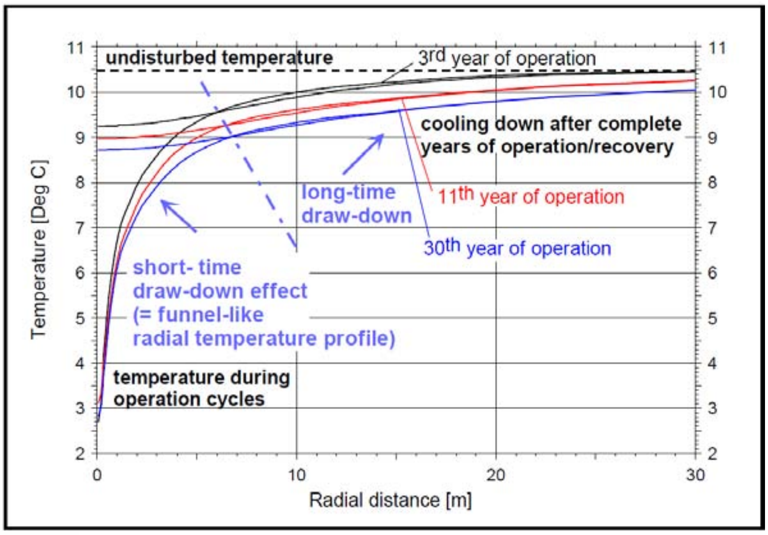

Profili di temperatura nel terreno intorno ad una sonda geotermica verticale (Funnel distribution, profilo ad imbuto)

Ground Temperatures and Heat Extraction (II)

The next pictures show a fundamental experiments in GCHP research of 20 yrs ago (Elgg, near Zurich). Ground Temperatures have been measured close to a 105m deep BHE at a radial distance of 0.5 and 1m and at different depths (1, 2, 5, 10, 20, 35, 50, 65, 85, and 105 m).

The experiment lasted 5 yrs and showed typical short (on/off cycles) and long term behaviour of the ground volume to the repeated sequences of heat extraction

Concering the short term transient (hourly scale), large temperature differences arise from far field, where the undisturbed temperature applies, and the BHE close surroundings (radial distances of order 0.1 meters), where ground temperature can drop of several degrees (5-10°C) depending on heat rate too. During the off cycles of the heat pump, a local heat recovery is observed in the near BHE ground

Ground temperature before and after heat extraction

Ground temperature profile 1m from BHE (Rybach e Eugster, 1997)

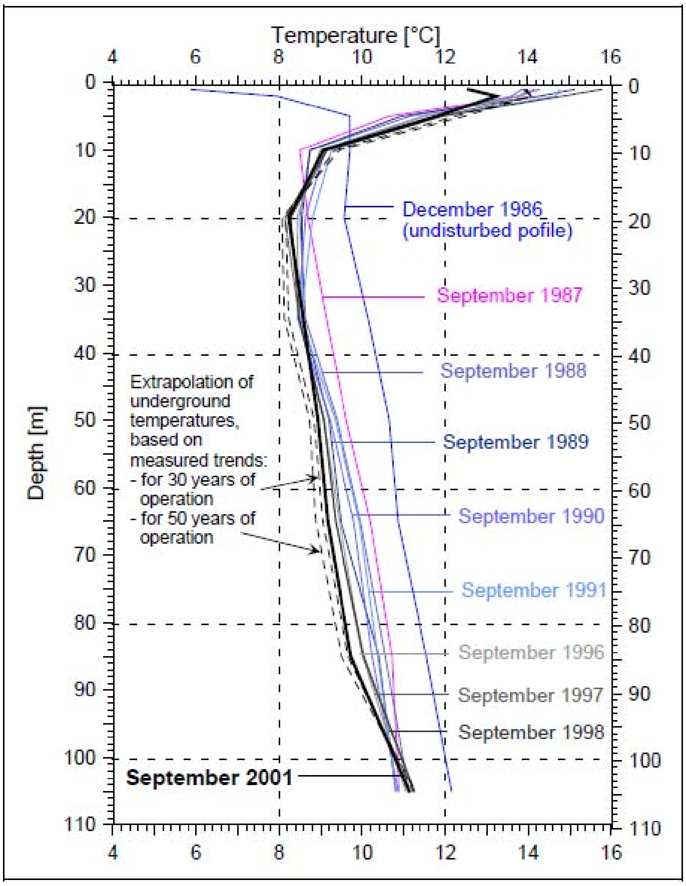

Ground temperature before, <u>during</u> and after heat extraction

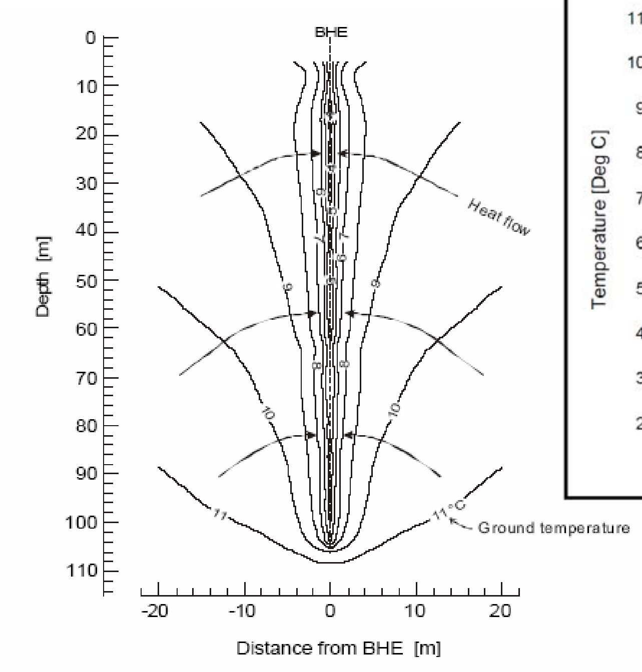

Isothermal profiles around a single BHE, 105m deep.
Elgg, Zurich, (Source: Rybach e Eugster, 1997)

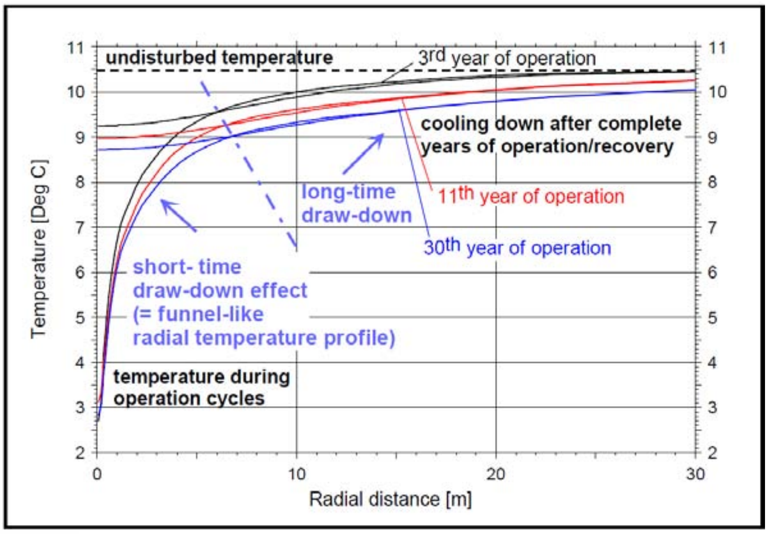

Temperature profile around a BHE in the short and long term (Funnel temperature distribution)

Two resistance model for GCHP simulation (I)

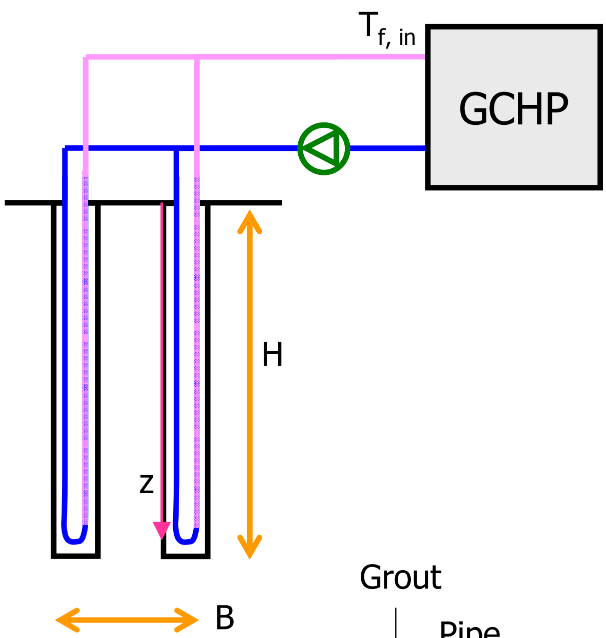

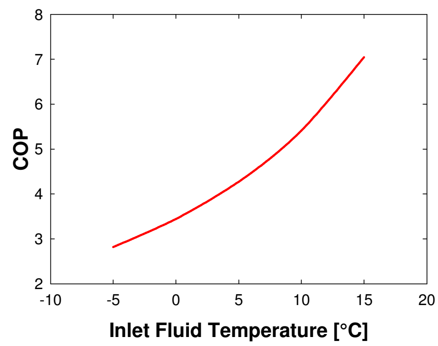

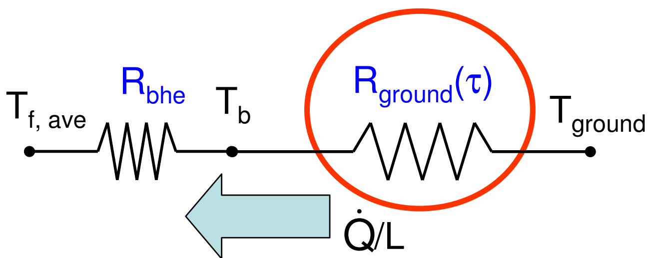

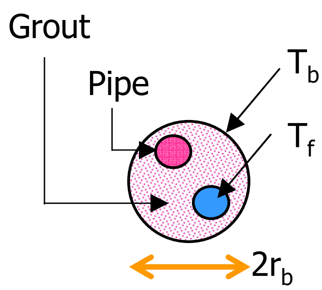

Two resistance model for GCHP simulation (II)

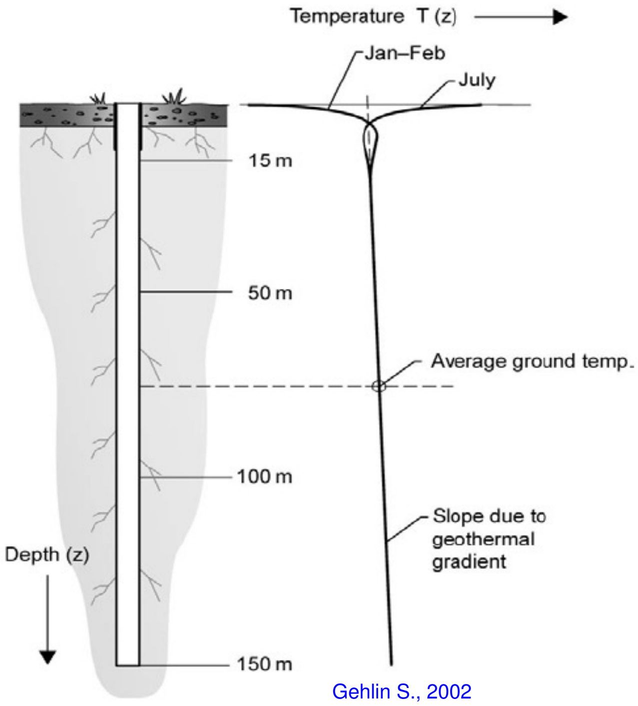

Undisturbed ground temperature, T_{ground}

•Depth < 15 m : Temperature variations according to seasonal fluctuations in air temperature $T_{air\ ext}$

•Depth~ 15 m
Ground Temp.= Yearly Ave $T_{air\ ext}$

•Depth > 15 m : Ground temp. increases with detph. Geothermal gradient is about 2-3°C every 100 m.

Ground Thermal response..

Courtesy of Prof. M. Bernier, EP Montreal

Conditions:
Borehole diameter = 6 inches
Ground conductivity = 2.1 W/m-K
Ground diffusivity = 0.08 m²/day
Far-field temperature = 10°C

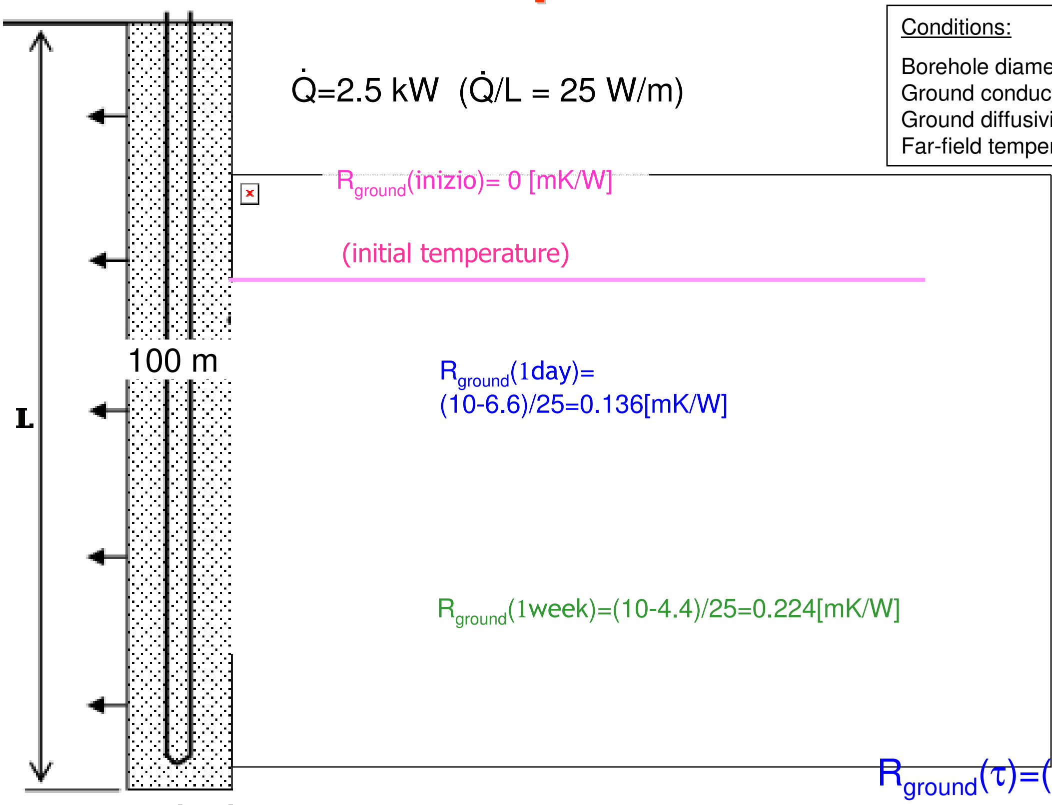

$R_{ground}(\tau)=(T_{bhe}-T_{gr})/(\dot{Q}/L)$

Two resistance model for GCHP simulation (III)

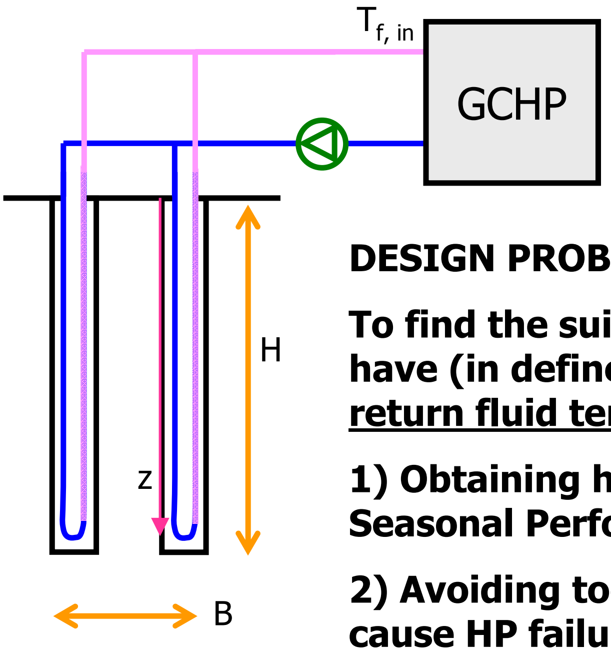

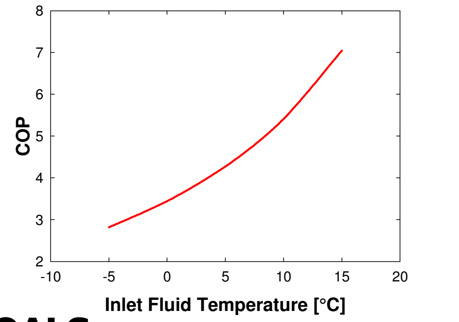

DESIGN PROBLEM AND GOALS

To find the suitable BHE overall length in order to have (in defined working conditions) a proper <u>return fluid temperature</u> ($T_{f,\ in}$) from ground for:

1) Obtaining high average seasonal COPs (SPF Seasonal Performance factor)

2) Avoiding too low temperatures (which can cause HP failure) during the peak working conditions

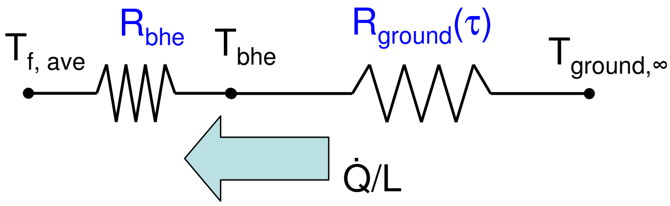

Two resistance model for GCHP simulation (IV)

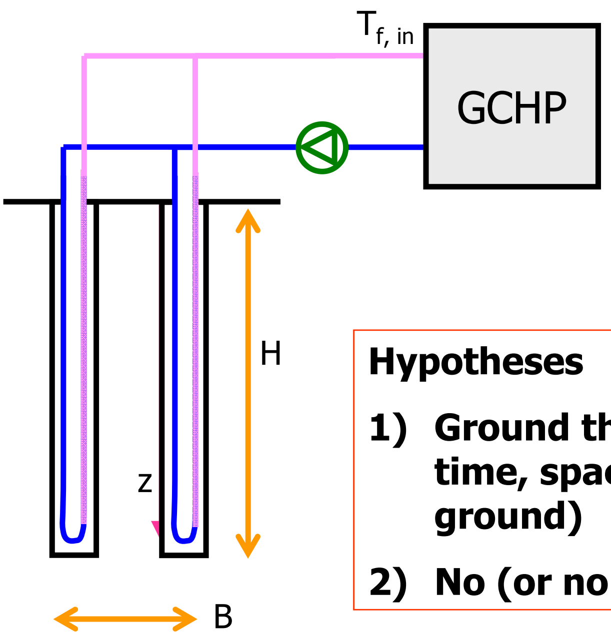

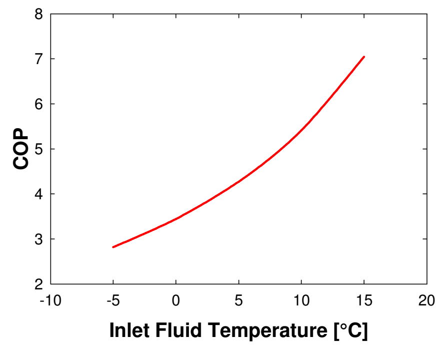

Hypotheses

1) **Ground thermal properties do not depend on time, space and temperature (homogeneous ground)**
2) **No (or no meaningful) groundwater flow**

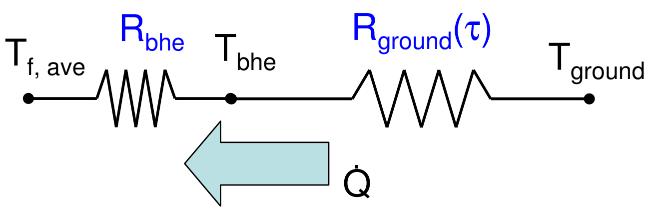

Two resistance model for GCHP simulation (V)

DESIGN STEPS AND MAIN CONCEPTS

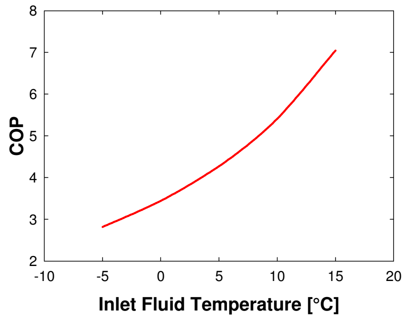

$T_{f,in}$ is related to the BHE wall temperature along the depth

$T_{f,ave}=(T_{f,\ in}+T_{f,out})/2$

<u>At given heat transfer rate Q</u>, $T_{f,ave}$ depends on $T_{ground,inf}$ and on BHE and Ground thermal resistances

HENCE:

It's mandatory to evaluate either R_{bhe} or R_{ground}

Input of the problem is the heat transfer rate Q [W] extracted/injected in the ground as a function of time (hourly, dayly or monthly values...)

$Q=Q_{ground} = Q_{build}(COP-1)/(COP)$

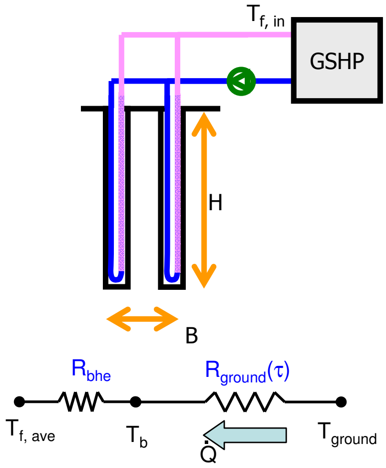

Two resistance model for GCHP simulation (VI)

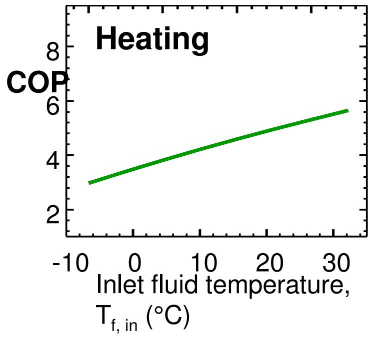

The starting point is the knowledge of the builing heating and cooling requirements Q_{build} [W], better in terms or energy required E_{build} [J or Wh] at given time intervals (again hours, days or months..)

$Q=Q_{ground} = Q_{build}(COP-1)/(COP)$

$E_{ground} = E_{build}(COP-1)/(COP)$

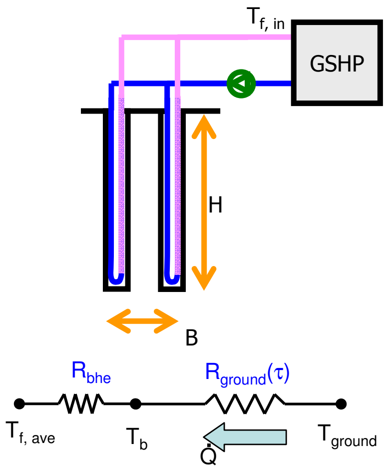

(e.g. the building monthly heat loads in kWh as calculated according to the standard UNI/EN 11300)

Ground Thermal Resistance and 1D models

General Heat Conduction Equation (cyl. Coordinates)

$$\frac{1}{r}\frac{\partial}{\partial r}\left(kr\frac{\partial T}{\partial r}\right)+\frac{1}{r^2}\frac{\partial}{\partial \phi}\left(k\frac{\partial T}{\partial \phi}\right)+\frac{\partial}{\partial z}\left(k\frac{\partial T}{\partial z}\right)+\dot{q}=\rho c\frac{\partial T}{\partial t}$$

1D transient heat conduction equation

$$\frac{1}{r}\frac{\partial}{\partial r}\left(kr\frac{\partial T}{\partial r}\right)'=\rho c\frac{\partial T}{\partial t}$$

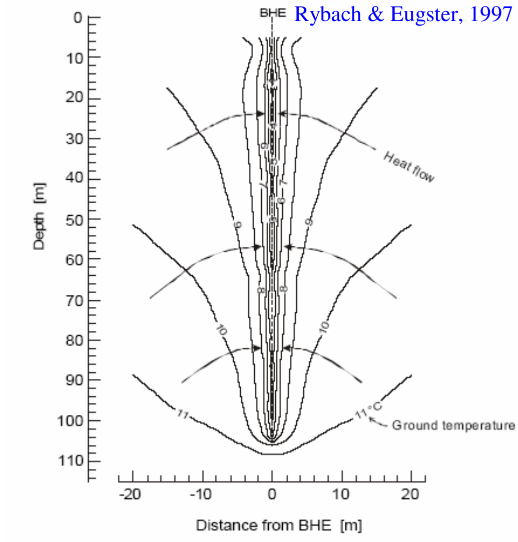

Ground Thermal Resistance and 1D models (IIIb)

1D transient heat conduction, constant thermal properties, no underground fluid flow, constant heat flux

Infinite Line Source Model (ILS)
The line source developed by Kelvin and later solved by Ingersoll and Plass (1948)

$$\Delta T=\frac{Q'}{4\pi k_{soil}}\int_x^{\infty}\frac{e^{-\beta}}{\beta}d\beta$$

$$x=\frac{r^2}{4\alpha_{soil}t}$$

$\dot{Q}'$ = heat transfer rate per length of line source $\left(\frac{W}{m}\right)$
ΔT = $T(r,\tau)-T_{gr,\infty}$
t = time (s)
α = ground diffusivity (m^2/s)
r = radius from the line source (m) or (ft)

$$\int_x^{\infty}\frac{e^{-\beta}}{\beta}d\beta=E_1(x)=-\gamma-\ln(x)-\sum_{n=1}^{m}\frac{(-1)^n x^n}{n\cdot n!}$$

$\gamma=0.577216$

Exponential integral

$x=1/(4Fo_r)$

$Fo=Fo_r=\alpha\tau/r^2$

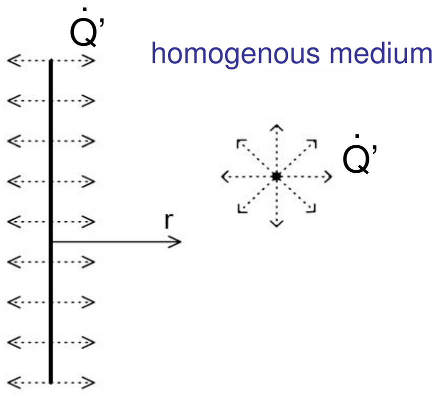

Ground Thermal Resistance and 1D models (IV)

$$\Delta T = \frac{\dot{Q}''}{k_s} G(F_0, p)$$

Fo=Fo$_{rb}$=$\alpha\tau/r_b^2$

$$p = \frac{r}{r_{bhe}}$$

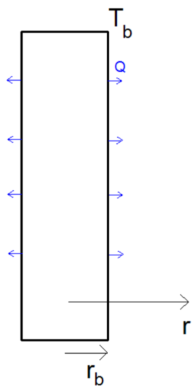

Infinite Cylindrical Source Model (ICS)
Ingersoll et al. (1950, 1954)

TABLE 13.2.—VALUES OF G(z,p) AS USED IN EQUATION (13.8f)

Fo$_{rb}$	G(Fo,p=1)	G(Fo,2)	G(Fo,5)	G(Fo,10)
0.10	0.049			
0.20	0.067			
0.30	0.080			
0.40	0.090			
0.50	0.099			
0.60	0.107			
0.70	0.113			
0.80	0.118			
1.00	0.128	0.035	0.001	0.000
1.20	0.137			
1.5	0.148			
2.0	0.163			
2.5	0.175			
3.0	0.186			
4.0	0.203			
5	0.217	0.112	0.0153	0.0001
6	0.228			
8	0.247			
10	0.263	0.155	0.0388	0.0024
12	0.275	0.167	0.0470	0.0042
15	0.291	0.182	0.0580	0.0072
20	0.312	0.203	0.0736	0.0129
25	0.328	0.219	0.0866	0.0188
30	0.342	0.232	0.0979	0.0246
50	0.380	0.271	0.132	0.0460
100	0.433	0.323	0.181	0.0842
500	0.560	0.449	0.304	0.197
1000	0.614	0.504	0.359	0.250
5000	0.742	0.632	0.486	0.376
10000	0.797	0.687	0.541	0.431
25000	0.870	0.760	0.614	0.504

Ground Thermal Resistance and 1D models (VI)

$$T(r_b) - T_{gr,\infty} = \frac{\dot{Q}'_{ave}}{C k_{gr}} \Gamma(Fo)$$

C=1 (ICS)
C=4π (ILS)
Γ=G (ICS)
Γ=E$_1$ (ILS)

Fo=Fo$_{rb}$=$\alpha\tau/r_b^2$

$$R_{ground}(\tau) = \frac{\Gamma(Fo)}{C k_{gr}}$$

Γ is a generic **Temperature Response Factor** able to describe the ground response under given assumptions

Ground thermal resistance: 2D models (III)

Finite line source in finite medium (FLS)

This solution can be obtained provided that a mirror source (of opposite strength) in introduced in the infinite medium (Eskilson, 1987, Zeng (2002)

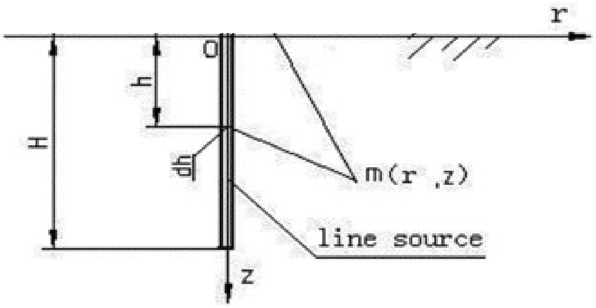

$$T(r,z)-T_{gr,\infty}=\frac{\dot{Q}'}{4\pi k_{gr}}\int_0^H\left(\frac{erfc\left(\frac{\sqrt{(z-h)^2+r^2}}{2\sqrt{\alpha\tau}}\right)}{\sqrt{(z-h)^2+r^2}}-\frac{erfc\left(\frac{\sqrt{(z-h)^2+r^2}}{2\sqrt{\alpha\tau}}\right)}{\sqrt{(z-h)^2+r^2}}\right)dh$$

Ground thermal resistance: 3D models (I)

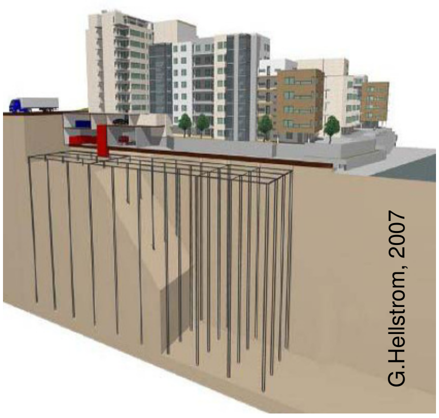

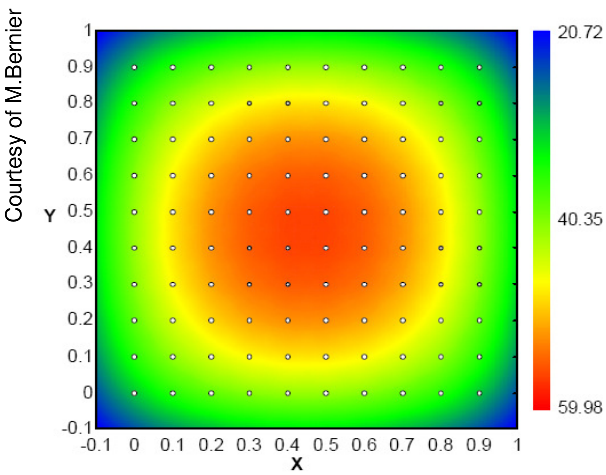

The g functions are TRF able to describe the overall behaviour of a BHE field. Eskilson first numerically calculated different g-functions for different BHE field geometries. These functions provide the dimensionless and average borehole temperature for constant heat transfer rate per unit length (Eskilson 1987, Hellstrom, 1997)

Ground thermal resistance: 3D models (II)

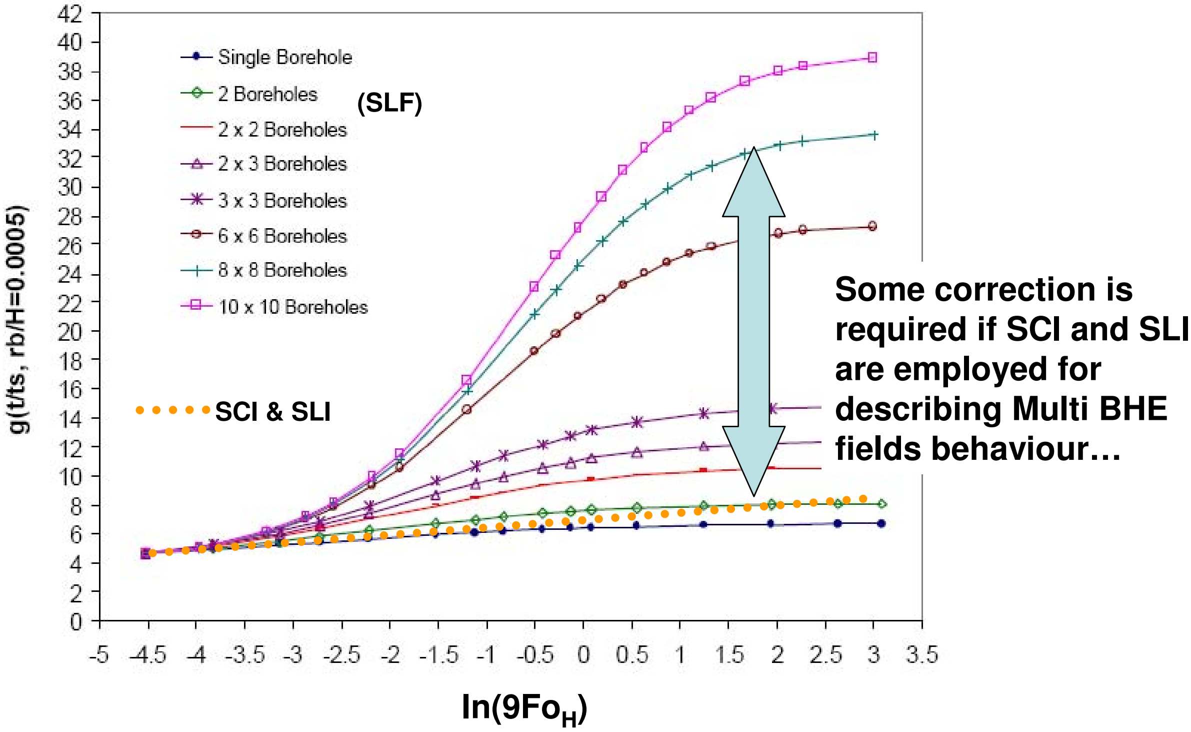

$$T_{ave}(r_b,\tau)-T_{gr,\infty}=\frac{Q'_{ave}}{2\pi k_{gr}}\,g\left(\ln(9Fo_H),\ r_b/H\ ,\ B/H\ ,borefield\ \ geometry\right)$$

Temporal superposition and Ashrae/UNI 11466 design method

Temporal superposition and the Ashrae-UNI method

The Ashrae method (Kavanaugh & Rafferty) is based on the hypothesis that the borefield behaviour under real operating conditions can be described by 3 elementary thermal loads to the ground, namely a multiyearly one (that lasts 10 years), o montly one and a multihourly one (6 hours)

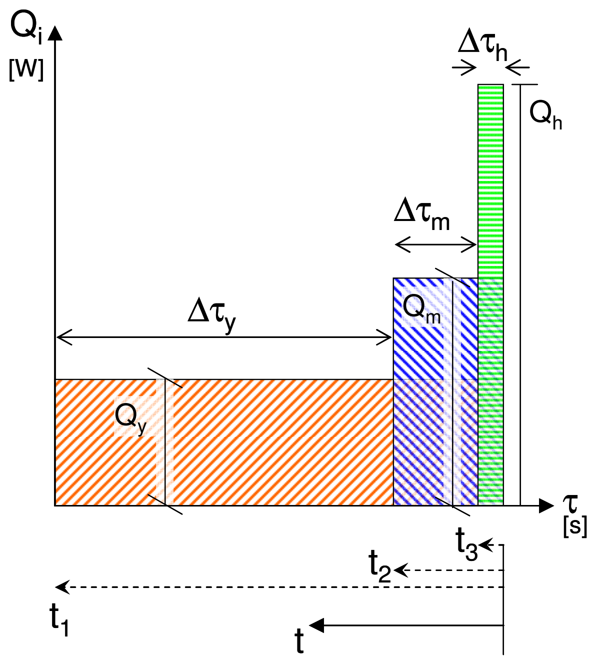

$\Delta\tau_y = 10\text{yrs}$ $\Delta\tau_m = 1\text{month}$ $\Delta\tau_h = 6\text{hrs}$

M.Fossa, The Temperature Penalty Approach to The Design Of Borehole Heat Exchangers For Heat Pump Applications, *Energy and Buildings*, to be published, (2011).

Temporal superposition and the Ashrae-UNI method

The Ashrae method (Kavanaugh & Rafferty) is based on a simple formula for evaluating the overall BHE length L as a function of ground thermal loads and expected fluid return temperature

$$L = \frac{\left\{\dot{Q}_y R_y + \dot{Q}_m R_m + \dot{Q}_h \left(R_h + R_{bhe}\right)\right\}}{T_{gr,\infty} - T_{f,ave}(\tau_N) - T_p}$$

The heat transfer rates (in [W]) Q_y, Q_m e Q_h represent the average values exchanged at ground level in three periods, 10 years, monthly and along 6 hours, respectively

Temporal superposition and the Ashrae-UNI method

The Ashrae method adopts the ICS solution for calculating the ground resistances R [Wm/K]

$$L = \frac{\left\{\dot{Q}_y R_y + \dot{Q}_m R_m + \dot{Q}_h \left(R_h + R_{bhe}\right)\right\}}{T_{gr,\infty} - T_{f,ave}(\tau_N) - T_p}$$

In order to take into account the "interference of adjacent bores" a correction factor T_p is introduced. Temperature Penalty

CHAPTER 32

GEOTHERMAL ENERGY

t_p = temperature penalty for interference of adjacent bores, °C

Temporal superposition and the Ashrae-UNI method

T_p is proportional to the error of G solution (single infinite cylindrical source) with respect to the "true" solution wich is named g-functionsPossibilities for calculating T_p

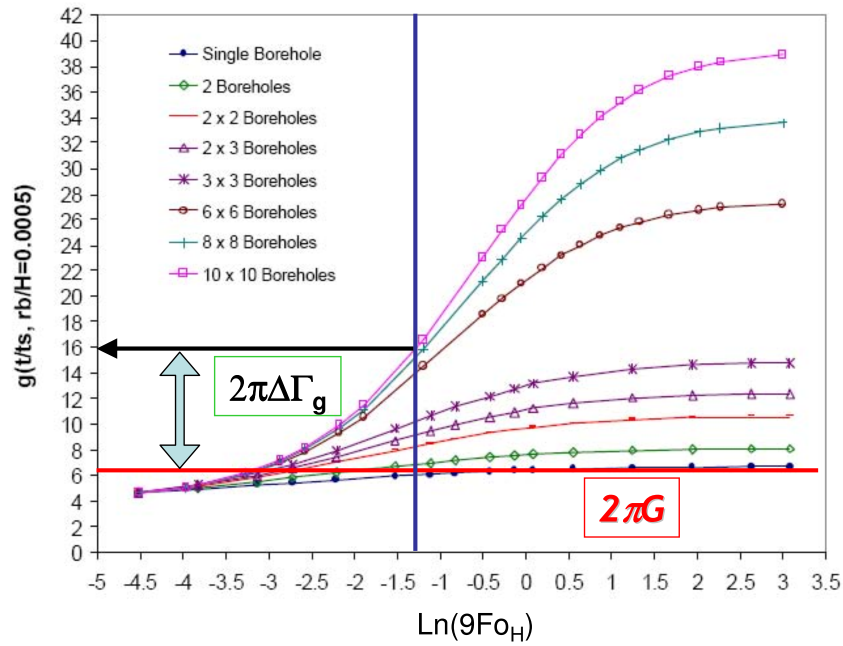

Temporal superposition and the Ashrae-UNI method

$$L = \frac{\left\{ \dot{Q}_y R_y + \dot{Q}_m R_m + \dot{Q}_h \left(R_h + R_{bhe} \right) \right\}}{T_{gr,\infty} - T_{f,ave}(\tau_N) - T_p}$$

Possibilities for calculating T_p

1) Empirical tables as in Ashrae standard
2) Bernier formula with 36 costanti (Bernier, ASHRAE Transactions 2008)
3) Diagrams of the g-function pertaining the BHE configurations chosen
4) Calculation of $\Gamma(t_1)$ according to MF method (2011, 2013, 2014)

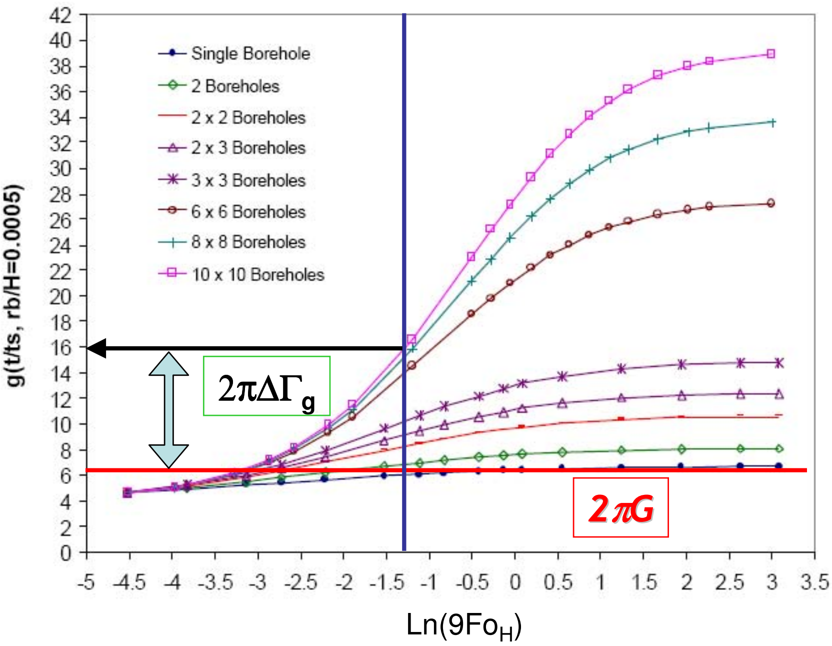

Temporal superposition and the Ashrae-UNI method

$$L = \frac{\left\{ \dot{Q}_y R_y + \dot{Q}_m R_m + \dot{Q}_h \left(R_h + R_{bhe} \right) \right\}}{T_{gr,\infty} - T_{f,ave}(\tau_N) - T_p}$$

Heat transfer rates (in [W]) Q_y, Q_m e Q_h are a synthetic representation of the heat profile at the ground in the long term, namely 10 yrs

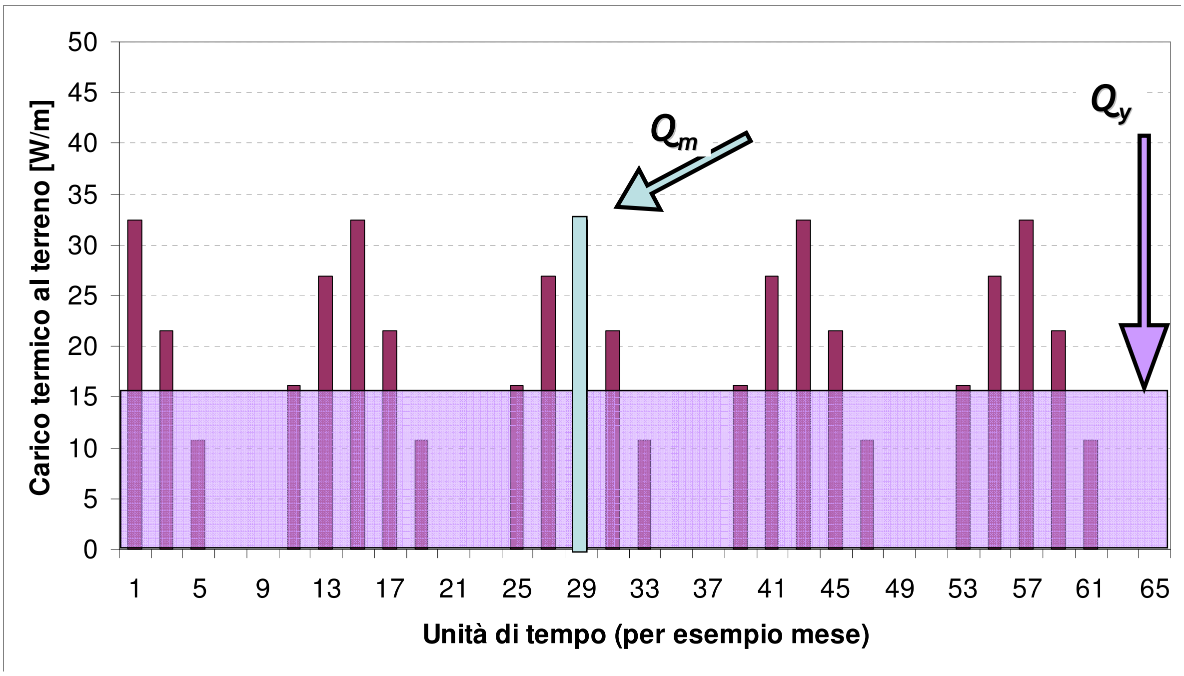

Temporal superposition and the Ashrae-UNI method

$$L = \frac{\{\dot{Q}_y R_y + \dot{Q}_m R_m + \dot{Q}_h (R_h + R_{bhe})\}}{T_{gr,\infty} - T_{f,ave}(\tau_N) - T_p}$$

Resistances R_y, R_m, R_{bhe} according to the standard have to be calculates as follows:

$$R_y = (G(Fo_f) - G(Fo_1))/k_{gr}$$

$$R_m = (G(Fo_1) - G(Fo_2))/k_{gr}$$

$$R_{6h} = G(Fo_2)/k_{gr}$$

$$\begin{aligned} Fo_f &= 4\alpha\tau_f/d_b^2 \\ Fo_1 &= 4\alpha(\tau_f - \tau_1)/d_b^2 \\ Fo_2 &= 4\alpha(\tau_f - \tau_2)/d_b^2 \end{aligned}$$

$$\begin{aligned} \tau_1 &= 3650 \text{ days} \\ \tau_2 &= 3650 + 30 = 3680 \text{ days} \\ \tau_f &= 3650 + 30 + 0.25 = 3680.25 \text{ days} \end{aligned}$$

R_{bhe} is the BHE resistance, to be calculated starting from TRT measurements or with proper formulas

Temporal superposition and the Ashrae-UNI method

$$L = \frac{\{\dot{Q}_y R_y + \dot{Q}_m R_m + \dot{Q}_h (R_h + R_{bhe})\}}{T_{gr,\infty} - T_{f,ave}(\tau_N) - T_p}$$

For t_1 = 3680.25 days,

Fo_{rb} is about $1.25 \cdot 10^5$

Fo_H is about di $3.2 \cdot 10^2$

$\ln(9Fo_H)$ is about -1.25

G(t1)=0.99

$G \cdot 2\pi = 6.3$

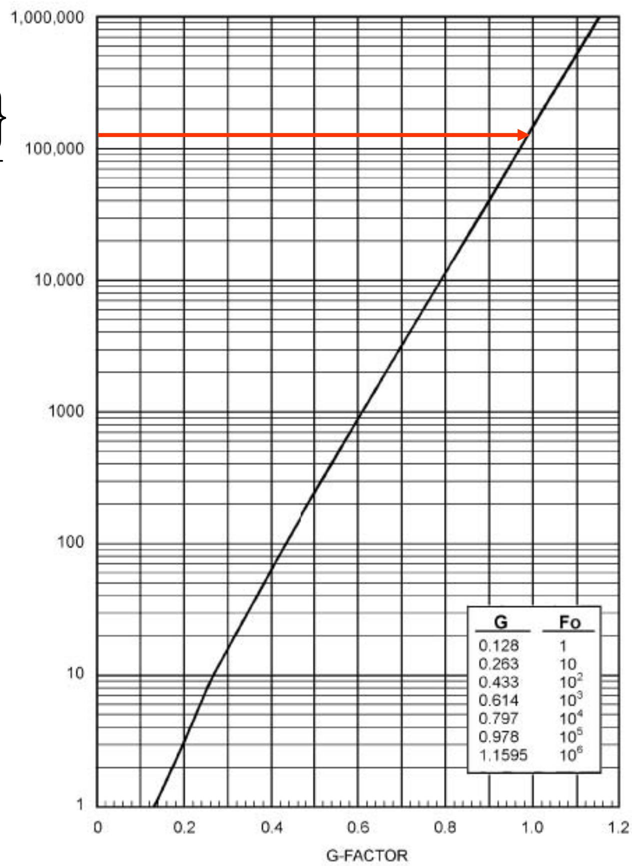

Tp evaluation according to Tp8 approach
(MF&DR 2015)

$$\theta_8 = \dot{Q}_y \frac{E_1\left[Fo^*(\tau_N, B)\right] + E_1\left[Fo^*(\tau_N, B\sqrt{2})\right]}{\pi k_{gr} L}$$

$$Fo^* = Fo(\tau_N, R) \cdot \left(\frac{H_{ref}}{H}\right)$$

$$T_{p8} = \theta_8 \frac{aN_4 + bN_3 + cN_2 + dN_1}{N_{tot}}$$

R configurations					
B/H	**0.03**	**0.05**	**0.075**	**0.1**	**0.125**
a	5.41	3.90	3.07	2.42	1.93
b	0.280	0.280	0.280	0.280	0.280
c	0.450	0.450	0.450	0.450	0.450
d	0	0	0	0	0

non-R configurations					
B/H	**0.03**	**0.05**	**0.075**	**0.1**	**0.125**
a	0	0	0	0	0
b	0.950	0.950	0.950	0.950	0.950
c	0.744	0.620	0.498	0.412	0.345
d	0.05	0.05	0.05	0.05	0.05

$$a(\text{R configs}) = 1.95005 + \frac{0.105215}{(B/H)} - 55.6543\left(\frac{B}{H}\right)^2$$

$$c(\text{non-R configs}) = -0.28174 \cdot \ln\left(\frac{B}{H}\right) - 0.23546$$

Notice:

1) Href=100m

2) N4, N3, N2 and N1 are the number of boreholes surrounded by "only" 4 other ones, only 3 other ones, and so on, respectively. As an example for clarifying the criterion, a rectangular borefield constituted by 3x4 BHEs has N4=2, N3=6, N2=4, N1=0, Ntot=12, while an in-line configuration 4x1 has N4=0, N3=0, N2=2, N1=2

Tp8 Method results (vs reference solution based on exact g-functions)

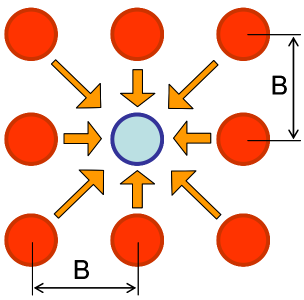

Reference BHE heights H and T_p values vs Tp8 method predictions. Effects of ground properties and BHE depth on model estimates.
R-type: Rectangular and square configurations.
Non-R: slender rectangular, , in-line, L, O and U BHE field geometries.

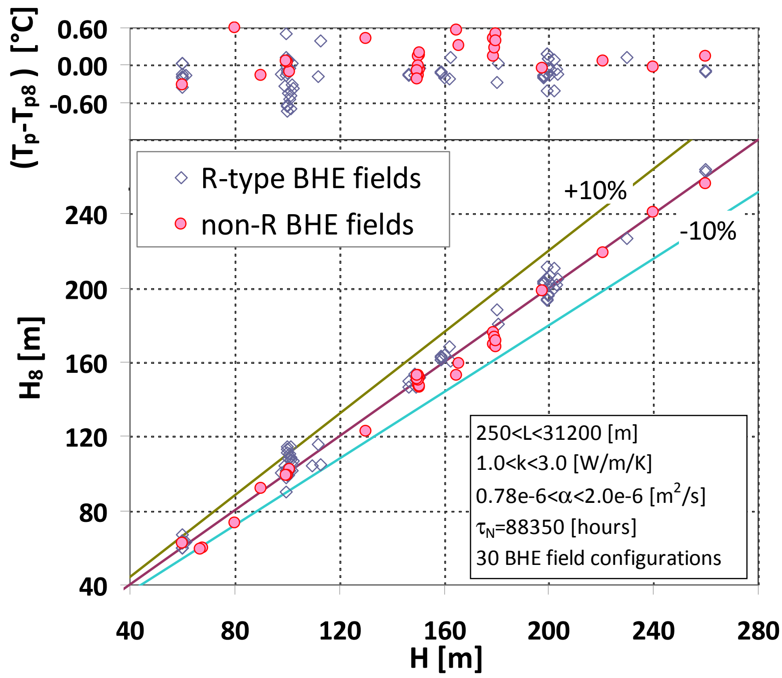

Source: Energy and Buildings 116 (2016) 114–121

Tp8 Method Annexes (G-Function analytical approximation, MF 2016)

$$G = \sum_{j=0}^{6} c_j Log_{10}(Fo_{rb})$$

c_0= 1.2777E-01 c_1= 1.0812E-01

c_2=3.0207E-02 c_3= -2.3037E-03.

c_4= -1.4459E-03

c_5= 3.6415E-04 c_6= -2.4889E-05

Quick.., sorry) Calculation example with the Ashrae/Tp8 method

$$L = \frac{\left\{\dot{Q}_y R_y + \dot{Q}_m R_m + \dot{Q}_h \left(R_h + R_{bhe}\right)\right\}}{T_{gr,\infty} - T_{f,ave}(\tau_N) - T_p}$$

$$PLF = \frac{n_{ore\ mese\ funz\ nom}}{n_{ore\ mese\ tot}} = \frac{Q_{month} / \dot{Q}_{nom,pdc}}{n_{giorni} * 24}$$

$$Q_{month} \quad [kWh] \quad \dot{Q}_{nom} \quad [kW]$$

$$\dot{Q}_{nom} = \dot{Q}_h$$

$$Allora\ PLF = \dot{Q}_{month} \Big/ \dot{Q}_{6h}$$

Building and ground heat loads

Building side	Qm [kWh]			Ground side	
gennaio	96680			76109.79	
febbraio	80110			63065.32	
marzo	67120			52839.15	
Aprile	40980			32260.85	
Maggio	17580			13839.57	
ottobre	23170			18240.21	
Novembre	54900			43219.15	
Dicembre	85490			67300.64	
Seasonal COP	4.7		Qy, gr	41.9	[kW]
Peak COP	4.05			41900	[W]
Qnom, bldg	350	[kW]	Qm, gr	102.3	[kW]
(PLF=0.372)				102300	[W]
			Qnom, gr=Q	263.6	[kW]
				263600	[W]

$$\dot{Q}_{m,gr} = \frac{Q_{m,bldg}}{24 \times 31} \times \frac{cop_{ave} - 1}{cop_{ave}}$$

$$\dot{Q}_{y,gr} = \frac{1}{8760} \sum Q_{m,bldg,i} \times \frac{cop_{ave} - 1}{cop_{ave}}$$

$$\dot{Q}_h = \dot{Q}_{nom,gr} = \dot{Q}_{nom,bldg} \times \frac{cop_{peak} - 1}{cop_{peak}}$$

Ground thermal resistances, calculated with G solution

k_ground	2.7	[W/m/K]
alpha_gr	1.62E-06	[m2/s]
rb	0.06	[m]

$$R_{6h} = \frac{1}{k_{gr}} \times \left[G\left(Fo\left(\tau_{6h}\right)\right)\right]$$

$$R_y = \frac{1}{k_{gr}} \times \left[G\left(Fo(\tau_{tot})\right) - G\left(Fo(\tau_m + \tau_{6h})\right)\right]$$

$$\tau_{tot} = (365 \times 10 + 30 + 0.25) \times 24 \times 3600 = 3.180E08$$

$$Fo(\tau_{tot}) = \frac{\alpha \tau_{tot}}{r_b^2} = 143090$$

$$Fo(\tau_{m+6h}) = \frac{\alpha(\tau_m + \tau_h)}{r_b^2} = 1176 \quad Fo(\tau_{6h}) = 9.7$$

$$G\left[Fo(\tau_{6h})\right] = 0.261$$

Ry	0.145	[mK/W]
Rm	0.134	
R6h	0.097	

BHE thermal resistance and Tp correction evalution

R_{bhe} is the BHE resistance, to be calculated starting from TRT measurements or with proper formulas

Let's select R_{bhe} =0.1[mK/W], Tgr=16.1[°C], Tf,ave=4

$$T_{p8} = \theta_8 \frac{aN_4 + bN_3 + cN_2 + dN_1}{N_{tot}}$$

$$L = \frac{\left\{\dot{Q}_y R_y + \dot{Q}_m R_m + \dot{Q}_h \left(R_h + R_{bhe}\right)\right\}}{T_{gr,\infty} - T_{f,ave}(\tau_N) - T_p(L)}$$

$$\theta_8 = \dot{Q}_y \frac{E_1\left[Fo^*(\tau_N, B)\right] + E_1\left[Fo^*(\tau_N, B\sqrt{2})\right]}{\pi k_{gr} L}$$

Iterations start by imposing Tp=0 and calculating first attempt L value. Also a BHE field configuration is chosen. Then a new Tp is calculated, here according to Tp8 approach. Iterations go on till convergence.

If BHE field selection is 10x10 and B/H=0.05,

Ntot=64, N4=36, N3=24, N2=4 Tp8 constants: a=3.90, b=0.28 c=0.45

Final overall Length at convergence is 13800m and Tp=6.7°C

MARUEEB

Co-funded by the Erasmus+ Programme of the European Union

Thanks for your attention